

TRANSITION METAL INDUCED HIGH SPIN POLARIZATION IN ZIGZAG SiCNT AND BLACK ARSENIC PHOSPHORUS: MATERIALS FOR SPINTRONIC APPLICATIONS

**A Thesis Submitted
In Partial Fulfilment of the Requirements
for the Degree of**

DOCTOR OF PHILOSOPHY
by

**ANURAG CHAUHAN
(Roll No. 2K18/PhDIT/07)**

Under the Supervision of

Dr. KAPIL SHARMA
Delhi Technological
University, India

Dr. SUDHANSHU CHOUDHARY
University of North Dakota,
USA



Department of Information Technology

DELHI TECHNOLOGICAL UNIVERSITY
(Formerly Delhi College of Engineering)
Shahbad Daultpur, Main Bawana Road, Delhi-110042. India

September, 2024



DELHI TECHNOLOGICAL UNIVERSITY

(Formerly Delhi College of Engineering)

Shahbad Daultapur, Main Bawana Road, Delhi-42

CANDIDATE'S DECLARATION

I, **ANURAG CHAUHAN**, hereby certify that the work which is being presented in the thesis entitled "*Transition Metal Induced High Spin Polarization in Zigzag SiCNT and Black Arsenic Phosphorus: Materials for Spintronic Applications*" in partial fulfilment of the requirements for the award of the Degree of Doctor of Philosophy, submitted in the Department of Information Technology, Delhi Technological University is an authentic record of my own work carried out during the period from **August 2018 to June 2024** under the supervision of **Prof. Kapil Sharma**, Professor of Information Technology Department, Delhi Technological University, Delhi and **Dr. Sudhanshu Choudhary**, Instructor at School of Electrical Engineering and Computer Science, University of North Dakota, Grand Forks, ND, USA.

The matter presented in the thesis has not been submitted by me for the award of any other degree of this or any other Institute.

Candidate's Signature



DELHI TECHNOLOGICAL UNIVERSITY

(Formerly Delhi College of Engineering)

Shahbad Daultapur, Main Bawana Road, Delhi-42

CERTIFICATE BY THE SUPERVISOR(s)

Certified that **Anurag Chauhan** (2K18/PhDIT/07) has carried out their search work presented in this thesis entitled **“Transition Metal Induced High Spin Polarization in Zigzag SiCNT and Black Arsenic Phosphorus: Materials for Spintronic Applications”** for the award of **Doctor of Philosophy** from Department of Information Technology, Delhi Technological University, Delhi, under our supervision. The thesis embodies results of original work, and studies are carried out by the student himself and the contents of the thesis do not form the basis for the award of any other degree.

Signature

(Prof. Kapil Sharma)

(Professor)

(Delhi Technological University, India)

A handwritten signature in black ink, appearing to read 'Sudhanshu', with a stylized flourish at the end.

Signature

(Dr. Sudhanshu Choudhary)

(Instructor)

(University of North Dakota, ND, USA)

ABSTRACT

This thesis explores the potential of transition metal-induced high spin polarization in zigzag Silicon Carbide Nanotubes and Black Arsenic Phosphorus for spintronic device applications. Spintronics, an emerging field of technology, leverages the intrinsic spin of electrons along with their charge to revolutionize data storage, magnetic sensing, and advanced computing technologies. Despite advancements in spintronics, several challenges persist, including limited spin diffusion lengths, finite defect densities, low energy density of existing materials, bias-dependent decrease in tunnel magnetoresistance and temperature sensitivity of MTJs. Additionally, materials like SiCNTs and b-AsP possess excellent properties such as tunable band gaps and thermal stability but lack intrinsic magnetism, hindering their direct application in spintronic devices.

This research employs density functional theory calculations to study the adsorption of transition metals on SiCNTs and b-AsP. The investigation focuses on the electronic and magnetic properties of these materials upon transition metal adsorption. Different transition metals (Ag, Co, Cr, Cu, Fe, Mo, Ti, Zr) are adsorbed on various chiralities of SiCNTs (zigzag (4,0), (6,0), and (8,0)) and pristine b-AsP to analyze their impact on spin polarization and magnetization. Computational simulations and optimizations are performed to evaluate the stability and feasibility of TM adsorption on these materials.

The study of SiCNTs reveals significant changes in their electronic and magnetic properties upon TM adsorption. The adsorption of Co, Cr, Fe, Mo, and Ti on SiCNTs induces substantial magnetic moments, transforming the non-magnetic SiCNTs into ferromagnetic (FM) or half-metallic ferromagnetic (HMF) states. The strength of the induced ferromagnetic behaviour varies with the various transition metals and is then related to the calculated magnetic moment in the adsorbed structure. The Cr adsorbed (8,0) SiCNT indicated strong HMF behaviour with a magnetic moment of 5.4 μ_B . These findings suggest that TM adsorption can significantly enhance the spintronic properties of SiCNTs and will be helpful in designing devices like spin-valves, MTJs, and MRAMs in the field of spintronics.

The electronic and magnetic properties of two-dimensional black Arsenic Phosphorus (b-AsP) on adsorption of Transition Metals (TM) on its surface are investigated using density functional theory (DFT) based on first principles calculations. The spin-density of states (s-DOS) and the bandstructure of all the transition metals adsorbed structures have been plotted, which shows their transformation from non-magnetic to magnetic behaviour. The results suggest that pristine b-AsP, which is a non-magnetic semiconductor, turns into an HMF on the adsorption of Co, Fe and Ti, and it turns into

an FM on the adsorption of Cr and Zr. The total magnetic moments were also calculated to further support our results and findings. Strong magnetic moments were observed for Cr, Fe, and Ti adsorbed b-AsP structures. Ag, Cu and Mo adsorption over b-AsP results in non-magnetic metallic characteristics with very weak magnetic moments. This transformation from a non-magnetic semiconductor to a magnetic HMF or FM material demonstrates the potential use of b-AsP in designing spin magnetic devices for various spin-based applications.

The enhanced spintronic properties of TM-adsorbed SiCNTs and b-AsP open new avenues for their application in spintronic devices. The high spin polarization and induced magnetism in these materials can improve the performance of data storage technologies, magnetic sensors, and advanced computing systems. The thermal stability and tunable electronic properties of SiCNTs and b-AsP further enhance their suitability for high-performance spintronic applications.

The application of spintronic devices using a standard mCell has also been proposed to show how spintronic technology coexists with conventional electronic circuits. A fault-tolerant Arithmetic Logic Unit (ALU) has been proposed and simulated. Magnetic cell (mCell)-based logic is an efficient approach for the construction of digital circuits as it occupies less area, is non-volatile, and has negligible static power consumption. This study proposes a new design for an ALU that is made using mCell logic. Simulation results show that the proposed ALU design achieves a power delay product of 88.98 fJ through the F_{out} pin and 112.76 fJ through the C_{out} pin, which is very low compared with traditional CMOS-based designs.

Future research should focus on experimental validation, further optimization of TM adsorption techniques, device integration, and exploring other two-dimensional (2D) materials with similar tunable properties to expand the scope of spintronic applications. This research contributes to the advancement of spintronics by providing insights into the potential of TM-induced high spin polarization in SiCNTs and b-AsP, paving the way for the development of next-generation spintronic devices.

ACKNOWLEDGEMENT

I would like to express my heartfelt gratitude to my supervisor, Prof. Kapil Sharma, and co-supervisor, Dr. Sudhanshu Choudhary, for their invaluable guidance, support, and encouragement throughout my doctoral studies. Their expertise in the field and dedication to research have been instrumental in shaping my research and fostering my growth as a scholar. I am deeply grateful for their insightful feedback and contributions to my research. Their thoughtful critiques and suggestions have challenged me to think more deeply and critically about my work.

I am profoundly grateful to the Hon'ble Vice Chancellor of the University for his visionary leadership and unwavering support for research endeavours.

My deepest appreciation goes to Prof. Dinesh Kumar Vishwakarma, Head of the Department of Information Technology. It is indeed my privilege to submit this thesis during his headship.

I would also like to extend my sincere thanks to Prof. O.P. Verma, Head of the Department of Electronics and Communication Engineering, for his unconditional support and encouragement during my PhD work. His guidance and support have been invaluable in the successful completion of this thesis.

I am also indebted to my colleague and friend, Mr Piyush Tewari, for providing any possible support and to Dr Kriti Suneja for her invaluable guidance and assistance during this period.

My colleagues at DTU have been a constant source of support, encouragement, and camaraderie. Working alongside them has been a pleasure and has made my experience in the doctoral program truly memorable. I would especially like to acknowledge the PhD scholars for their collaborative spirit and mutual support.

I extend my gratitude to the reviewers of this thesis for their meticulous evaluation and constructive feedback, which have greatly enhanced the quality of my research.

I am profoundly indebted to my family and friends for their unwavering love and support, even during the most challenging times. My parents have always been an inspiration to me; their constant support has been the foundation upon which I have built my life and career.

Special credit goes to my beloved wife, Renuka, for her invaluable understanding and patience during the long hours I spent on my work. Her love and encouragement have been my anchor.

I am at a loss for words to thank my wonderful children, Mivaan and Heyaansh, whose boundless love and motivation have been my driving force to complete what I started. They have looked so patiently to finish my PhD so that they can play with me. Their innocent eyes have waited so eagerly for me for months so as to spend quality time with me. Their smiles and hugs have been my greatest source of joy and inspiration.

In particular, I want to honor the memory of my late younger brother, Abhishek, whose presence and love continue to inspire me. Though he is no longer with us, his memory has been a guiding light throughout this journey.

Without the collective support and guidance of these individuals, this research would not have been possible.

Finally, I thank the Almighty for giving me the strength to carry out the present research work.

Anurag Chauhan

Dedicated To My Family

LIST OF PUBLICATIONS

Journals

1. **Anurag Chauhan**, Kapil Sharma, and Sudhanshu Choudhary, Transition metal induced-magnetization in zigzag SiCNTs. J Comput Electron 22, 964–970 (2023). <https://doi.org/10.1007/s10825-023-02030-y> (IF: 2.1)
2. **Anurag Chauhan**, Kapil Sharma, and Sudhanshu Choudhary, “Transition metal induced- magnetization and spin-polarisation in black arsenic Phosphorus,” Ain Shams Eng. J., p. 102632, 2024, doi:<https://doi.org/10.1016/j.asej.2024.102632>. (IF: 6.0)

International Conferences:

1. **Anurag Chauhan**, Kapil Sharma, and Sudhanshu Choudhary “Transition Metal-induced Magnetization in (6,0) SiCNT” in the 2nd International Conference on Recent Advances in Functional Materials (RAFM-2024).
2. **Anurag Chauhan**, Kapil Sharma, and Sudhanshu Choudhary “Implementation of Fault Tolerant Arithmetic Logic Unit Using mCell” in the 2nd International Conference on Atomic, Molecular, Material, Nano and Optical Physics with Applications (ICAMNOP- 2023)

TABLE OF CONTENTS

Title	Page No.
Candidate declaration	ii
Certificate	iii
Abstract	iv
Acknowledgement	vi
List of Publications	ix
Chapter 1 INTRODUCTION	1
1.1 Background	1
1.2 History of Spintronics Development	2
1.3 Importance and Potential of Spintronics	4
1.4 Motivation	5
1.5 Research Gaps	7
1.6 Research Objectives	9
1.7 Thesis Organization	10
Chapter 2 LITERATURE REVIEW	12
2.1 Introduction	12
2.2 Early Developments and Key Concepts	12
2.3 Spintronic Device Applications	15
2.4 Materials for Spintronic Device Applications	19
2.5 Potential for Spintronic Applications	26
2.6 Summary	27
Chapter 3 TRANSITION METAL INDUCED MAGNETIZATION IN ZIGZAG SiCNTs	28
3.1 Introduction	28
3.2 Computational Details	29
3.3 Results and Discussions	31
3.4 Summary	65
Chapter 4 TRANSITION METAL INDUCED MAGNETIZATION AND SPIN-POLARIZATION IN BLACK ARSENIC PHOSPHORUS	67
4.1 Introduction	67
4.2 Computational Details	69
4.3 Results and Discussions	70
4.4 Summary	82

Chapter 5 IMPLEMENTATION OF FAULT TOLERANT ARITHMETIC LOGIC UNIT USING MCELL	84
5.1 Introduction	84
5.2 Structure of The Proposed Logic Gates	85
5.3 Implementation of Basic Logic Gates Using mCell	87
5.4 Implementation of Complex Logic Circuits Using mCell	89
5.5 Proposed Arithmetic Logic Unit	92
5.6 Setup and Simulation	94
5.7 Results and Discussions	94
5.8 Summary	96
Chapter 6 CONCLUSION, FUTURE SCOPE AND SOCIAL IMPACT	97
6.1 Conclusion	97
6.2 Future Scope	99
6.3 Social Impact	100
REFERENCES	102
List of Publications And their proofs	112

LIST OF FIGURES

Fig. 1.1 Present and future applications of spintronic devices	3
Fig. 2.1 MTJ consisting of carbon nanotube sandwiched between left-right CrO₂ HMF electrodes	16
Fig. 2.2 Zigzag (4,0) SiCNT	21
Fig. 2.3 Black Arsenic Phosphorus	25
Fig. 3.1(a) Zigzag (4,0) SiCNT (b) Co atom adsorbed (4,0) SiCNT	30
Fig. 3.2(a) Zigzag (6,0) SiCNT (b) Cr atom adsorbed (6,0) SiCNT	30
Fig. 3.3(a) Zigzag (8,0) SiCNT (b) Ag atom adsorbed (8,0) SiCNT	30
Fig. 3.4 DOS and bandstructure of pristine SiCNT(4,0)	33
Fig. 3.5 DOS and bandstructure of Ag adsorbed SiCNT(4,0)	34
Fig. 3.6 DOS and bandstructure of Co adsorbed SiCNT(4,0)	35
Fig. 3.7 DOS and bandstructure of Cr adsorbed SiCNT(4,0)	36
Fig. 3.8 DOS and bandstructure of Cu adsorbed SiCNT(4,0)	37
Fig. 3.9 DOS and bandstructure of Fe adsorbed SiCNT(4,0)	38
Fig. 3.10 DOS and bandstructure of Mo adsorbed SiCNT(4,0)	39
Fig. 3.11 DOS and bandstructure of Ti adsorbed SiCNT(4,0)	40
Fig. 3.12 DOS and bandstructure of Zr adsorbed SiCNT(4,0)	41
Fig. 3.13 DOS and bandstructure of pristine SiCNT(6,0)	45
Fig. 3.14 DOS and bandstructure of Ag adsorbed SiCNT(6,0)	46
Fig. 3.15 DOS and bandstructure of Co adsorbed SiCNT(6,0)	47
Fig. 3.16 DOS and bandstructure of Cr adsorbed SiCNT(6,0)	48
Fig. 3.17 DOS and bandstructure of Cu adsorbed SiCNT(6,0)	49

Fig. 3.18 DOS and bandstructure of Fe adsorbed SiCNT(6,0)	50
Fig. 3.19 DOS and bandstructure of Mo adsorbed SiCNT(6,0)	51
Fig. 3.20 DOS and bandstructure of Ti adsorbed SiCNT(6,0)	52
Fig. 3.21 DOS and bandstructure of Zr adsorbed SiCNT(6,0)	53
Fig. 3.22 DOS and bandstructure of Pristine SiCNT(8,0)	56
Fig. 3.23 DOS and bandstructure of Ag adsorbed SiCNT(8,0)	57
Fig. 3.24 DOS and bandstructure of Co adsorbed SiCNT(8,0)	58
Fig. 3.25 DOS and bandstructure of Cr adsorbed SiCNT(8,0)	59
Fig. 3.26 DOS and bandstructure of Cu adsorbed SiCNT(8,0)	60
Fig. 3.27 DOS and bandstructure of Fe adsorbed SiCNT(8,0)	61
Fig. 3.28 DOS and bandstructure of Mo adsorbed SiCNT(8,0)	62
Fig. 3.29 DOS and bandstructure of Ti adsorbed SiCNT(8,0)	63
Fig. 3.30 DOS and bandstructure of Zr adsorbed SiCNT(8,0)	64
Fig. 4.1 (a) Pristine Semiconducting AsP-3 (b) Co- adsorbed AsP-3	69
Fig. 4.2 DOS and bandstructure of pristine AsP3	72
Fig. 4.3 DOS and bandstructure of Ag adsorbed AsP3	73
Fig. 4.4 DOS and bandstructure of Co adsorbed AsP3	74
Fig. 4.5 DOS and bandstructure of Cr adsorbed AsP3	75
Fig. 4.6 DOS and bandstructure of Cu adsorbed AsP3	76
Fig. 4.7 DOS and bandstructure of Fe adsorbed AsP3	77
Fig. 4.8 DOS and bandstructure of Mo adsorbed AsP3	78
Fig. 4.9 DOS and bandstructure of Ti adsorbed AsP3	79
Fig. 4.10 DOS and bandstructure of Zr adsorbed AsP3	80
Fig. 5.1 Schematic diagram of an mCell	86

Fig. 5.2 General structure of logic gates	86
Fig. 5.3 mCell Based NOT Gate	87
Fig. 5.4 mCell Based NOR Gate	88
Fig. 5.5 mCell Based NAND Gate	88
Fig. 5.6 Schematic Diagram of PPRG	90
Fig. 5.7 Double Feynman Gate	91
Fig. 5.8 PPRG based Full Adder	92
Fig. 5.9 Operation Selector Circuit of ALU	93
Fig. 5.10 Block Diagram of ALU	93
Fig. 5.11 Transient Response of ALU	95

LIST OF TABLES

Table 3.1 Magnetic Properties of (4,0) SiCNT after adsorption of TM	42
Table 3.2 Magnetic Properties of (6,0) SiCNT after adsorption of TM	54
Table 3.3 Magnetic Properties of (8,0) SiCNT after adsorption of TM	55
Table 4.1 Magnetic Properties of b-AsP-3 after adsorption of TM	81
Table 5.1 Truth Table of Implemented Logic Gates	89
Table 5.2 Truth Table of PPRG	90
Table 5.3 Functional Table of ALU	94
Table 5.4 Power Delay Product of ALU and its Subcomponents	95

LIST OF SYMBOLS AND ABBREVIATIONS

2D	Two-Dimensional
ALU	Arithmetic Logical Unit
b-AsP	Black Arsenic Phosphorus
CMOS	Complementary Metal Oxide Semiconductor
CMP	Chip Multi-Processors
CNTs	Carbon Nanotubes
DFG	Double Feynman Gate
DFT	Density Functional Theory
DOS	Density of States
FM	Ferromagnetic
FPGA	Field Programmable Gate Arrays
GMR	Giant Magnetoresistance
HMF	Half-Metal Ferromagnetic
LCAO	Linear Combination of Atomic Orbitals
MRAM	Magnetic Random Access Memory
PPRG	Parity Preserving Reversibility Gate
RAM	Random Access Memory
s-DOS	Spin Density of States
SGGA	Spin-Polarized Generalized Gradient Approximation
SiCNTs	Silicon Carbide Nanotubes
SOC	Spin-Orbit Coupling
Spin-FET	Spin-Field Effect Transistors
STO	Spin-Torque Oscillators
STT	Spin-Transfer Torque
TM	Transition Metal
TMD	Transition Metal Dichalcogenide
TMR	Tunnel Magnetoresistance

Chapter 1

INTRODUCTION

Spintronics, leveraging electron spin rather than charge, promises to extend Moore's Law, driving advancements in data storage, speed, and energy efficiency beyond traditional semiconductor limits. This revolutionary approach will open new frontiers in developing cutting-edge technology.

1.1 Background

Spintronics refers to an emerging technology acquired from spin-based electronics, a type of electronic device that exploits the intrinsic spin of electrons as well as their charge for information processing. This dual use of the electron could pave the path for new high-density data storage, magnetic sensing, and advanced computing technologies. Spintronics uses this charge and the quantum-mechanical property of the spin, giving rise to additional degrees of freedom that may be manipulated to provide devices with superior capabilities [1].

Conventional electronic devices are mostly based on the charge of electrons to carry any information. Due to miniaturization, which almost tends to saturate the limits set by Moore's Law for the nanometre-scale electronic components of today, there are quantum size effects and heat dissipation issues due to leakage currents in the electronics industry. Spintronics offers the prospect of creating devices with larger storage densities, smaller consumption of power, and larger speeds [2].

The principle of spintronics is manifested via the manipulation of electron spin. An electron is a fundamental particle with a quantum number known as spin, the direction of which can be either "up" or "down." In spintronic devices, information can be stored and manipulated through the manipulation of electron spin states, eventually working in a way fundamentally different from traditional charge-based electronics. This capability opens up the possibility of developing devices that are more energy-efficient and capable of operating at higher speeds compared to their conventional counterparts [3].

The discovery of Giant Magnetoresistance (GMR) in the late 1980s by Baibich et al. was the one that sparked the concept of spintronics [4]. GMR refers to the enormous change in electrical resistance when an external magnetic field is imposed on certain materials. These gave way to the invention of high-density hard disk drives and

bridged the possibility of manipulating electron spins into practical reality. This was one of the defining moments for the field that opened the route to further developments in the ability to manipulate spin.

This ability to manipulate electron spin has far-reaching consequences across a number of various disciplines; the use of spintronic devices integrated with conventional electronics devices and circuits may lead to the enhancement of storage densities with significant reductions in data storage power consumption. The high sensitivity of spintronic materials to magnetic fields can be utilized in sensors to create highly accurate, compact magnetic sensors. Spins can also be manipulated at the quantum level, giving the ability to change the information processing in computing and hence leading to the possibility of quantum computers solving problems far beyond the reach of classical computers [1].

It is, in essence, the ability to control and use spin in electronic devices which fundamentally changes the way in which information can be processed and stored — a point that can lead to the realization of the next generation of high-performance and energy-efficient devices. The promise of integrating spintronic components in conventional electronic systems is revolutionary when it comes to the capability of the electronics industry to bring major improvements in computing, storage, and communication technologies.

1.2 History of Spintronics Development

Since its discovery, spintronics has progressed tremendously and has witnessed a number of principal discoveries and technological advances. For example, one of the most important is the discovery of GMR by Baibich et al.[5] and Binasch et al. [6], which established the usability of the spintronic effect in traditional electronic circuits. Fig. 1.1 shows the applications of spintronics in various fields [7]. The GMR-based read heads became the standard for hard disk drives, expanding data storage capacity at an enormous rate. This, in turn, led to the wide application of spintronics devices in the consumer electronics market.

Following GMR, MTJs were developed, which again proved the potential success of spintronics. Moodera et al.[8] demonstrated large Tunnel Magneto Resistance (TMR) at room temperature, an important development in increasing the functionality and feasibility of Magnetic Random Access Memory (MRAM). MRAM is a type of non-volatile memory that employs the magnetic state of MTJs for information storage, which offers faster reading and writing times, better endurance, and lower power dissipation compared to conventional memory technologies. MRAM opened a new frontier in memory technology by providing a reliable and efficient alternative to existing memory solutions.

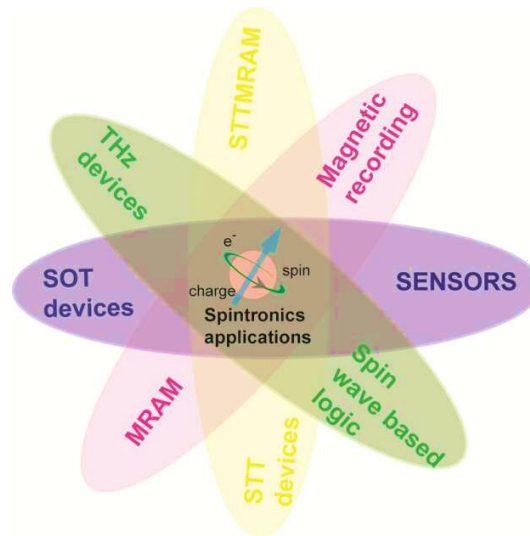


Fig. 1.1 Present and future applications of spintronic devices

Second, but very essential to the field of spintronics, was the well-documented discovery of the spin Hall effect by Kato et al.[9]. The devices based on this effect are more efficient for applications related to spintronics because spin currents can be generated without an externally applied magnetic field. After this discovery, it was much easier to develop new spintronics materials and subsequently integrate them into conventional semiconductor technology. The spin Hall effect did open up new routes toward the realization of electrically controllable spintronic devices, hence enhancing the potential applications of spintronics.

Another breakthrough in the development of spintronics was the exploration of materials known as topological insulators. Topological insulators are materials that present insulating characteristics in bulk, while surface states support spin-polarized currents. Their surface states are protected through time-reversal symmetry, ensuring the perfect conduction of spin-polarized currents with no dissipation. That makes topological insulators very promising materials for applications in spintronics because they can support spin-polarized currents with less energy loss [10].

The discovery of two-dimensional (2D) materials such as graphene and Transition Metal Dichalcogenides (TMD) has again put new life into spintronics research programs. These materials possess excellent electronic and spintronic properties, including tunable bandgap, high carrier mobility and strong spin-orbit coupling. 2D materials are unique in their properties and stand as ideal candidates for next-generation spintronic devices with enhanced performance features [11].

The continuous evolution of spintronic materials and devices will solve the most critical challenges in modern electronics, thereby leading to next-generation technologies. Spintronics, combined with other advanced technologies, such as

quantum computing and neuromorphic computing, can change information processing and storage, which will mean various unprecedented developments.

1.3 Importance and Potential of Spintronics

In principle, the prospective uses of spintronics are innumerable and multifarious, ranging from data storage and magnetic sensing to quantum computing and advanced communication systems. In such domains, the potential added value that spintronic devices can bring concerning performance, efficiency, and functionalities is immense.

1.3.1 Data Storage and Memory

Spintronic devices, like MRAM, come up with solutions for non-volatile memory in which read and write times are improved, endurance is high, and power consumption is low compared to traditional memory technologies. Such advantages make spintronic memory devices quite suitable for a wide variety of applications, starting from consumer electronics to high-performance computing systems [12]. The non-volatility feature of MRAM makes it particularly essential for applications requiring the integrity of data and speed. Moreover, the scalability of this technology will further perpetuate the relevance of MRAM in high-density memory applications in the future as well.

1.3.2 Magnetic Sensors

Giant magnetoresistive and tunnel magnetoresistive spintronic sensors find extensive uses in hard disk drives, automotive systems, biomedical devices, and so on. Such sensors exhibit a high level of sensitivity, stability, and potential for miniaturization; therefore, they are quite suitable for magnetic field detection in various environments [3]. High sensitivity and high precision are two critical properties of medical imaging and automotive safety systems. The fact that these sensors can be miniaturized without losing their performance makes them very useful in the development of compact and portable diagnostic tools.

1.3.3 Quantum Computing

Spintronics enables quantum computing technologies. The electron spin permits the realization of qubits in a very efficient and scalable way. This would yield very high coherence times and fidelity of operations from spin-based qubits with unique properties of spin, making them useful for practical quantum computing [13]. This manipulation at the quantum level of spin will further give way to radical computing power and efficiency, surmounting traditional computing capabilities. Through quantum mechanics combined with the principles of spintronics, quantum spintronics promises new paradigms in information processing and communication.

1.3.4 Advanced Communication Systems

Spintronic devices can be used to develop advanced communication systems, exploiting the spin degree of freedom for information transfer. Spin-based communication technologies have huge potential to deliver higher data rates, improve security, and bring down power consumption in comparison with traditional electronic communication systems; this becomes very relevant in the backdrop of ever-increasing data demands and the quest for more secure and efficient channels of communication[14]. Spintronic components, if integrated into communication systems, might improve data integrity and transmission efficiency in answering the rising challenges in modern communication networks.

The broad applicability and potential of spintronics point toward its role as a transformative technology. Overcoming some of the challenges and exploiting some of the unique properties attributed to spin could mean that spintronic devices will set a basis for new generations of technologies in many multidisciplinary fields. Further development and integration of spintronics technologies into a variety of applications is expected to change the face of information storage, processing, and communication in the future of electronics and information technology.

1.4 Motivation

The main motivations behind the present work are driven by the promise of spintronics to revolutionize the platform of electronic devices and circuits that can be achieved through high spin polarization in novel materials. After many years of research and development, a few issues still remain, among which determining and optimizing materials that can achieve strong spin polarization at room temperature are two of the most demanding problems.

The growing demands for high-performance electronic devices make the search for new materials with improved spintronic properties very relevant. Traditional materials like silicon and germanium have weak performance in spintronics due to their weak spin-orbit coupling and low spin polarization. This boosts the interest in finding alternative materials that could be developed to help surmount these limitations and produce better performances in spintronic applications.

1.4.1 Silicon Carbide Nanotubes and Spintronics:

Silicon carbide nanotubes (SiCNTs) are a class of promising materials merged with the excellent properties of both silicon and carbon. Nanotubes have huge mechanical strength, chemical stability, and tunable electronic properties; therefore, they can be suitable for many technological applications, including spintronics. Theoretical studies have shown that the adsorption of transition metals onto CNTs can induce magnetism;

hence, materials that are otherwise non-magnetic become potential candidates for spintronic devices [15]. Therefore, the influence of adsorption of transition metals on the electronic and magnetic properties of SiCNTs is very important to investigate if they are to be optimized for use in spintronics.

The ability to modify spin properties of SiCNTs by transition metal adsorption does open new routes toward advanced spintronic devices. For example, magnetism induced into SiCNTs can raise their spin polarization and make them usable for MTJs and spin valves. Such characteristics can be realized with higher performance parameters of magnetoresistance and thermal stability than those afforded by traditional spintronics materials [16].

1.4.2 Black Arsenic Phosphorus and Spintronics

b-AsP is a relatively new class of 2D material that has more recently come up as a potential candidate for spintronics. Apart from having some structural similarity with black phosphorus, it incorporates arsenic atoms modulating the electronic and magnetic properties. This makes b-AsP an ideal candidate for exploring new avenues in spintronics research due to its unique properties, such as tunable bandgap and high carrier mobility [17].

This is a spin-driven semiconductor material with potential applications in modern spintronics; hence, the incorporation of transition metals in b-AsP can introduce magnetic properties into it. The doping of transition metals has been found to bring about impressive changes in the electronic and magnetic properties of b-AsP, making it potentially suitable for spintronic devices [18]. In this investigation, researchers have attempted to discover new opportunities for developing state-of-the-art spintronic devices with enhanced performance and functionality by exploring the interaction between transition metals and b-AsP.

Research into materials with particular spintronic properties is a consequence of the bottleneck in the applications of currently available technologies that have to meet the ever-growing demands for faster, more efficient, yet reliable electronic devices. Considering the interaction between transition metals and novel materials such as SiCNTs and b-AsP, this research aims to tackle the challenges that exist in achieving high spin polarization and, hence, boosting the performance of spintronic devices. It may realize new materials and technologies that will advance the current possibilities in spintronics.

1.4.3 mCell Technology

The rapid advancement of integrated circuit (IC) technology, driven by Moore's Law, has reached a critical juncture where traditional CMOS scaling faces significant

physical and economic barriers. This necessitates the exploration of alternative technologies that can sustain the momentum of innovation in electronics. Among the promising candidates is magnetic logic technology, particularly mCell-based logic circuits. mCell technology represents a novel approach to designing digital circuits by exploiting the spintronic properties of magnetic materials, specifically leveraging current-driven magnetic devices for non-volatile logic and memory applications [19].

mCell, or magnetic cell technology, integrates the principles of spintronics into a four-terminal device capable of isolated read and write operations. This isolation between read and write paths is a significant advantage over traditional magnetic memory elements, as it mitigates the issues related to current sneak paths, thereby enhancing the reliability and scalability of the circuits. The fundamental operation of a mCell relies on manipulating the magnetization state of a ferromagnetic material using spin-transfer torque (STT) or the spin Hall effect (SHE) [20].

The potential applications of mCell technology are vast, ranging from non-volatile memory elements to logic circuits. In memory applications, mCells can be used to design all-magnetic MRAM bitcells, eliminating the need for CMOS transistors and enabling ultra-low power operation. In logic circuits, mCells can be arranged in current-steering networks to perform complex computational tasks with high energy efficiency and reduced voltage requirements. The inherent non-volatility of mCells also makes them ideal for applications requiring persistent state retention, such as in power-constrained environments and portable devices.

mCell technology can be integrated with other spintronic devices to enhance their functionality and performance. For example, combining mCells with magnetic tunnel junctions (MTJs) can result in highly efficient memory and logic elements with superior data retention and low power consumption. The compatibility of mCells with existing semiconductor fabrication processes further facilitates their adoption in a wide range of electronic applications, paving the way for next-generation computing and data storage solutions.

1.5 Research Gaps

Despite the progress being made in the field of spintronics, there exist several vital gaps that have to be filled if this technology is to keep on evolving. These research gaps are the foundations of all objectives of this study:

1. Finite Spin Diffusion Lengths and Defects: A number of already reported MTJs use insulating oxides and carbon-based nanotubes as tunnelling barriers. However, in most instances, the performance of these junctions is still limited by finite spin diffusion lengths and defects that generally impact the overall efficiency and reliability of the devices. Overcoming such limitations really requires an understanding of

mechanisms impacting spin diffusion and, indeed, new materials that have an improved spin-transport property [21].

2. Low Energy Density of Current 2D Materials: Due to the low energy density associated with conventional 2D materials such as graphene, there has been an increased demand for new storage technology and electronic devices. This limitation has thus raised the chances of the quest for new alternative materials with better performance characteristics. All these are necessary due to the ever-increasing demands of modern electronic devices, which call for higher energy densities and still require new materials [22].

3. Bias-dependent decrease in TMR: MTJ with high TMR is a desirable property. Unfortunately, TMR decreases with increasing bias, which further decreases other desired properties, such as spin polarizing efficiency. It is thus challenging to confront this decline in performance under operating conditions. Understanding factors that lead to this decrease and developing ways to circumvent such problems is very important in improving MTJ's performance [16].

4. Temperature Sensitivity of MTJs: It reduces the spin polarizing efficiency of MTJ at a high temperature, hence rendering them temperature sensitive. This, therefore, limits their application in areas where there is a variation in temperature, and stable performance is a must. The main challenges in this device involve developing materials and a structure that would increase spin polarizing efficiency over a broad temperature range [21].

5. Non-magnetic nature of pristine SiCNT and black AsP: Materials such as SiCNT and black AsP possess very good properties such as tunable band gap and are thermally stable, and thus they can be used as electrodes for spintronic devices, including MTJs. However, they are non-magnetic in their pristine form, and that hinders their direct application in a spintronic feature. Therefore, more investigations must be done to develop methodologies to induce magnetic properties, such as transition metal adsorption in these materials, to be useful in spintronic applications [23], [24].

6. Limited Studies on Transition Metal Adsorption: Very few theoretical studies have been conducted on the effect of transition metal adsorption on tunable bandgap materials. These new materials can be designed with enriched properties in spintronics only if the interaction is well understood. Extensive studies on the adsorption of transition metals and their effects on the electronic and magnetic properties of materials like SiCNT and b-AsP are, therefore, needed if the full potential is to be brought out in this regard [18].

These gaps need to be filled to develop a basic understanding required for further growth in the field of spintronics and to advance the effectiveness, reliability, and

efficiency of spintronic devices. It is hoped that through due attention to these most relevant areas, the investigation reported will help develop next-generation spintronic technologies capable of overcoming the limitations of present devices.

1.6 Research Objectives

The intention of the major research is to find whether transition metal adsorption can modulate the electronic and magnetic properties of SiCNT and b-AsP to become promising materials for spintronics applications. These can be further broken down into the following specific research objectives.

1. To study the effect of adsorption of transition metals on pristine SiCNT using density functional theory: This objective seeks to understand, using density functional theory, how different transition metal adsorptions affect the electronic and magnetic properties of pristine SiCNTs. The variation in the electronic structure and magnetic moments caused by the adsorption of transition metals is going to be identified. It will, therefore, provide insight into the potential of SiCNTs as spintronic materials and help in the development of device architectures that are optimized for such applications.

2. To investigate the effects of adsorption of transition metals on SiCNTs by varying their chirality and find its application in designing spintronic devices: The present work aims to study the effect of chirality on the adsorption process and its resulting spintronic properties to identify configurations that can be used in designing spintronic devices. The research will investigate various chiralities of SiCNTs to determine how they impact spin polarization and magnetic properties. This study will provide valuable insights into the role of chirality in enhancing spintronic properties, thereby guiding the design of more efficient spintronic devices.

3. To study the effect of adsorption of transition metals on pristine AsP and find its utilisation for spintronics devices: These changes are looked at with the influence of transition metal adsorption on pristine black arsenic phosphorus to ascertain its possible application in spintronic devices. The said work will include studying the electronic and magnetic properties of b-AsP before and after the adsorption of transition metal to identify any enhancements in the spintronic performance. This work aims to set a basis for b-AsP to represent a material potentially feasible for spintronic devices and lay the basis for further research into b-AsP applications.

Therefore, the present research presents an understanding of the interactions of transition metals with SiCNTs and b-AsP, which can be used for the development of spintronic devices in the future. It is believed that the result of the present work would be helpful in overcoming the prevailing difficulties in spintronics and opening new ways to technological revolutions.

1.7 Thesis Organization

The thesis consists of six chapters, which focus on integral parts of the research objectives. The structure of the thesis is as follows:

Chapter 1: Introduction: This chapter provides a background study reviewing the basics of spintronic technology, the importance of the research study, motivation, research gaps, research objectives, research questions, and the structure of the thesis. In summary, this chapter sets the stage for all other chapters by introducing the major concepts and outlining research objectives.

Chapter 2: Literature Review: This chapter presents a review of the current research in areas of spintronics, SiCNT, b-AsP and the role of transition metals in inducing spin polarization. It provides the background necessary for understanding the research gaps and objectives of this study. It summarizes the major and principal research works executed within the scope of these areas, points out the gaps in existing knowledge, and locates the current research in relation to that background.

Chapter 3: Transition Metal Induced- Magnetization In Zigzag SiCNTs: This chapter gives a report on investigating the impact of transition-metal adsorption on the electronic and magnetic properties of zigzag SiCNTs using DFT calculations. It details the methods used, presents the findings, and discusses the implications of these findings for spintronics applications.

Chapter 4: Transition Metal-Induced Magnetization And Spin-Polarization In Black Arsenic Phosphorus: This chapter presents investigations into the effects of transition metal adsorption over b-AsP and also addresses its potential application in spintronics. The results of DFT calculations have shed light on changes in electronic and magnetic properties of b-AsP upon transition metal adsorption. It provides a comprehensive analysis of the interaction of transition metals and b-AsP and their potential for spintronic applications.

Chapter 5: Implementation of Fault-Tolerant Arithmetic Logic Unit using mCell: In this chapter, a novel design for a fault-tolerant ALU using mCell-based logic has been proposed and simulated. The proposed ALU design integrates PPRG logic, which ensures energy-efficient and error-detection capabilities by maintaining parity during computational operations. This chapter details the implementation of ALU using various basic and complex logic gates using mCell, including NOT, NAND, NOR, AND, OR, and PPRG-based full adders using Cadence Virtuoso. The study concludes that mCell-based logic circuits, with their non-volatility, low power consumption, and high-density integration, hold promise for future applications in spintronic devices, including magnetic memories, hybrid FPGAs, and non-volatile flip-flops.

Chapter 6: Conclusion, Future Scope and Social Impact: The final chapter summarizes the key findings of the research on the adsorption of transition metals on zigzag SiCNT and b-AsP, highlighting significant contributions to the field of spintronics. The chapter also explores the implementation of fault-tolerant ALUs using mCell technology, underscoring its advantages over traditional CMOS technology. Future research directions are proposed, focusing on experimental validation and the exploration of new transition metals. Finally, the chapter discusses the potential social and environmental impacts of these advancements, emphasizing their benefits for data storage, consumer electronics, economic growth, and sustainability.

Chapter 2

LITERATURE REVIEW

2.1 Introduction

Spintronics, from the terminology 'spin electronics', is a new field of research into the functionality of electronic materials based on the intrinsic spin of electrons and their associated magnetic moments in addition to their fundamental electronic charge. It would complement conventional electronics with spin degrees of freedom, hence potentially higher processing speeds and lower power consumption. Therefore, one of the core ideas driving spintronics is the manipulation of spin currents in a very large variety of materials that turn out to be quite important in applications related to data storage, sensing, and quantum computing [25].

The devices associated with this area of spintronics function based on the spin-dependent transport of electrons, which may be controlled by external magnetic fields or spin-polarized currents. One of the primary discoveries in this domain is GMR, which fundamentally changed data storage technologies by making possible the development of very sensitive read heads in hard disk drives [3]. Since the discovery of GMR, huge steps forward in understanding and manipulation of spin currents have been realized, including MTJs, spin valves, and other components for spintronics.

The power of spintronics lies beyond conventional electronics in solving some of the most pressing challenges that modern technology faces. By making use of the spin degrees of freedom, spintronic devices can achieve non-volatile memory states that do not require power to hold information, unlike conventional Random Access Memory (RAM). This becomes particularly advantageous while trying to develop energy-efficient computing systems. Moreover, spintronics can contribute to quantum computing by utilizing spin qubits in information processing to deliver utterly new computational powers and speeds [2], [13].

2.2 Early Developments and Key Concepts

The discovery of the GMR effect by Albert Fert and Peter Grünberg, working independently at the end of the 1980s, marked a milestone in the development of spintronics. GMR means that under an external magnetic field, a large change of electrical resistance exists in magnetic multilayers. This effect is that when two ferromagnetic layers are separated by a non-magnetic conductive layer, the resistance of the structure depends on whether the magnetic moments of the ferromagnetic layers are parallel or antiparallel. This discovery opened real ways for the creation of very

sensitive magnetic sensors and read heads for hard disk drives that would boost the then-existing data storage technology diagnosed [2], [14], [26].

Soon after the discovery of GMR, research in this field became focused on mechanisms involved in GMR and enhancing spintronic device efficiency. One very important development in this context was MTJ. MTJs basically consist of two ferromagnetic layers separated by an insulating barrier, normally magnesium oxide (MgO). The current that tunnels through the barrier are extremely sensitive to the relative orientation of the magnetizations in the ferromagnetic layers. Under these circumstances, when the magnetizations are parallel, the resistance is low, and when they are antiparallel, the resistance is high, leading to TMR [16]. This property is used in magnetic random access memory and read heads for hard drives. While offering great promise, MTJs using oxides and carbon-based nanotubes for the tunnel barrier generally had to contend with a finite spin diffusion length and defects that further degraded performance. The finite spin diffusion length denotes the distance over which spin information can be conveyed without large losses; with defects, however, scattering sites are introduced that further lower the values of spin coherence and polarization. These limitations also necessitate seeking other alternative materials with better spin transport properties and fewer defects.

The discovery of half-metallic ferromagnets has taken the entire concept of spintronics to a new level. These materials have a special property in that they act like conductors for electrons of one spin orientation and like insulators or semiconductors for electrons of opposite spin. This means that nearly 100% of the spin is polarized at the Fermi level, making them good for efficient spin injection in spin-based devices. For instance, well-studied half-metallic ferromagnets are chromium dioxide (CrO_2) and magnetite (Fe_3O_4), which have a strong suitability for spintronics applications. High spin polarization in these materials enhances the performance of devices like spin transistors and spin valves used in spintronics [27], [28].

Another key development in spintronics is the research on carbon-based materials, particularly in carbon nanotubes (CNTs) and graphene. Indeed, the pristine mechanical and electrical properties of carbon nanotubes have already been harnessed in several spintronic applications. For example, MTJs using carbon nanotubes are very promising since they have long spin coherent lengths and low spin-orbit coupling. It has been shown that filling CNTs with transition metals such as cobalt can give rise to huge magnetism, making them very suitable for spin transport and polarized applications [29]. The unique properties of the CNT, therefore, open up new views on the development of efficient and viable spintronic devices.

Graphene, a single layer of carbon atoms in a hexagonal lattice, has lately attracted much attention in the field of spintronics due to its high carrier mobility and long spin diffusion lengths. The combination of graphene with ferromagnetic materials has

resulted in graphene-based spintronic devices exhibiting improved performance. They showed promising results for graphene-based spin valves and spin transistors, proving that graphene can be a game-changer in spintronics technology. This concept—the ease of control of the spin currents in graphene by external magnetic fields and gate voltages creates new perspectives for developing advanced tunable spintronics devices [30].

The integration of transition metals with carbon-based materials further broadened the scope of spintronics. Transition metals like cobalt, nickel, and iron combined with carbon nanotubes or graphene exhibit huge enhancements in magnetic properties and spin polarization. For instance, high spin polarization at the Fermi level and large magnetic moments have been identified in cobalt-filled CNTs, a feature that can be quite relevant for spintronics applications. Besides having very good spin transport properties, these hybrid structures also manifest scalability and compatibility with conventional semiconductor technologies, which would, therefore, make them quite appealing for any future spintronic device [31].

A major development in spintronics has been the improvement of techniques for measuring and controlling spin polarization. In this direction, most of the preliminary efforts were made to unravel the principles underlying the transport of spins and how they could be maximized in various materials. This resulted in the study of several ferromagnetic materials and their interfaces with non-magnetic materials. The key challenges to be met in this context were the creation of materials and structures capable of retaining high spin polarization over practical distances and at room temperature. Progress in materials science, especially in the growth of high-quality thin films and in control of their precise composition and interfaces, was essential to achieving this progress [3], [32].

The early part of 2000 saw formidable advances made in the integration of spintronic components with conventional semiconductor technology. This integration was imperative in the functioning of spintronics devices within consumer electronics. One of the major breakthroughs was in the development of spin transistors; these are the current flow controllers based on the spinning of electrons. Unlike conventional transistors that are controlled by charges, spin transistors consume low power and high switching speed. It became possible due to advances in material science, for example, the creation of high-quality ferromagnetic contacts and the possibility of precise control over spin injection and detection [33], [34].

On the other hand, spintronics benefited tremendously from theoretical advances. Computational models and simulations gave profound insights into the behaviour of spin currents and the interaction of spin with different materials. Those have been instrumental in predicting new phenomena and guiding experimental research. For example, studies on the electronic structure and magnetic properties of spintronic

materials have been done pretty well using functional density theory. Theoretical prediction will, in general, open the pathway to discover new materials and optimize existing ones for better performance in spintronics devices [16], [30], [35], [36], [37], [38], [39].

The latest research has been directed toward developing new materials with improved spintronic properties. Particularly promising materials are the TMDs and topological insulators. Compounds like MoS₂ and WS₂ in TMDs have peculiar electronic and optical properties, which can be modulated by compositional and thickness variations. In such materials, strong spin-orbit coupling was observed, making them suitable for applications in spintronics. On the other hand, topological insulators have time-reversal symmetry-protected surface states, resulting in robust spin-polarized surface currents. These materials open a new path to higher-efficiency and higher-functionality spintronic devices [18], [40], [41].

Another emerging trend in the field of spintronics is related to the prospects of research into spin caloritronics, which studies the interplay between spin and heat currents. It involves the development of devices that can directly transform thermal energy into spin currents and vice versa. The field of spin caloritronic devices might open new routes to thermal management in electronic devices or lead to more efficient ways of energy harvesting. For instance, the spin Seebeck effect, a spin voltage generated by the temperature gradient, is seen in a large number of compounds being considered for practical application [40], [42].

The various early developments and key concepts of spintronics have laid a robust foundation in the field. The discovery of the GMR effect, the development of MTJs and HMF, and research on carbon-based materials like CNTs and graphene have dramatically advanced the understanding and capability to manipulate spin currents for a wide range of applications. Such successes further enable a new generation of spintronic devices with better performance, scalability, and energy efficiency, thus potentially redefining data storage, sensing, and quantum computing technologies.

2.3 Spintronic Device Applications

2.3.1 Magnetic Random-Access Memory

MRAM is the most promising application of spintronics technology. MRAM uses magnetic states for storage; hence, it offers a host of advantages that include non-volatility, high speed, and endurance. The core component of the MRAM is the MTJ, which comprises two ferromagnetic layers separated by an insulating barrier. The resistance of the MTJ depends on the relative alignment of the magnetizations of the ferromagnetic layers and hence can be utilized for binary data representation [16], [36].

Significant advancements were made with the development of spin-transfer torque MRAM technology. STT-MRAM technology uses the spin-transfer torque (STT) effect to postulate that a spin-polarized current can induce switching of the magnetic state of a ferromagnetic layer without the use of an applied magnetic field. This translates into lower power consumption and very high speed in writing compared to traditional MRAM. Recent investigations have led to the development of STT-MRAM, demonstrating its effectiveness for high-density memory applications that require low power consumption [41], [43].

2.3.2 Magnetic Tunnel Junction (MTJ)

An MTJ consists of two magnetic layers separated by a thin insulating tunnel barrier, typically an oxide (Fig. 2.1). One magnetic layer is designed to be 'hard' to switch; that is, it has a fixed magnetization and is called the reference layer. The other magnetic layer is engineered to switch more easily with externally applied magnetic fields or currents and is called the free layer. The key principle behind MTJ operation is the tunnelling magnetoresistance (TMR) effect, where the electrical resistance of the junction varies based on the relative alignment of the magnetizations in the two ferromagnetic layers. The MTJ's conductance depends on the relative orientation of magnetization in the free and reference layers. In the case of their parallel orientation, MTJ exhibits low resistance; otherwise, it shows high resistance when the magnetizations are antiparallel [19].

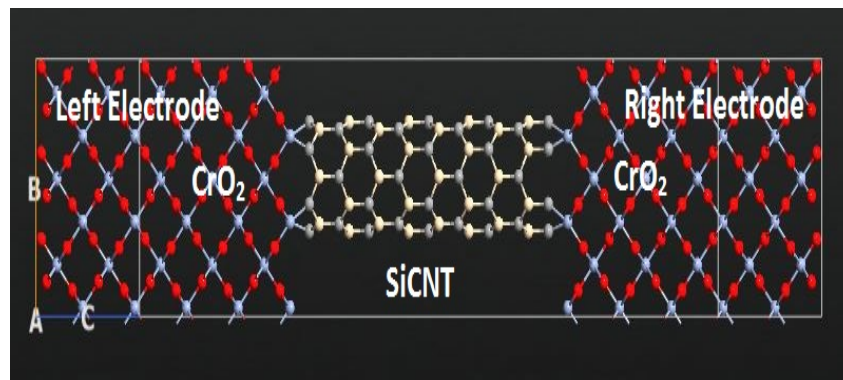


Fig. 2.1 MTJ consisting of carbon nanotube sandwiched between left-right CrO_2 HMF electrodes

The tunnel magnetoresistance (TMR) ratio, which measures the change in resistance from the low state (R_P) to the high state (R_{AP}), is given by:

$$TMR = \frac{R_{AP} - R_P}{R_P} \quad (2.1)$$

TMR turns out to be the differences in the electron density of states at the Fermi level for majority and minority spins. Since electron spin is conserved during tunnelling, electrons can tunnel only into states having the same spin orientation. That means the tunnelling conductance depends on the product of the density of states at the Fermi level: large when there are many states available for tunnelling on both sides of the barrier—parallel magnetizations—and low when fewer states are available—antiparallel magnetizations [36].

This bistable resistance state enables MTJs to serve as memory elements in MRAM, providing non-volatility, high endurance, and fast read/write speeds. MTJs are pivotal in the advancement of spintronic technologies, offering advantages in data storage density, power efficiency, and integration with existing semiconductor technologies, making them ideal for applications in next-generation memory devices, sensors, and logic circuits [41]. Recently, many MTJs have been simulated using CNTs and SiCNTs as the insulating layer, providing a very high TMR value of nearly 100% [16], [36].

2.3.3 Spin-Field Effect Transistors (Spin-FET)

A more significant application in the field is in spin-field effect transistors, or Spin-FETs, which are devices that can replace conventional transistors in normal electronic devices. Unlike conventional transistors, wherein the current flow is modulated by charges, Spin-FETs modulate the flow of electrons depending on their spin, which means that these devices possess the potential to conduct at much lower powers as well as switch at faster speeds. The principle of a Spin-FET is injected with spin-polarized electrons in a semiconductor channel whereby the spin orientation is controlled by the gate voltage.

The development of Spin-FETs has been driven in large part by advances in material science and spin injection techniques. Proposing the first theoretical model for Spin-FETs, pioneers in this area have proven that it is feasible to integrate spintronic devices with the existing technology [44]. Their work laid a foundation for experimental studies, which have lately shown successful spin transport and manipulation inside semiconductor channels.

Recently, there has been increased research focused on efficiently achieving spin injection and detection in Spin-FETs. Among the structures that have been developed are the integration of high spin-polarized materials, HMF, and TMD, which hold great

promise for enhancing Spin-FET performance [33], [45], [46]. Recent investigations show that it has been possible to realize efficient spin injection with the use of ferromagnetic contacts, and this has since opened the possibility of producing practical devices based on spin-FET.

2.3.4 Spin-Valves and Spin-Torque Oscillators

The simplest spintronic devices from which a vast majority of devices are built are known as spin-valves. Examples include read heads used in hard disks and magnetic sensors. A spin-valve consists of a sandwich-like structure – two ferromagnetic layers separated by a non-magnetic spacer [21]. The resistance of the spin-valve changes based on the relative orientation of magnetizations in the ferromagnetic layers with respect to one another – the same working principle as MTJs. This is used to sense magnetic fields and attempt to read data from magnetic storage media [47].

Another exciting application of spintronics is spin-torque oscillators (STO). STOs generate microwave frequencies due to the effect of spin-transfer torque, whereby a current polarized in spin causes the precession of magnetization in a ferromagnetic layer. Because of this, it can be used to make tunable microwave oscillators for telecommunications and sensing applications [48], [49].

2.3.5 Quantum computing and spin-qubit technology

Quantum computing is an emerging field that leverages quantum mechanical principles to carry out calculations that are infeasible with conventional computers. Qubits based on spin represent one of the possible avenues to implement such a quantum computer and are generally referred to as spintronics, which is the ultimate end of science. Here, spin qubits use the spin state of either an electron or a nucleus as a fundamental unit of information, possibly offering advantages such as long coherence times and compatibility with pre-existing semiconductor technologies [13].

The coherence time of spin qubits has undergone tremendous improvement over the past years, and schemes for reliable spin manipulation and readout have been established. Gate-defined quantum dots and nitrogen-vacancy centers in diamonds have already resulted in very encouraging results in the operations of high-fidelity spin qubits [50].

2.3.6 Spin Caloritronic and Energy Harvesting

Spin caloritronic is a type of emerging field that considers the interaction of spin with heat currents. The field is aiming to realize devices that will convert thermal energy into a spin current, and vice versa, in what could be a new means for handling heat externally from electronic devices, thus furthering energy efficiency [40]. A key factor

in blade efficiency is the so-called spin Seebeck effect, where a gradient in temperature yields a spin voltage.

Dr. Uchida and Dr. Saitoh are leading researchers in the field of spin caloritronics. They have demonstrated the spin Seebeck effect in various materials and explored its potential applications. Their research shows that spin caloritronic devices can be used for energy harvesting, converting waste heat into electrical energy, and for the thermal management of electronic devices [51].

This development of spin caloritronic devices will have a huge impact on a new generation of energy-efficient technologies. For example, thermoelectric generators that are based on the spin Seebeck effect have a huge potential to power low-energy sensors and devices, which would help reduce the reliance on batteries in electronic systems and make them more sustainable. Spin caloritronic cooling systems offer new ways of managing heat within high-performance electronic devices to enhance their efficiency and reliability [52].

2.4 Materials for Spintronic Device Applications

2.4.1 Carbon Nanotubes

CNTs are a potential material in which spintronic applications can be realized due to their excellent mechanical, electrical, and thermal properties. CNTs are cylindrical nanostructures consisting of rolled-up graphene sheets, which promote special electronic properties such as metallic or semiconducting behaviour, depending on their chirality and diameter. Their large aspect ratio, high conductivity, and ability to transport spin coherently over long distances make them perfect candidates for applications in spintronics [53].

Much research has been done on the integration of transition metals into CNTs for the enhancement of their magnetic properties and spin polarization. Transition group metals, such as cobalt, nickel, and iron, show really high magnetism when filled into a CNT. For instance, cobalt-filled CNTs show strong spin polarization at the Fermi level and a large magnetic moment, which are two basic needs that a spintronic device should meet in order to perform successfully and effectively [29], [31]. This enhancement will be in the magnetic properties due to strong hybridization between the transition metal d orbitals and carbon atom π orbitals in the CNT, resulting in the formation of a robust magnetic structure.

Recent research regarding the magnetic properties of transition metal/CNT structures suggests their use in spintronics. It has been demonstrated that CNTs on doping/adsorption with transition metals induce magnetism and, therefore, are suitable

for applications in spin-polarized devices. These findings underscore the importance of material integration in enhancing the performance of spintronic devices [15].

The further ability to maintain long spin coherence lengths in the presence of low spin-orbit coupling additionally makes CNTs promising for spintronics. It has been reported that the use of CNTs in MTJs as one of the electrodes also acquires promising results in terms of high spin polarization and efficient spin transport properties. These qualities make CNTs a very promising material in developing next-generation spintronics devices such as spin transistors and spin valves, which require high performance and scalability [21], [36].

Even though CNTs exhibit high spin coherence lengths and low spin-orbit coupling (SOC) at the same time, some of their properties limit their usability in this field. In particular, the presence of finite spin diffusion lengths and defects limit their suitability for spintronics applications. This has led to the need for alternative materials that can offer superior spin transport properties with effective defect management [16].

2.4.2 Silicon Carbide Nanotubes

SiCNTs, because of their remarkable structural, electronic, and magnetic properties, maybe a promising material for the realization of spintronic applications. SiCNT resembles CNT in structure but is made of silicon and carbon atoms. Apart from these, there are other advantages over CNT, such as better thermal stability and chemical resistance, which make the material well-fit for high-performance applications in extreme environments [27]. This is interesting because it has been shown that SiCNTs are rich in morphology and can show huge differences in their electronic and transport properties depending on their structural configuration. DFT calculations have revealed different chiralities of SiCNTs, and through them, different electronic properties have been found. Some of them have semiconducting behaviour, but others have metallic behaviour. This tunability in electronic properties makes SiCNT a versatile material for spintronic applications [54], [55].

The integration of transition metals into SiCNTs has been a key focus of research to enhance their magnetic properties and spin polarization. Transition metals such as chromium, iron, and cobalt, when incorporated into SiCNTs, induce strong magnetic moments and high spin polarization. Dr. Ernst Richter's work on the structural and electronic properties of SiCNTs has provided valuable insights into their stability and potential for spintronic applications. Richter et al. (2004) demonstrated that doping SiCNTs with chromium and iron significantly enhances their magnetic properties, making them suitable for next-generation spintronic devices [27].

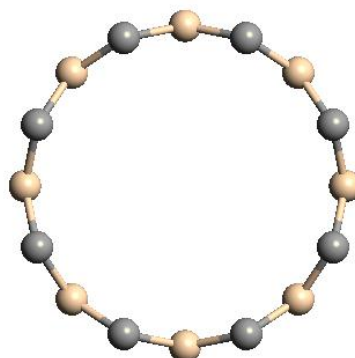


Fig. 2.2 Zigzag (4,0) SiCNT

The potential of SiCNTs in spintronic applications is further enhanced by their high thermal conductivity and mechanical strength. These properties make SiCNTs ideal for applications in high-performance electronic devices that require efficient heat dissipation and structural stability. The combination of these properties with enhanced magnetic behaviour through transition metal doping positions SiCNTs as a promising material for advanced spintronic technologies.

2.4.3 Two-Dimensional (2D) Materials

The concept of 2D crystalline materials dates back to 1962 when the surface characteristics of ultra-thin graphite layers were first documented. Following this, in 1963, researchers synthesized 2D MoS₂ and analysed its optical properties [56]. However, the pivotal breakthrough came with the successful isolation of graphene as a distinct 2D nanomaterial [57], which subsequently paved the way for the discovery of various other 2D structures [32], [58].

2D nanomaterials are characterized by their minimal thickness, typically only one or a few atomic layers. These layers can be composed of identical atoms, such as in graphene and black phosphorus, or different atoms, as seen in hexagonal boron nitride (h-BN) and TMDs [59], [60]. The extremely thin nature of these materials results in a high surface area-to-volume ratio, coupled with exceptional mechanical flexibility and optical transparency. Their notable mechanical strength is due to strong intraplanar covalent, metallic, or ionic bonding. Additionally, the confinement of electrons within two dimensions and the absence of electron scattering between layers impart unique electrical, thermal, and magnetic properties [58], [61]. These distinctive features make 2D nanomaterials ideal candidates for use in electronic and optoelectronic devices, supercapacitors, sensors, solar cells, electrocatalysts, and photocatalysts [62].

Two-dimensional (2D) materials have garnered significant interest in the field of spintronics due to their unique electronic, optical, and mechanical properties. Due to their brilliant features, They find numerous applications like gas sensing, rechargeable ion batteries and hydrogen storage. Presently, a lot of research is going on 2D materials like novel perovskites and Heusler alloys, as each material possesses unique characteristics that make it appropriate for a particular application [63]. The ability to engineer and manipulate these properties at the atomic level makes 2D materials highly suitable for spintronic applications [25].

In the field of spintronics, these research efforts can lead to the discovery of novel spintronic properties, allowing for the customization of features to meet specific needs. This can improve scalability and integration with existing technologies, thereby advancing the creation of highly efficient, cost-effective, and powerful spintronic devices. The integration of magnetic and semiconducting characteristics on a single chip has attracted significant interest in the field of condensed matter physics. To achieve the desired properties, researchers modify the characteristics of various 2D materials by employing techniques such as metal doping or adsorption [24], [63], [64], [65], [66], [67].

2.4.3.1 Graphene

Graphene is a widely recognized two-dimensional material composed of a single layer of carbon atoms organized in a hexagonal pattern. It exhibits exceptional electronic properties, including high carrier mobility, long spin diffusion lengths, and excellent thermal conductivity. These properties make graphene an ideal candidate for spintronic applications [32], [68].

Graphene's high carrier mobility allows for efficient electron transport, which is crucial for spintronic devices. Its long spin diffusion length, which can reach up to several micrometres at room temperature, enables the transport of spin information over long distances without significant loss of spin coherence. This property is particularly important for the development of spintronic devices such as spin valves and spin transistors, where maintaining spin coherence is critical for device performance [69].

The electronic properties of graphene can be further enhanced by introducing various types of defects or doping with other elements. For instance, the introduction of boron or nitrogen atoms into the graphene lattice can modify its electronic properties, making it more suitable for specific spintronic applications. Additionally, the application of an external electric field can induce a bandgap in graphene, which is otherwise a zero-bandgap semiconductor. This tunability of electronic properties makes graphene a versatile material for a wide range of applications [70], [71], [72].

While pristine graphene is non-magnetic, its magnetic properties can be significantly enhanced by doping with transition metals. The incorporation of transition into the graphene lattice can induce localized magnetic moments, leading to high spin polarization. This enhancement in magnetic properties is attributed to the interaction between the d-orbitals of the transition metals and the π -orbitals of the carbon atoms in graphene [69], [71], [72].

Recent studies have demonstrated that doping graphene with transition metals can significantly enhance its spintronic properties. For instance, the deposition of cobalt on graphene leads to the formation of robust magnetic structures, making it suitable for spintronic applications [30], [73].

Despite its exceptional properties, graphene also has limitations that affect its suitability for certain spintronic applications. One of the major challenges is its zero-bandgap nature, which limits its use in applications that require a semiconducting behaviour. While techniques such as doping and the application of electric fields can induce a bandgap, these methods often result in reduced carrier mobility and increased scattering, which can affect the overall performance of spintronic devices [74].

Another limitation of graphene is its relatively weak spin-orbit coupling, which makes it challenging to achieve efficient spin manipulation. While spin transport in graphene is efficient over long distances, the lack of strong spin-orbit interaction limits its ability to generate and manipulate spin currents effectively. This limitation has led researchers to explore other 2D materials with stronger spin-orbit coupling for advanced spintronic applications [75].

2.4.3.2 Transition Metal Dichalcogenides

TMDs are another class of 2D materials that have shown great promise for spintronic applications. TMDs, such as Molybdenum Disulfide (MoS_2) and tungsten disulfide (WS_2), exhibit unique electronic and optical properties that can be tuned by varying their composition and thickness. These materials have been shown to have strong spin-orbit coupling, making them suitable for spintronic applications [76].

TMDs exhibit a direct bandgap when in monolayer form, which is different from their bulk counterparts that have an indirect bandgap. This direct bandgap is crucial for optoelectronic applications, as it allows for efficient light absorption and emission. The strong spin-orbit coupling in TMDs leads to spin-split energy bands, which are essential for spintronic devices. This property enables the manipulation of spin states using external electric fields, making TMDs attractive for developing spintronic transistors and other devices [77], [78].

The electronic properties of TMDs can be further tuned by applying strain or electric fields. For example, applying strain to a monolayer of MoS_2 can significantly alter its

electronic band structure, making it possible to engineer its properties for specific applications. Similarly, applying an external electric field can control the spin and valley degrees of freedom in TMDs, enabling the development of advanced spintronic devices [76].

The magnetic properties of TMDs can be enhanced by doping with transition metals. Researchers have shown that incorporating transition metals such as chromium and manganese into the TMD lattice can induce strong magnetic moments, leading to high spin polarization. These doped TMDs exhibit robust magnetic properties, making them suitable for spintronic applications [79], [80].

Recently, many researches on TMDs have highlighted the potential of these materials for spintronic applications. His studies have demonstrated that doping TMDs with transition metals can significantly enhance their spintronic properties. For instance, doping MoS₂ with chromium results in a material with strong spin polarization and robust magnetic properties, making it suitable for developing spintronic devices [81], [82], [83].

Despite their promising properties, TMDs also face limitations that can affect their performance in spintronic applications. The major challenge with TMDs is their sensitivity to defects and impurities. The presence of defects can significantly affect the electronic and magnetic properties of TMDs, leading to reduced spin coherence and lower spin polarization. Ensuring high-quality material synthesis and minimizing defects are critical for optimizing the performance of TMD-based spintronic devices [39].

2.4.3.3 Black Arsenic Phosphorus

b-AsP is a layered material that exhibits excellent electronic and magnetic properties, making it a promising candidate for spintronic applications. This material consists of a mixture of arsenic (As) and phosphorus (P) atoms, and its unique structural configuration endows it with remarkable physical and chemical properties. When combined with transition metals, b-AsP shows high spin polarization and enhanced magnetic properties, which are essential for efficient spintronic devices [38].

b-AsP can exist in various allotropes depending on the arrangement of arsenic and phosphorus atoms. The α -phase, which consists of a honeycomb lattice structure, is one of the most stable configurations. In this configuration, the atoms are arranged in a way that forms a two-dimensional puckered layer, similar to black phosphorus but with the added complexity of arsenic atoms. The α -phase can further branch into different allotropes, such as α_1 , α_2 , and α_3 , each with distinct structural properties. The α_1 allotrope is the most stable among these phases. It features a direct bandgap semiconductor structure, which is beneficial for electronic and optoelectronic

applications. The $\alpha 2$ and $\alpha 3$ allotropes, while also showing promising properties, are less stable compared to $\alpha 1$. The stability of these allotropes is determined by the specific bond lengths and angles within the lattice, as well as the presence of any strain or external forces applied to the material [84].



Fig. 2.3 Black Arsenic Phosphorus

The $\alpha 1$ phase of b-AsP is characterized by alternating arsenic and phosphorus atoms arranged in a puckered structure. This phase exhibits a direct bandgap of approximately 1.63 eV at the Γ point, which is crucial for optoelectronic applications such as photodetectors and light-emitting devices. The bandgap can be tuned by applying strain, making it versatile for various technological applications

The electronic properties of the $\alpha 1$ phase are highly anisotropic, meaning they vary depending on the direction of the applied strain. This anisotropy is advantageous for designing devices that require specific directional properties. For instance, carrier mobility, which is a measure of how quickly electrons can move through a material, is significantly higher along certain crystallographic directions. This high carrier mobility enhances the performance of electronic devices, making the $\alpha 1$ phase of b-AsP particularly attractive for high-speed electronics [84].

The $\alpha 1$ phase also exhibits high thermal stability, which is essential for devices operating under high temperatures or in harsh environments. The strong covalent bonds between the arsenic and phosphorus atoms provide robustness against thermal degradation, ensuring long-term stability and reliability of the material in practical applications [38].

The magnetic properties of b-AsP, particularly in the $\alpha 1$ phase, can be significantly enhanced by doping with transition metals. Transition metal doping induces localized magnetic moments within the b-AsP lattice, which are crucial for achieving high spin polarization. When transition metals such as nickel, cobalt, or manganese are

incorporated into the b-AsP structure, they interact with the arsenic and phosphorus atoms, leading to the formation of robust magnetic moments. The research on the electronic structure and carrier mobility of 2D arsenic phosphide has been pivotal in understanding the potential of this material for spintronic applications. The studies have demonstrated that the incorporation of transition metals into b-AsP can lead to significant enhancements in electronic and magnetic properties, making it suitable for high-performance spintronic devices. The results also suggest that the electronic properties of b-AsP can be finely tuned by varying the composition of arsenic and phosphorus, as well as by applying strain. These tunable properties make b-AsP a versatile material for various spintronic applications [23], [84].

The thermal conductivity of b-AsP is another important property that makes it suitable for various applications. The lattice thermal conductivity of monolayer b-AsP has been investigated using first-principles molecular dynamics. These studies have shown that b-AsP exhibits relatively low thermal conductivity compared to other 2D materials, which is advantageous for thermoelectric applications where low thermal conductivity and high electrical conductivity are desired [38].

The mechanical properties of b-AsP are also noteworthy. The material exhibits high tensile strength and flexibility, making it suitable for flexible electronic applications. The puckered structure of b-AsP allows it to withstand significant mechanical deformation without breaking, which is essential for developing durable and reliable electronic devices [84].

2.5 Potential for Spintronic Applications

The high spin polarization in transition metal-doped b-AsP makes it a promising candidate for various spintronic applications. The tunable electronic properties of b-AsP, combined with its enhanced magnetic behaviour, position it as an ideal material for developing advanced spintronic devices. Applications include spin transistors, spin valves, and MTJs, where high spin polarization is crucial for efficient performance.

Additionally, the ability to maintain high spin polarization at room temperature further enhances the potential of b-AsP for practical spintronic devices. The integration of transition metal-doped b-AsP in spintronic devices can lead to improved performance in terms of spin injection, transport, and detection. These advancements underscore the importance of b-AsP in the future development of high-performance spintronic devices [23], [38].

In conclusion, b-AsP exhibits unique structural, electronic, and magnetic properties that make it a highly promising material for spintronic applications. The $\alpha 1$ phase of b-AsP, with its direct bandgap and high carrier mobility, stands out as the most stable and versatile configuration. The ability to enhance its properties through transition

metal doping and the application of strain further broadens its potential for various advanced technological applications. Continued research and development in this area are expected to lead to significant advancements in the field of spintronics, paving the way for new applications and improved device performance.

2.6 Summary

The literature review has covered the foundational concepts and advancements in the field of spintronics, focusing on key developments and materials that have significantly contributed to the progress of this technology. We began by exploring the early developments in spintronics, such as the discovery of GMR and the development of MTJs, which have been pivotal in enhancing data storage technologies.

We then delved into various spintronic device applications, including MRAM, MTJs, spin-FETs, spin-valves, STOs, quantum computing with spin qubits, and spin caloritronics. Each of these applications leverages the unique properties of spintronic materials to achieve high performance, efficiency, and scalability in practical devices.

The review also highlighted the significant role of transition metals in inducing high spin polarization in various materials. We discussed the integration of transition metals with CNTs, SiCNTs, graphene, TMDs, and b-AsP. The enhanced magnetic and electronic properties of these materials, achieved through transition metal doping, make them ideal candidates for advanced spintronic application

Chapter 3

TRANSITION METAL INDUCED MAGNETIZATION IN ZIGZAG SiCNTs

3.1 Introduction

In the last two decades, carbon nanotubes have opened a new world of possibilities for researchers and the semiconductor industry. They are considered promising candidates for designing nanodevices like nanosensors due to their high stability, unique electronic and mechanical properties and high-frequency response [34], [53].

The successful synthesis of the Boron-Nitride nanotube showed that nanotubes synthesized from other materials are also feasible [85], [86]. Later, silicon carbide nanotubes were also reported to be grown using the self-assembling technique [87]. These nanostructures showed very different and unique properties compared to their bulk forms due to their small size and tubular structure. The nanotubes could behave as metallic or semiconducting based on their chirality and diameter dimensions. Compared to CNTs, SiCNTs are more suitable in the electronics industry field due to their unique physical and electronic properties. Therefore, SiCNTs are more suitable for higher power, temperature, and frequency operations [27], [88], [89], [90]. The studies report that the nature of SiCNTs depends on the value of (n, m) , where n and m are the chirality vectors. The $(n, 0)$ nanotubes are identified as zigzag nanotubes, whereas (n, n) nanotubes are identified as armchair nanotubes. It also states that $(n, 0)$ i.e., zigzag SiCNTs for $n = (7, 9)$ are semiconducting in nature, and their bandgap increases with the value of the chiral vector n , whereas they are metallic for $n \leq 6$ [54], [91]. For the case of (n, n) , i.e., armchair nanotubes, SiCNTs are metallic for $n = 5$ and 6 but semiconducting in the range $n = (7, 10)$ with their bandgap decreasing with an increasing value of n . Due to these properties of SiCNTs, they make a very suitable material to be used as the channel in developing spintronic devices [16], [28].

Spintronic devices find their applications in designing programmable logic elements, magnetic sensors, MTJ and MRAM. When choosing an electrode material for a spintronic device, half-metallicity is the most important characteristic. Materials possessing half metallicity are highly selective to the spin orientation of the electron and, hence, are used as electrode material in the design of MTJs. The efficiency of an MTJ is decided by its property to allow/ block electrons of a particular spin (up/ down).

A very high ($\sim 100\%$) TMR was reported for an MTJ designed with CrO_2 as half-metallic electrodes and SiCNT as the channel [16].

SiCNT in intrinsic form is non-magnetic in nature. For the SiCNT to be used in spin-dependent transport, it is highly desired that the SiCNT should itself be made spin-polarized. It has been implemented for the CNTs by either doping the nanotube with transition metals or adsorption of transition metals on the surface of the CNTs [29]. Recent studies have demonstrated that the electrical properties and the conductivity of the CNTs can be manipulated by the adsorption of transition metals on their surface. It will use the hybrid structure in the field of spintronics generation of magnetic sensors and biosensors [31]. A very recent study has reported that the semiconducting CNT can behave as HMF or FM on the adsorption of transition metals [15], [29], [92].

Therefore, it would be interesting to study the impact of the adsorption of transition metals on the surface of zigzag SiCNTs. Here, we have investigated the zigzag SiCNT(4,0), SiCNT(6,0), which are metallic and SiCNT(8,0), which are semiconducting in their pristine forms. Their electronic properties have been verified by calculating their bandstructures and spin-DOS and confirming the results with the existing literature. The magnetic properties of the adsorbed structures have also been analyzed by calculating their magnetic moments.

3.2 Computational Details

The transfer of electric charge from the transition metal to the SiCNT occurs due to the reciprocal effect, due to which SiCNT exhibits changed magnetic properties. In zigzag SiCNT, the ratio of Si: C ratio is fixed at 1:1, and the Si-C bond length is set at 1.78 Å. The changes in the magnetic properties of all SiCNT(4,0), SiCNT(6,0) and SiCNT(8,0) are studied by adsorbing transition metals on their surface. One atom of the transition metal to be adsorbed (Ti, Cr, Fe, Co, Cu, Zr, Mo and Ag) is placed near the surface of the SiCNT(4,0), SiCNT(6,0) and SiCNT(8,0), and the resulting geometry is relaxed till the forces on each atom have been reduced to not more than 0.05 eV/Å.

The s-DOS has been plotted for both the metallic SiCNT(4,0), SiCNT(6,0) as well as semiconducting SiCNT(8,0) based on density functional theory using the Atomistix simulation Toolkit [93], [94], [95]. Spin-polarized generalized gradient approximation (SGGA) has been used to provide the exchange-correlation energy using numerical LCAO (linear combination of atomic orbitals) basis sets. The threshold energy of 130 Rydberg has been specified with a k -point sampling of (1,1,100) along x , y and z directions, respectively.

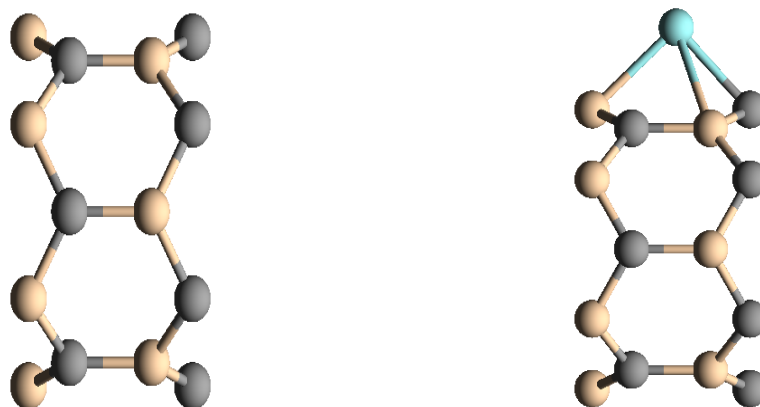


Fig. 3.1(a) Zigzag (4,0) SiCNT (b) Co atom adsorbed (4,0) SiCNT

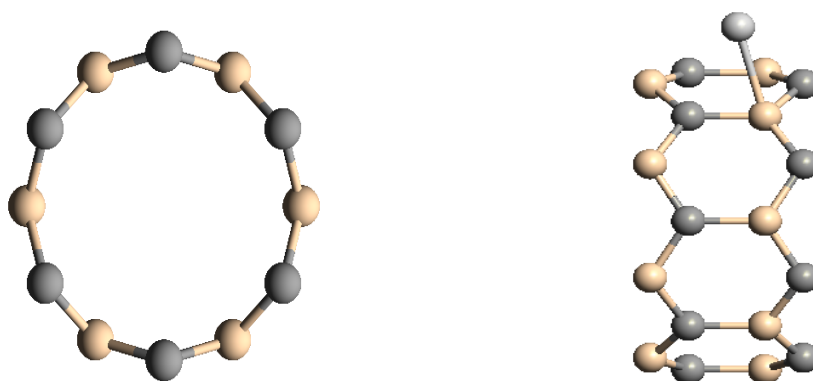


Fig. 3.2(a) Zigzag (6,0) SiCNT (b) Cr atom adsorbed (6,0) SiCNT

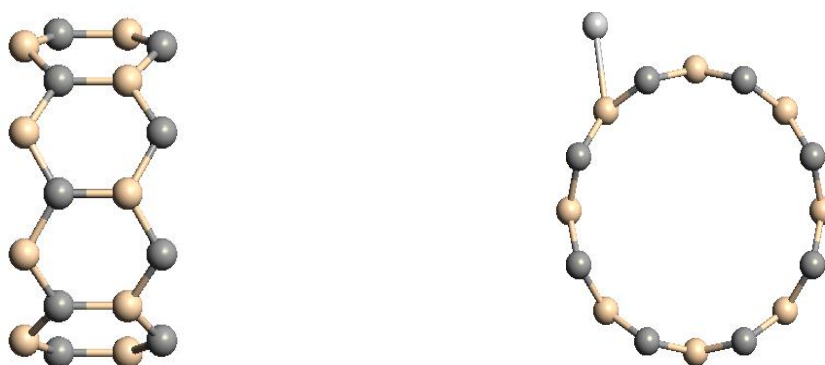


Fig. 3.3(a) Zigzag (8,0) SiCNT (b) Ag atom adsorbed (8,0) SiCNT

The band structure calculations have also been carried out to verify the results obtained from the spin-DOS analysis. The calculations have been done for all the adsorbed structures for both metallic (4,0) SiCNT, (6,0) SiCNT, and semiconducting (8,0) SiCNT. The sampling set has been set to (1,1,3) along the x , y and z directions, respectively, with the Brillouin zone set to G, Z, Y.

According to the energy distribution interpretation, the Density of States (DOS) provides the number of available states between energy E and $E + dE$ can be given as:

$$DOS(E) = \frac{\Delta n}{\Delta E \times L} = \frac{1}{\sqrt{2}\pi A} \left(E - \frac{E_g}{2}\right)^{-\frac{1}{2}} \quad (3.1)$$

Where $DOS(E)$ represents the density of states at a given energy level E , E_g is the energy gap, $A = at$ is the Taylor expansion coefficient, and L is the length of SiCNT.

Also, the carrier concentration of the material at a given energy E can be found using the density function and the probability density function as:

$$n(E) = \int DOS(E)f(E)dE \quad (3.2)$$

To ensure the feasibility of transition metals on the surface of SiCNT, adsorption energy can be calculated as:

$$E_{ads} = E_{structure} - [E_{TM} + E_{SiCNT}] \quad (3.3)$$

Where E_{ads} is the energy of adsorption, $E_{structure}$ is the total energy of the optimized structure after adsorption of transition metal on the surface of SiCNT, E_{SiCNT} is the total energy of the intrinsic SiCNT and E_{TM} is the total energy of one transition metal. Also, a larger negative value of E_{ads} means a more stable structure and the process is thermodynamically exothermic [96].

3.3 Results and Discussions

To understand the effect of adsorption, it is necessary to investigate the electronics and magnetic characteristics of the adsorbed structures. To investigate this, the transition metals were kept near the surface of pristine SiCNT, and the overall structure was relaxed. The relaxed structure of Ag-adsorbed (8,0) semiconducting SiCNT can be seen in Fig. 3.3. Similarly other transition metals were also adsorbed individually on the pristine (4,0) SiCNT, (6,0) SiCNT and (8,0) SiCNTs (see Fig. 3.1, Fig. 3.2 and Fig. 3.3). The resulting structures were then relaxed to optimize them. To ensure the feasibility of adsorption of different transition metals on the surface of SiCNT, the adsorption energy of the structure was calculated. The adsorption energy of all the structures came out to be negative, which means that the structure is stable. A larger

negative value of adsorption energy means stronger adsorption between the transition metal and the SiCNT.

To investigate the electronic structure of SiCNTs and the resulting adsorbed structures, we analyzed the s-DOS and their bandstructures. The s-DOS and bandstructure for all the SiCNT (4,0) structures are shown in Fig. 3.4 to Fig. 3.12. The s-DOS and their bandstructures for all SiCNT (6,0) structures are shown in Fig. 3.13 to Fig. 3.21. The s-DOS and their bandstructures for all the SiCNT(8,0) structures are available in Fig. 3.22 to Fig. 3.30.

3.3.1 SiCNT (4,0)

Fig. 3.1(a) shows the relaxed geometry of the pristine (4,0) SiCNT, which is very similar to the (4,0) CNT [15]. The geometry has been constructed by substituting half of the carbon (C) atoms in a dimer of (4,0) CNT with silicon (Si) atoms. The geometry was then optimized so that the resulting structure was stable and could be used for further analysis. The bandstructure and spin-density of states for pristine (4,0) SiCNT are plotted as shown in Fig. 3.4. It can be observed that the pristine (4,0) SiCNT is metallic as it has no bandgaps with bands crossing the Fermi level. It can be observed from its spin-DOS shown in Fig. 3.4 that both spin-states (spin-up and spin-down) are present at the Fermi level for (4,0) SiCNT. But its calculated zero magnetic moment, as shown in Table 3.1 preserves its non-magnetic nature. These results conclude that pristine (4,0) SiCNT is a non-magnetic metal, which is consistent with the existing research [91].

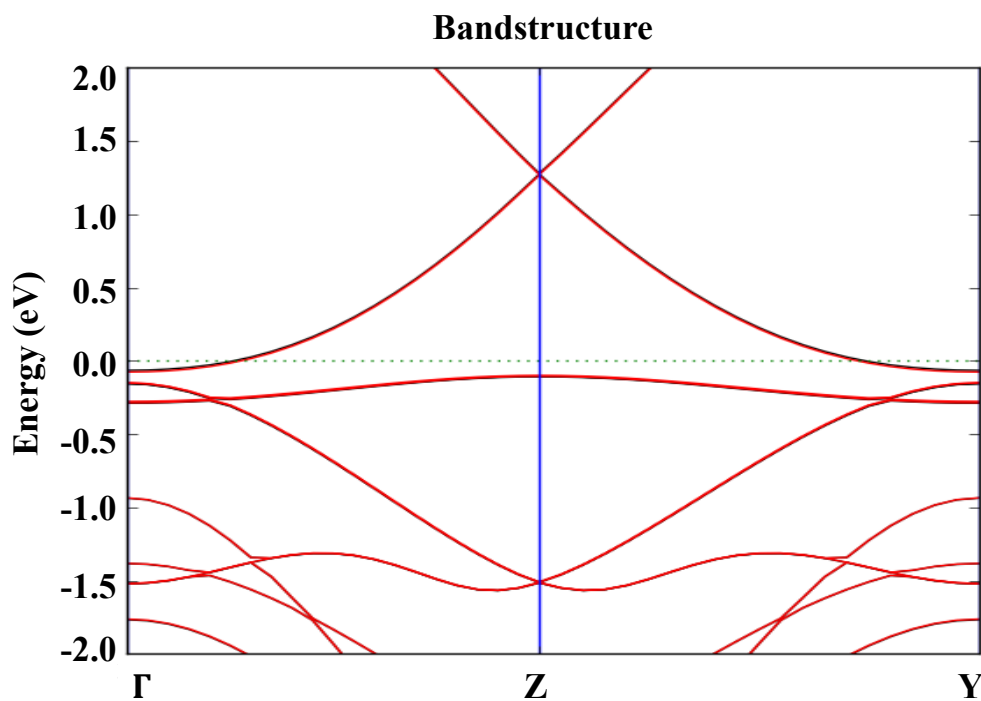
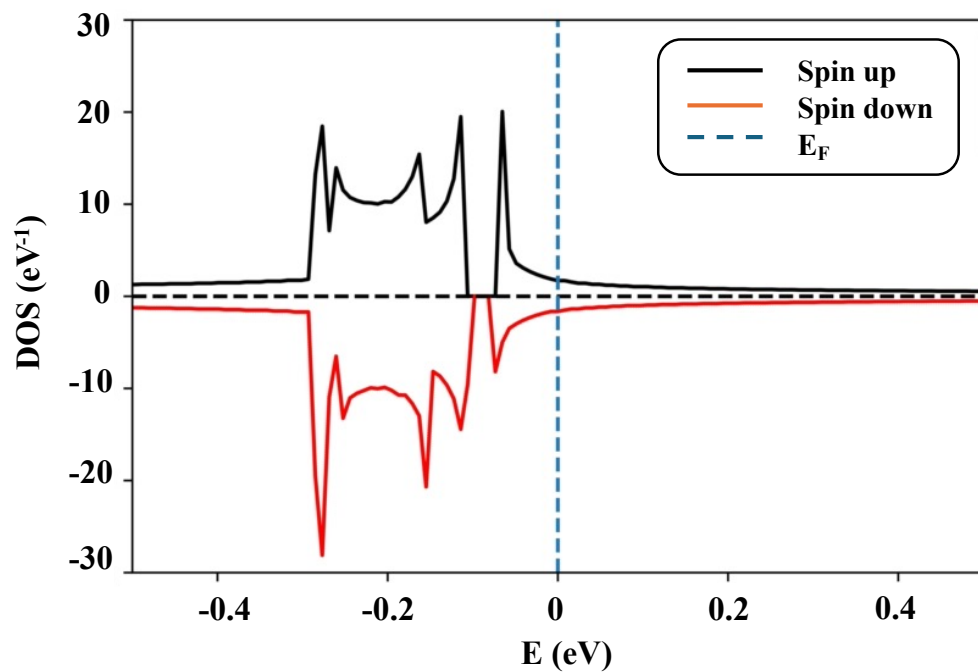


Fig. 3.4 DOS and bandstructure of pristine SiCNT(4,0)

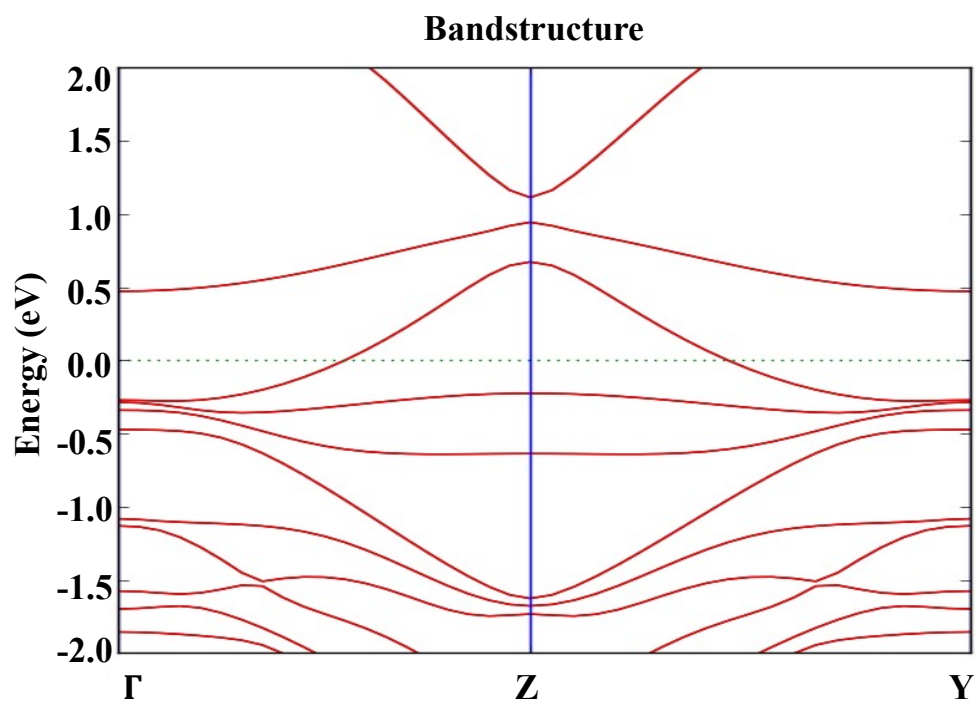
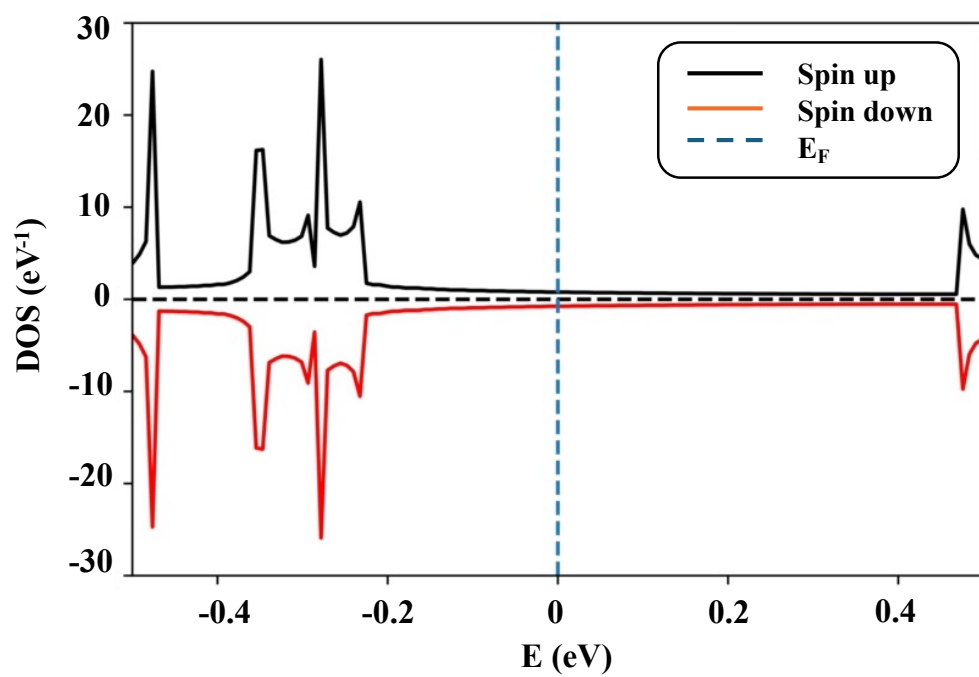


Fig. 3.5 DOS and bandstructure of Ag adsorbed SiCNT(4,0)

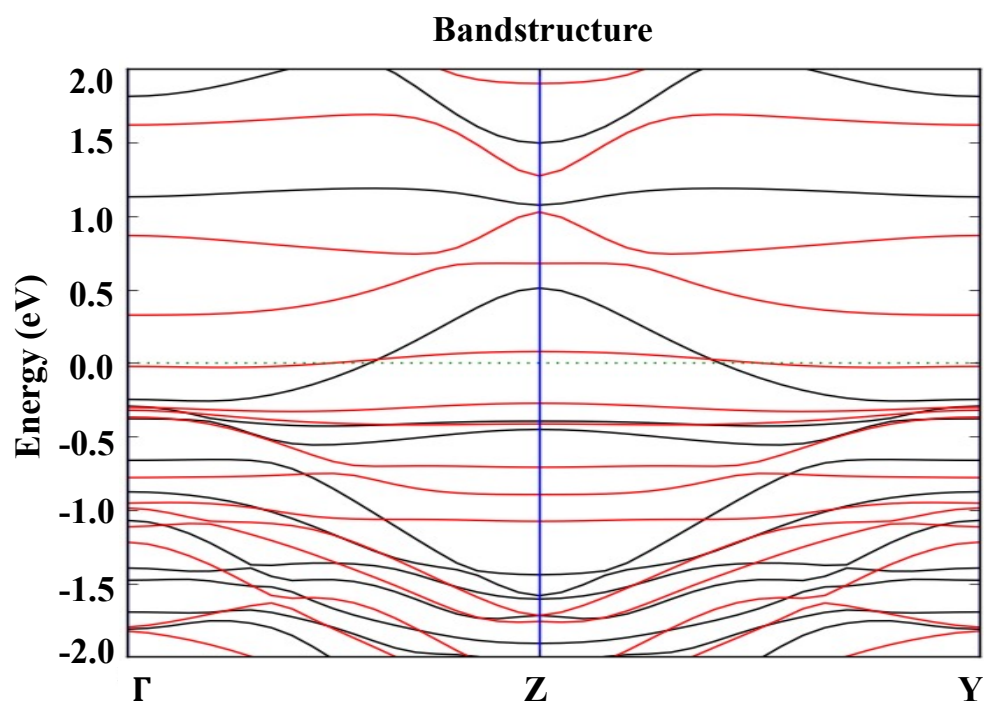
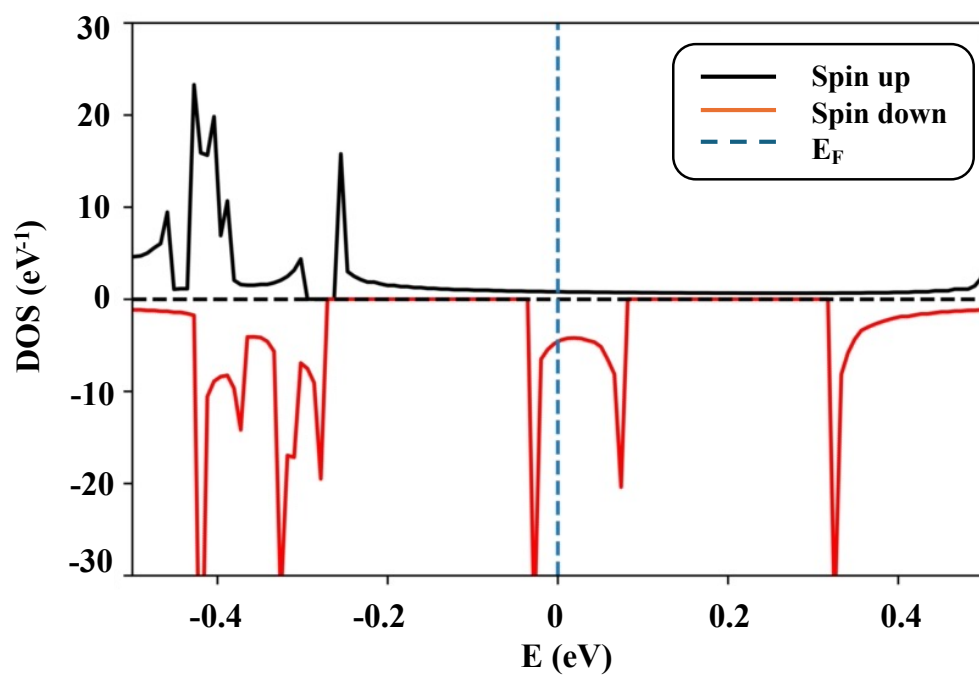


Fig. 3.6 DOS and bandstructure of Co adsorbed SiCNT(4,0)

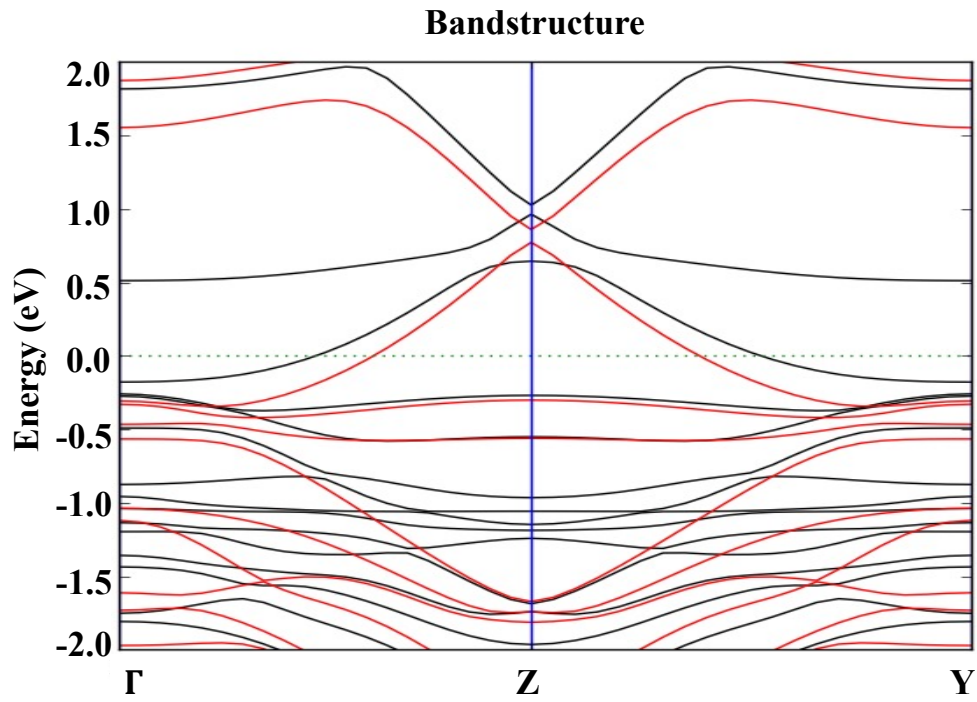
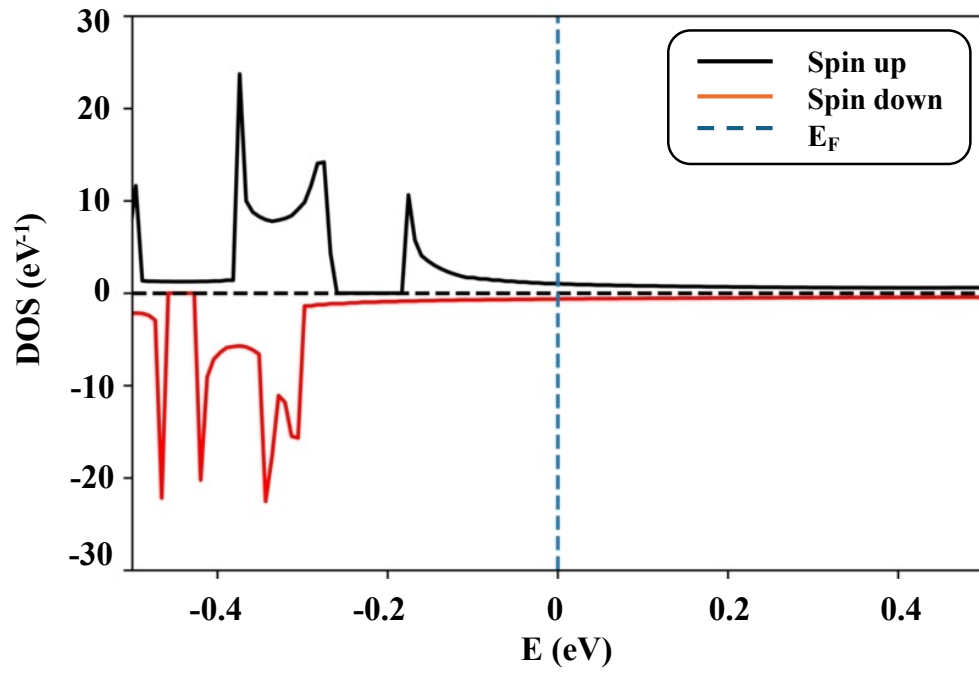


Fig. 3.7 DOS and bandstructure of Cr adsorbed SiCNT(4,0)

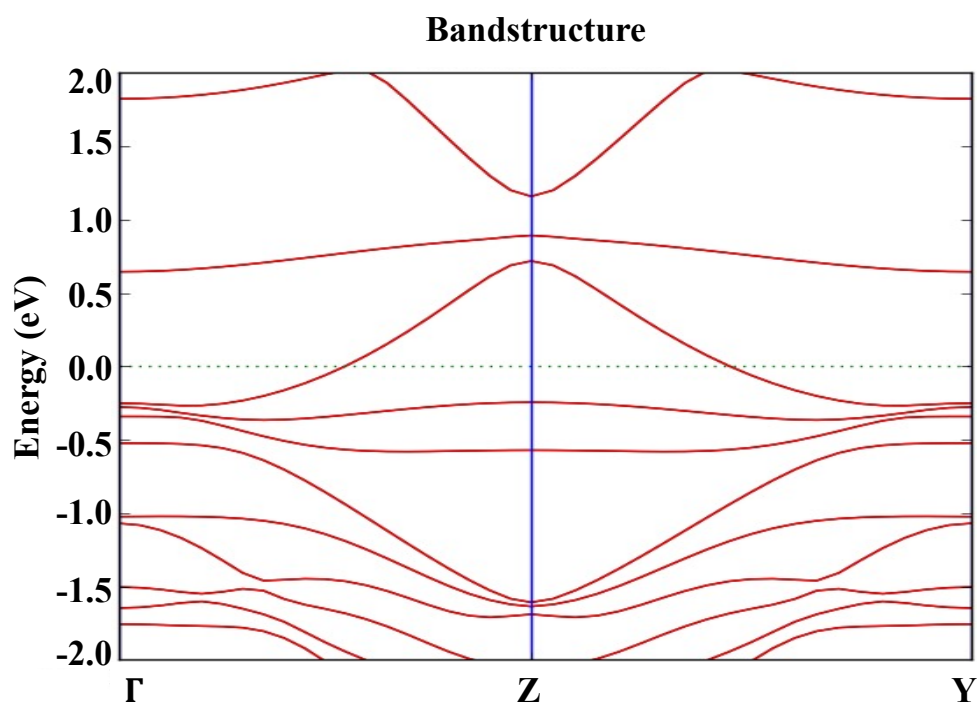
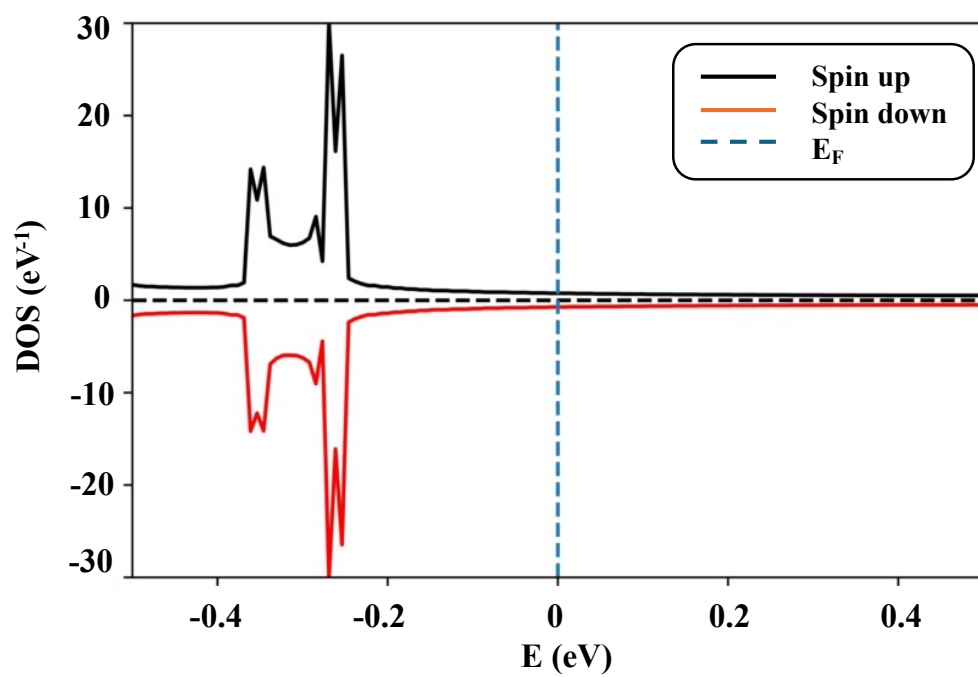


Fig. 3.8 DOS and bandstructure of Cu adsorbed SiCNT(4,0)

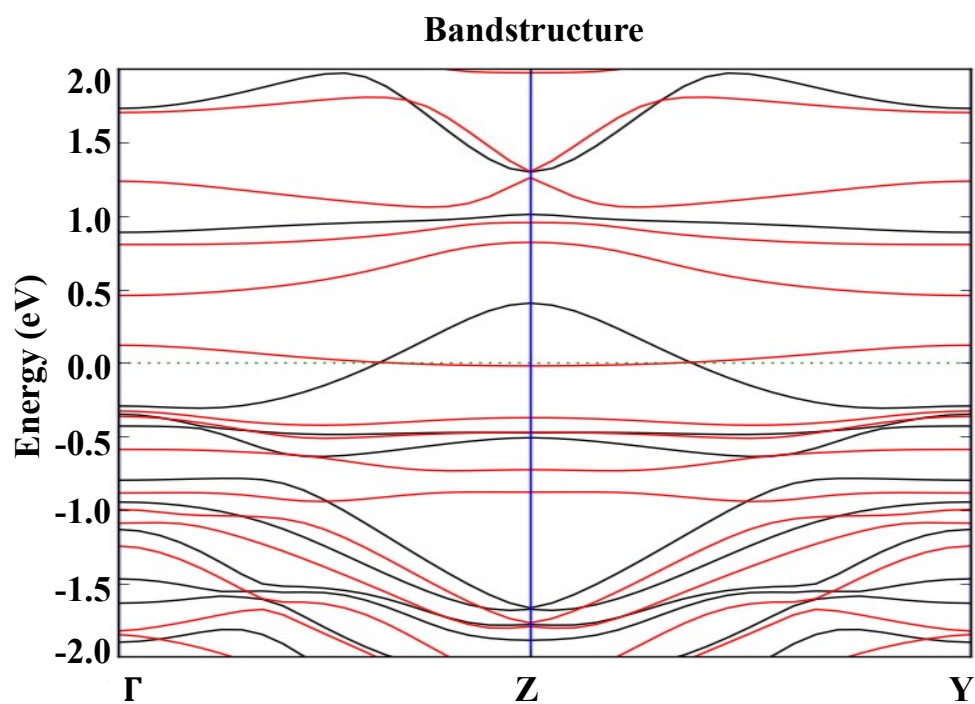
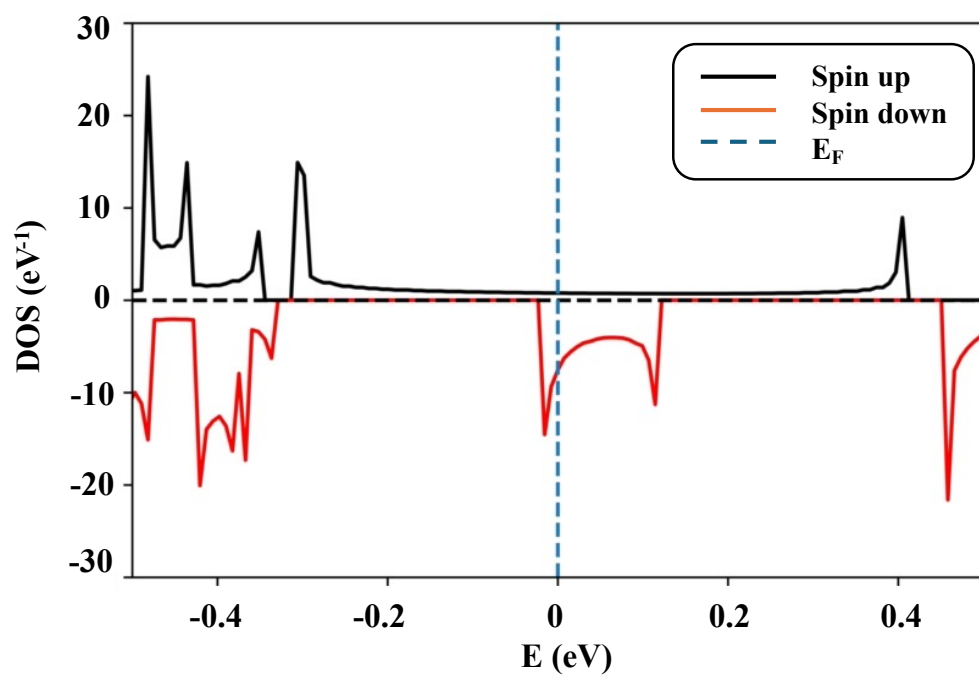


Fig. 3.9 DOS and bandstructure of Fe adsorbed SiCNT(4,0)

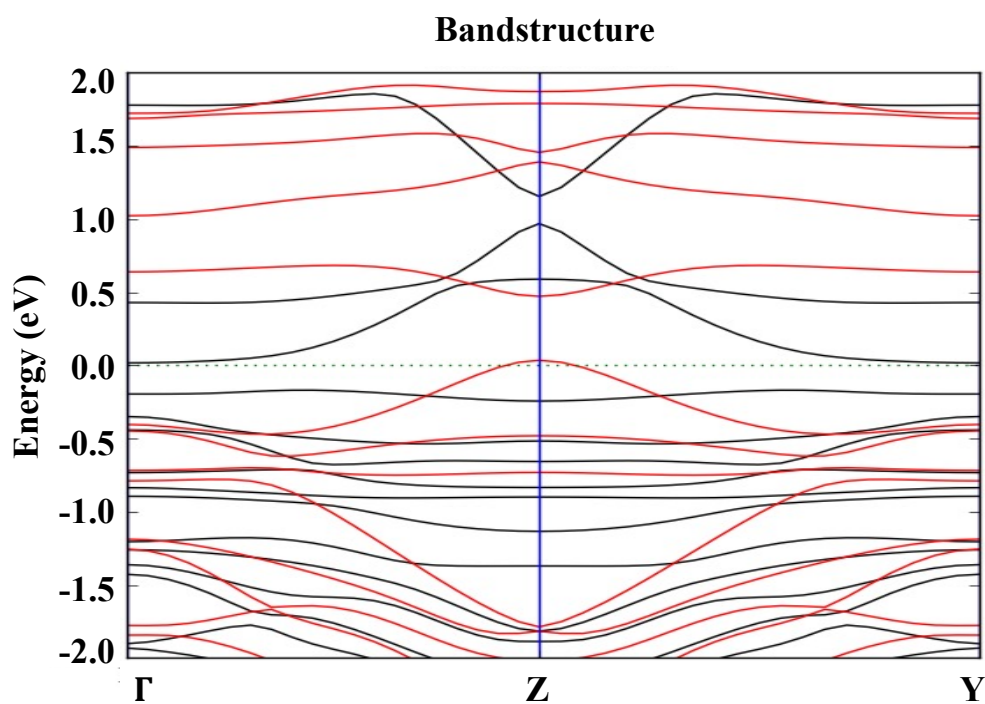
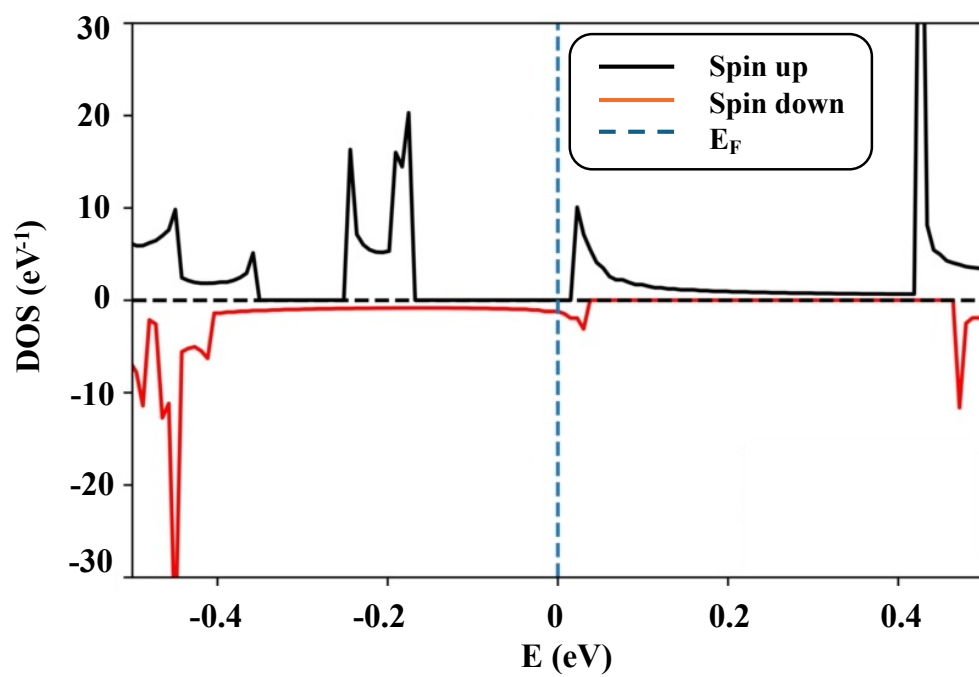


Fig. 3.10 DOS and bandstructure of Mo adsorbed SiCNT(4,0)

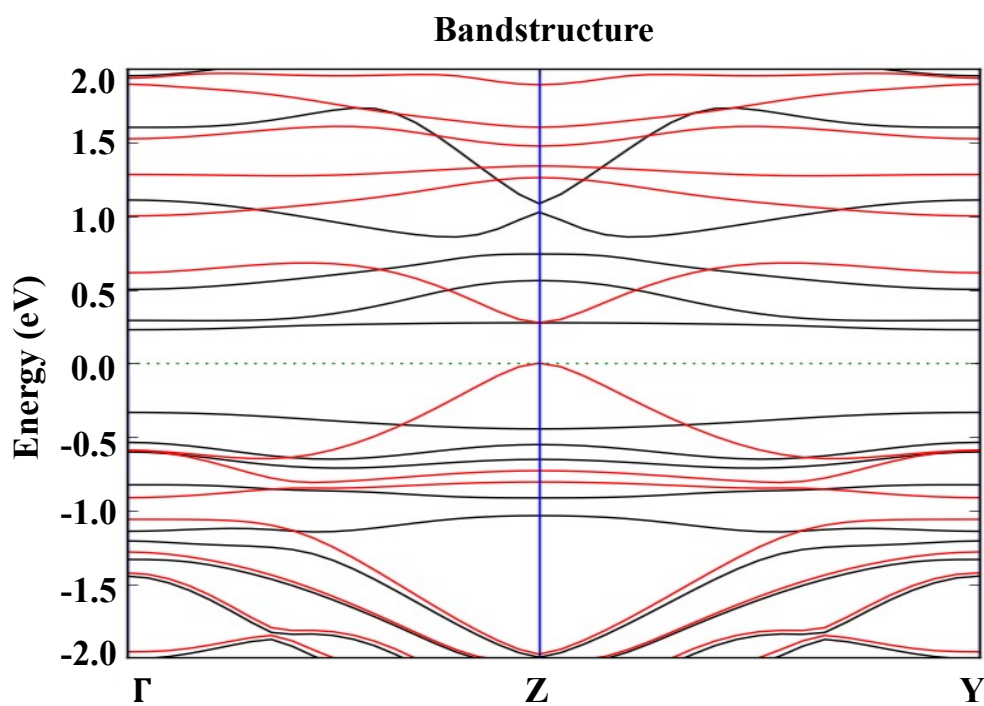
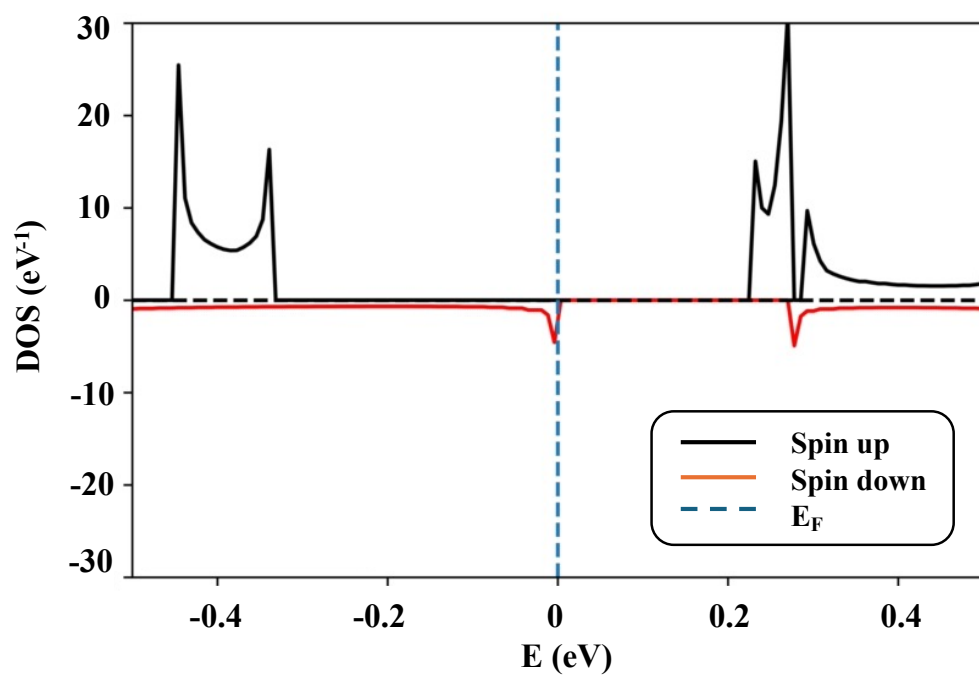


Fig. 3.11 DOS and bandstructure of Ti adsorbed SiCNT(4,0)

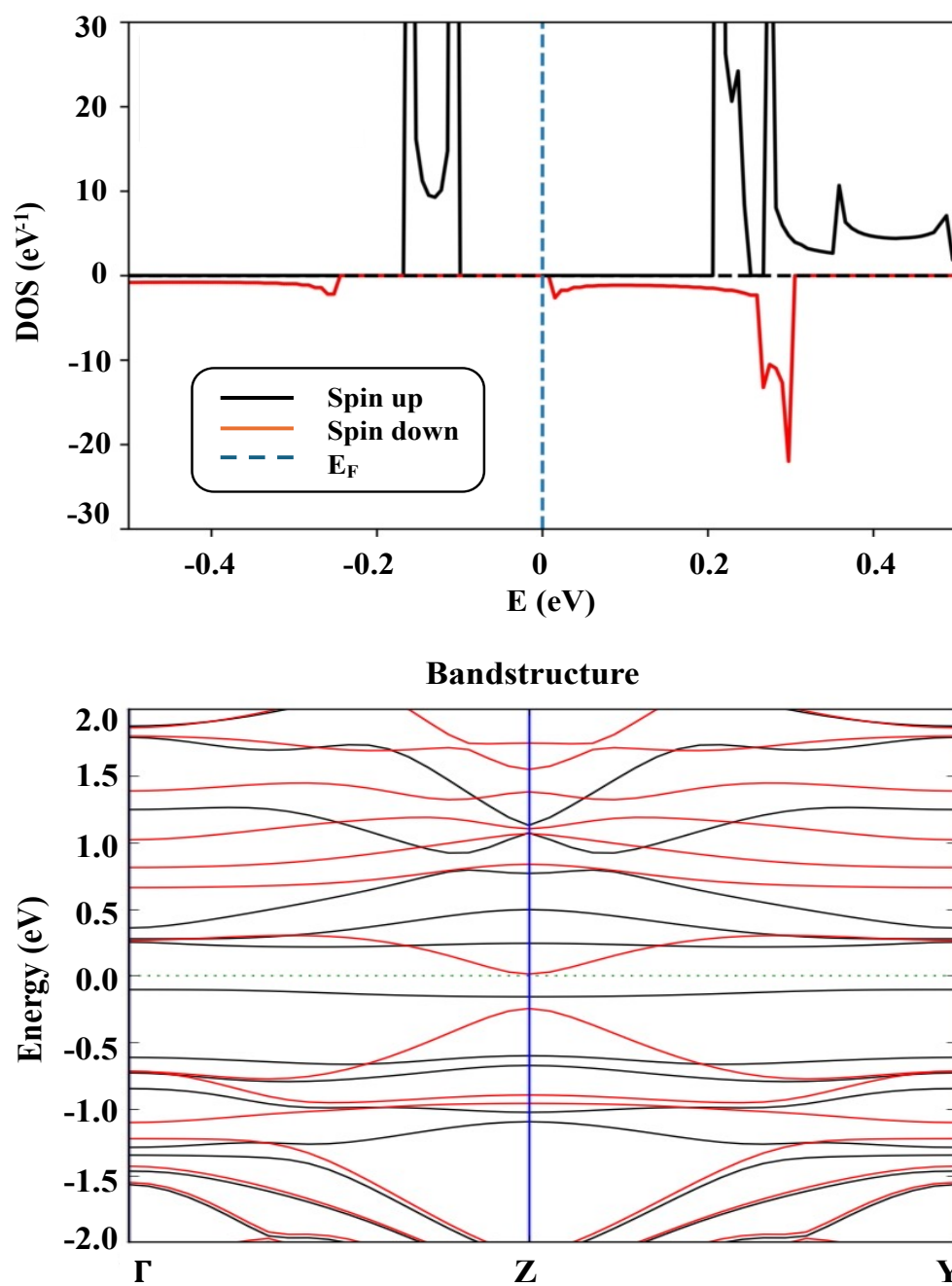


Fig. 3.12 DOS and bandstructure of Zr adsorbed SiCNT(4,0)

Table 3.1 Magnetic Properties of (4,0) SiCNT after adsorption of TM

Simulated structure	Spin- Up	Spin- Down	Magnetic Moment per atom (μ_B)	Magnetic Behaviour
Pristine (4,0)SiCNT	Passed	Passed	NIL	Non-Magnetic
Ag adsorbed (4,0)SiCNT	Passed	Passed	NIL	Non-Magnetic
Co adsorbed (4,0)SiCNT	Not Passed	Passed	+2.1	HMF
Cr adsorbed (4,0)SiCNT	Passed	Not Passed	+4.8	HMF
Cu adsorbed (4,0)SiCNT	Passed	Passed	+4.8	FM
Fe adsorbed (4,0)SiCNT	Not Passed	Passed	+3.2	HMF
Mo adsorbed (4,0)SiCNT	Not Passed	Passed	+4.2	HMF
Ti adsorbed (4,0)SiCNT	Not Passed	Passed	+2.1	HMF
Zr adsorbed (4,0)SiCNT	Not Passed	Not Passed	+1.8	Non-Magnetic

The bandstructure and s-DOS of the Ag-adsorbed zigzag (4,0) SiCNT shown in Fig. 3.5 shows its metallic nature. In addition, it also preserves its non-magnetic behaviour as the magnetic moment remains insignificant (see Table 3.1) even though its s-DOS shows conduction states in both spin-up and spin-down channels. However, the magnetic moment rises to significant levels when zigzag (4,0) SiCNT is adsorbed with Co. The zero bandgap at the Fermi level can be observed from its bandstructure in Fig. 3.6. Also, the majority of the conduction states for the Co-adsorbed structures are available in only the spin-down direction, and negligible states are available in the spin-down channel in comparison to the spin-up states. This shows its HMF nature. The HMF materials have this unique characteristic that they allow electrons of a particular spin (up/down) to conduct while blocking the electron having the opposite spin (down/up). This unique property of HMF allows their use in novel fields like spintronics for the fabrication of novel devices like spin valves and MTJs. The significant magnetic moment of $\sim 2 \mu_B$ for Co-adsorbed (4,0) SiCNT confirms its magnetic behaviour (see Table 3.1). Similar induction of HMF behaviour can be observed in Fe, Mo and Ti-adsorbed where most of the conduction is allowed in the spin-down states and no/negligible conduction is allowed in the spin-up states (see Fig. 3.9, Fig. 3.10 and Fig. 3.11). Their significant magnetic moments of ~ 3 , 4 and $2 \mu_B$ respectively indicate a transformation to a magnetic nature compared to the non-

magnetic nature of pristine (4,0) SiCNT (see Table 3.1). The Cr- adsorbed (4,0) SiCNT also shows half metallicity as it allows conduction only in the spin-up channels and blocks the conduction of spin-down electrons (see Fig. 3.7). Its significant magnetic moment of $4.8 \mu_B$ reflects its magnetic nature (see Table 3.1).

From the spin- DOS of Cu-adsorbed (4,0) SiCNT shown in Fig. 3.8, it can be observed that only Cu-adsorbed (4,0) SiCNT structure shows ferromagnetic behaviour as it has conducting states in both spin-up and spin-down channels. It also has a significant magnetic moment of $\sim 4.8 \mu_B$ (see Table 3.1). As shown in Table 3.1, the Zr-adsorbed (4,0) SiCNT, inspite of significant magnetic moment, is non-magnetic in nature since it does not have any conduction states at the Fermi level, which can be observed from its spin- DOS as shown in Fig. 3.12.

The bandstructures of all the transition metal adsorbed (4,0) SiCNT structures show zero bandgap at the Fermi level, indicating the metallic nature of all the adsorbed structures. The magnetic nature of the adsorbed structures is attributed to their significant magnetic moment and availability of conducting states in their spin-up and spin-down channels. The calculated magnetic moment in the TM-adsorbed (4,0) SiCNT results primarily due to the unpaired electrons present in the d-orbital of the transition metals. The carbon and silicon atoms have a negligible contribution to the overall magnetic moments of the adsorbed structures, which is verified by the obtained zero magnetic moments of the pristine (4,0) SiCNT. The adsorbed structures result in the metallic/half-metallic due to the transfer of charge from the transition metal to the carbon/ silicon atoms on which it is adsorbed. Therefore, the results suggest that the adsorption of transition metals on the pristine (4,0) SiCNT can transform its non-magnetic nature into FM/ HMF nature.

3.3.2 SiCNT (6,0)

The calculated spin-DOS for pristine (6,0) SiCNT, as well as TM adsorbed (6,0)SiCNT, are plotted as shown in Fig. 3.13 to Fig. 3.21. It is visible from the bandstructure and the spin-DOS in Fig. 3.13 that pristine (6,0) SiCNT is metallic. However, no spin-states (spin-down and spin-up) are present for the pristine (6,0) SiCNT, which shows that it preserved its non-magnetic behaviour on adsorption of Ag.

The Ag-adsorbed zigzag (6,0) SiCNT shows its transformation from non-magnetic behaviour to FM as its bandstructure, and s-DOS shows the availability of both spin-down and spin-up states as given in Fig. 3.14. However, Co-adsorbed (6,0) SiCNT in Fig. 3.15 shows the conduction states only in the spin-up direction, making it an HMF material. As given in Fig. 3.16, (6,0) SiCNT adsorbed with Cr also shows significant conduction states in the spin-up direction with no states in the spin-down direction. This makes Cr-adsorbed (6,0) SiCNT a promising HMF material. Similarly, in the case

of Cu-adsorbed (6,0) SiCNT, its demonstration of half-metallicity is evident as it predominantly facilitates conduction in the spin-up channels while exhibiting negligible conduction states in the spin-down channels (refer to Fig. 3.17). Ti adsorbed (6,0) SiCNT likewise demonstrates half-metallic behaviour. Its s-DOS in Fig. 3.20 shows that conducting states are only accessible in the spin-down channel, obstructing the conducting states in the spin-up channel. Moreover, it is intriguing to note that, according to Fig. 3.18 only the Fe-adsorbed (6,0) SiCNT structure exhibits non-magnetic behaviour, with minimal conducting states in the spin-up channel and zero conducting states in the spin-down channel. Similar non-magnetic behaviour is shown by Zr and Mo adsorbed (6,0) SiCNT (see Fig. 3.21, Fig. 3.19) as they have no conducting states at the Fermi level, making them non-magnetic in nature. The unpaired electrons present in the d-orbital of TM are the main cause of the ferromagnetic characteristics of TM-adsorbed (6,0) SiCNT. Hence, the findings imply that the metallic but non-magnetic nature of pristine (6,0) SiCNTs can also be changed to FM/HMF nature by adsorbing the transition metals.

The magnetic nature of the SiCNT(6,0) after adsorption was also verified by calculating the magnetic moment of individual adsorbed structures. The magnetic moment of each structure is given in Table 3.2. It can be seen from Table 3.2 that pristine SiCNT(6,0) has zero magnetic moments, which also confirms its non-magnetic nature. Ag on adsorption provides a small but significant magnetic moment of $0.44 \mu_B$ which shows its transformation to a magnetic material. Similarly, a small but significant magnetic moment was observed when Cu-atom was adsorbed on SiCNT(6,0). The resulting structure is FM, as confirmed by its DOS in Fig. 3.17. Co-atom on adsorption produces a magnetic moment of $1.26 \mu_B$ (Table 3.2), and it can also be observed from its s-DOS that conducting states are only available in the spin-down channel, transforming it into an HMF material. Cr-atom adsorbed SiCNT(6,0) produced the highest magnetic moment of all the adsorbed structures upon adsorption, measuring $+5.33 \mu_B$. Half metallicity was also observed on the adsorption of Fe- atom and Ti- atom, which produced magnetic moments of $2.83 \mu_B$ and $1.76 \mu_B$, respectively. These calculated magnetic moments, when correlated with bandstructure and s-DOS, reflects the conversion of non-magnetic materials to FM and HMF materials.

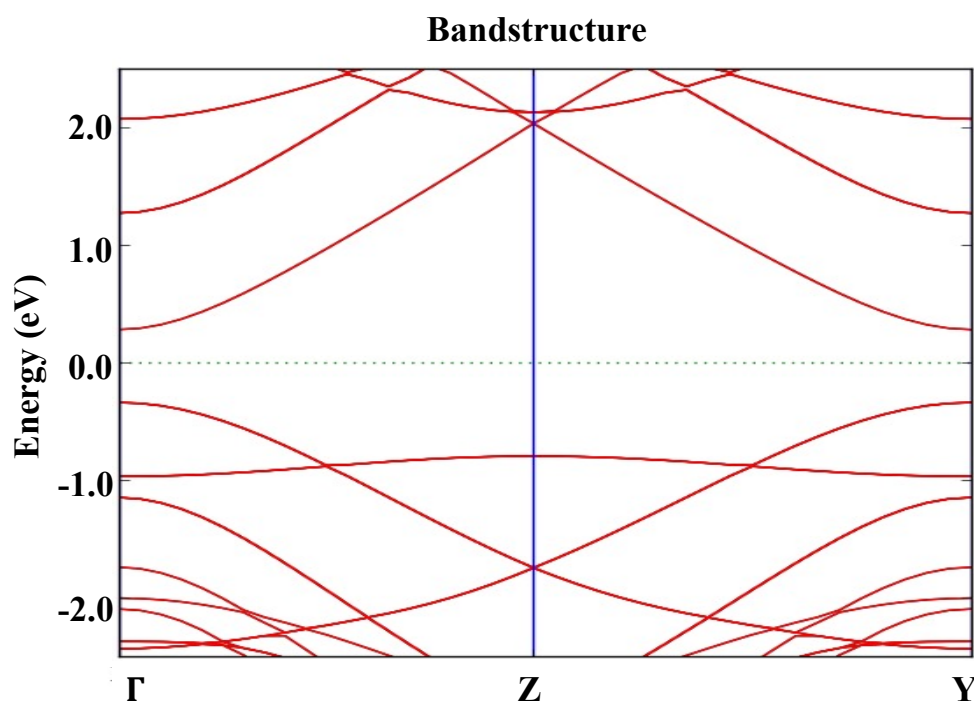
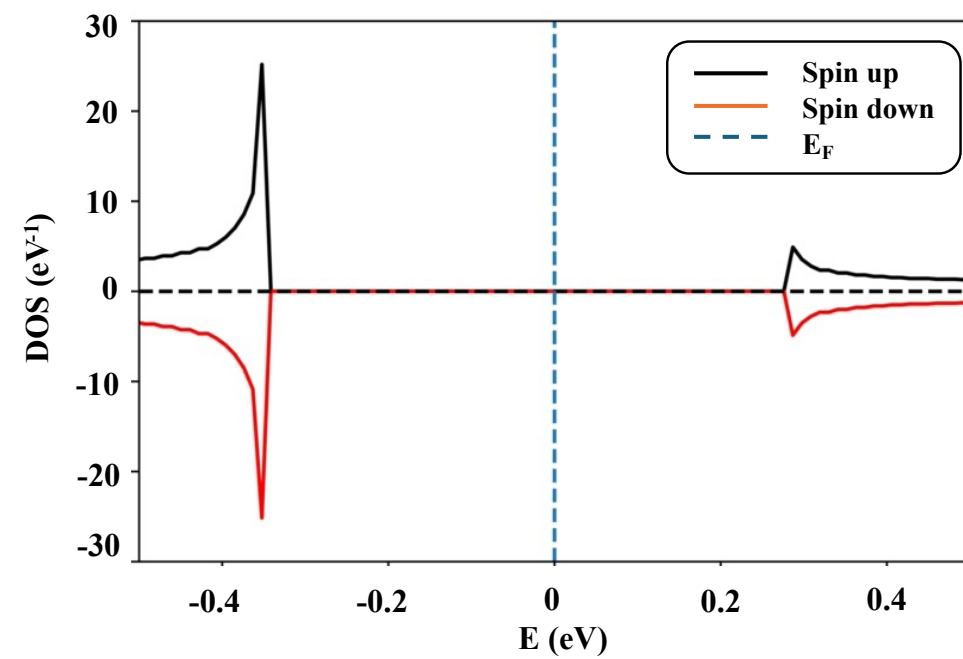


Fig. 3.13 DOS and bandstructure of pristine SiCNT(6,0)

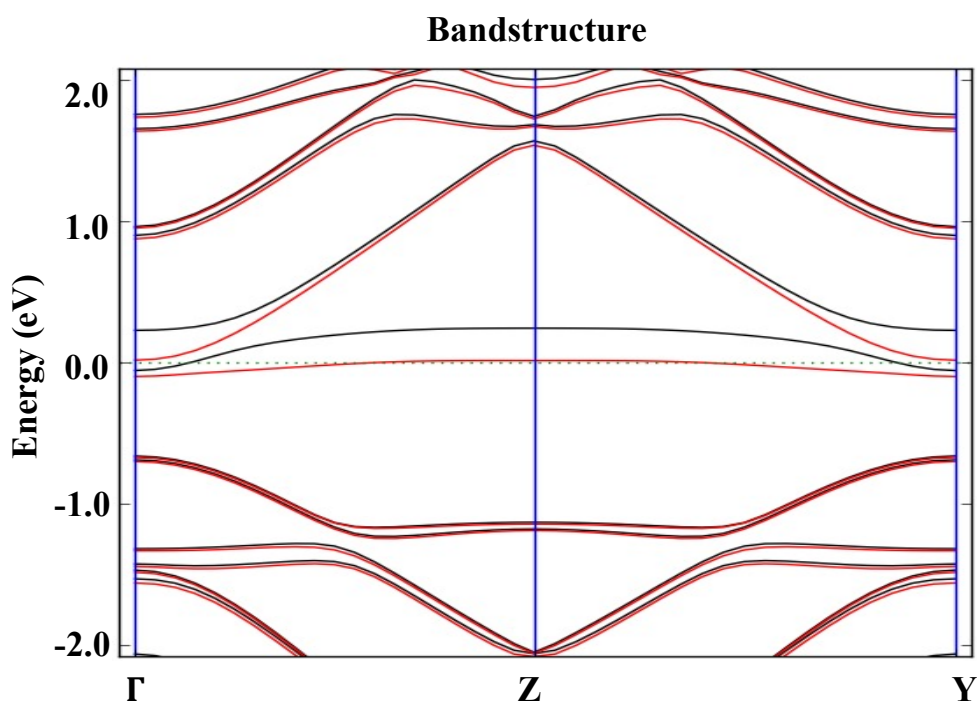
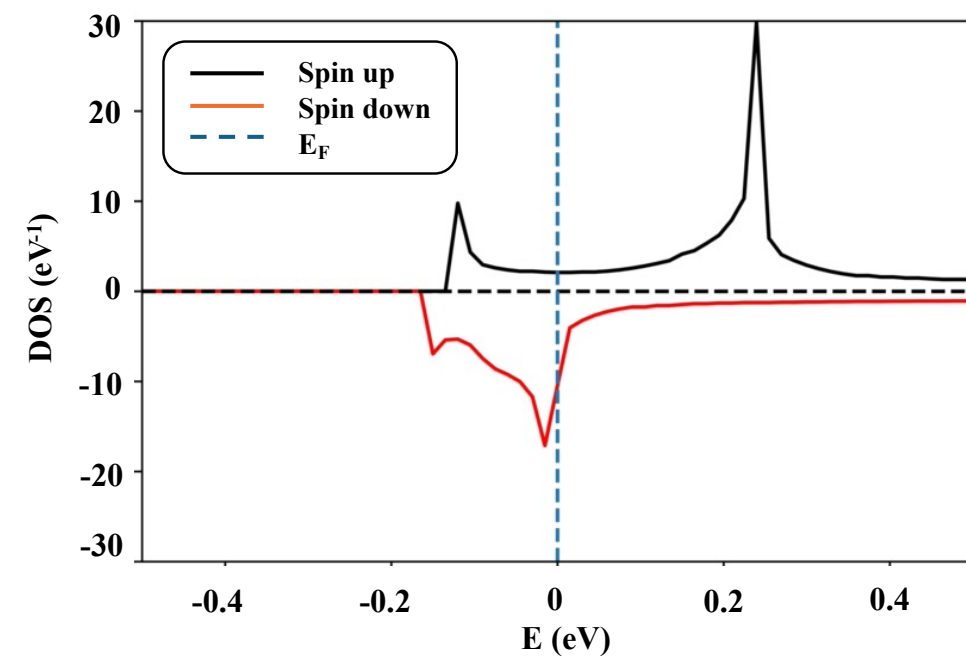


Fig. 3.14 DOS and bandstructure of Ag adsorbed SiCNT(6,0)

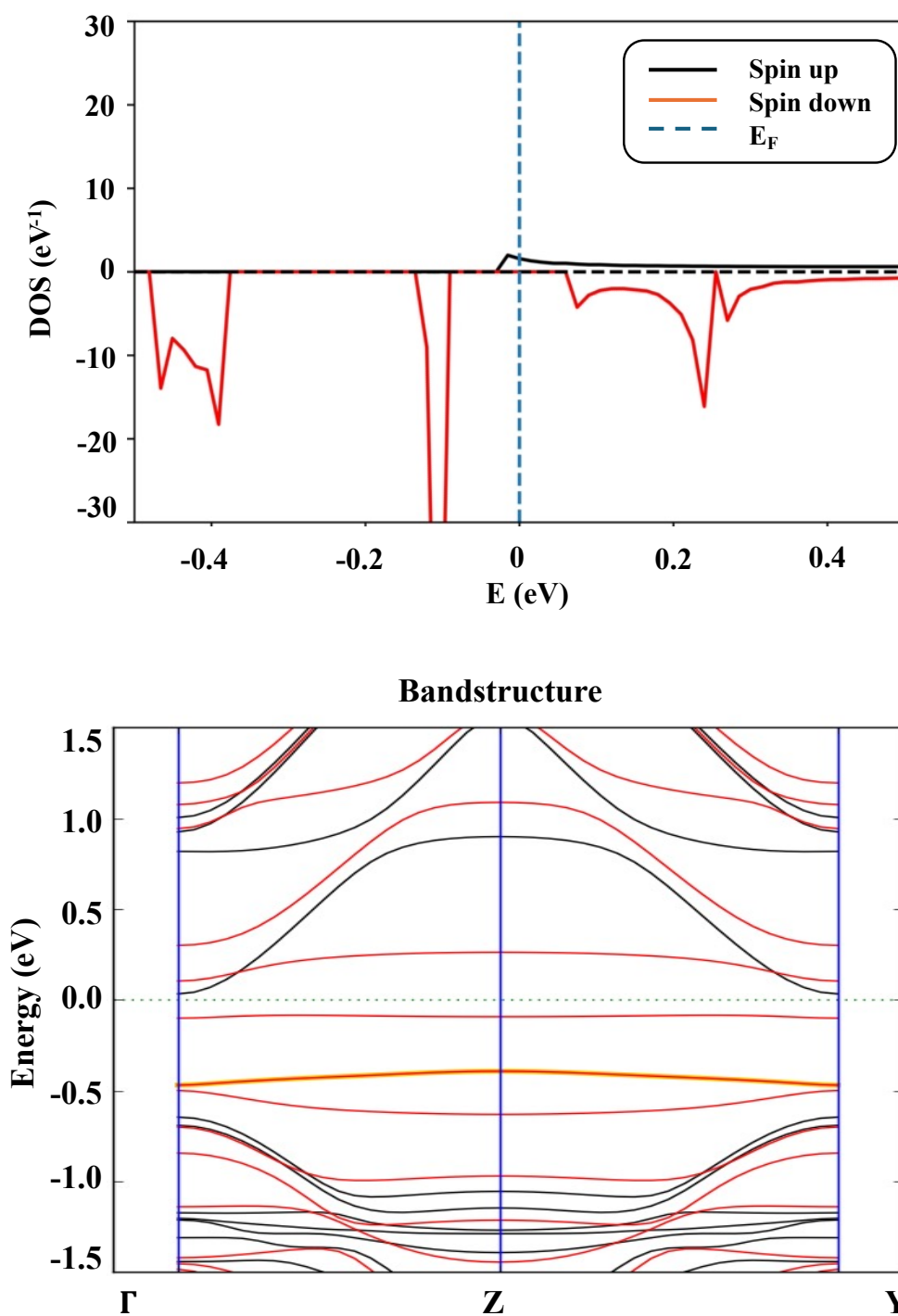


Fig. 3.15 DOS and bandstructure of Co adsorbed SiCNT(6,0)

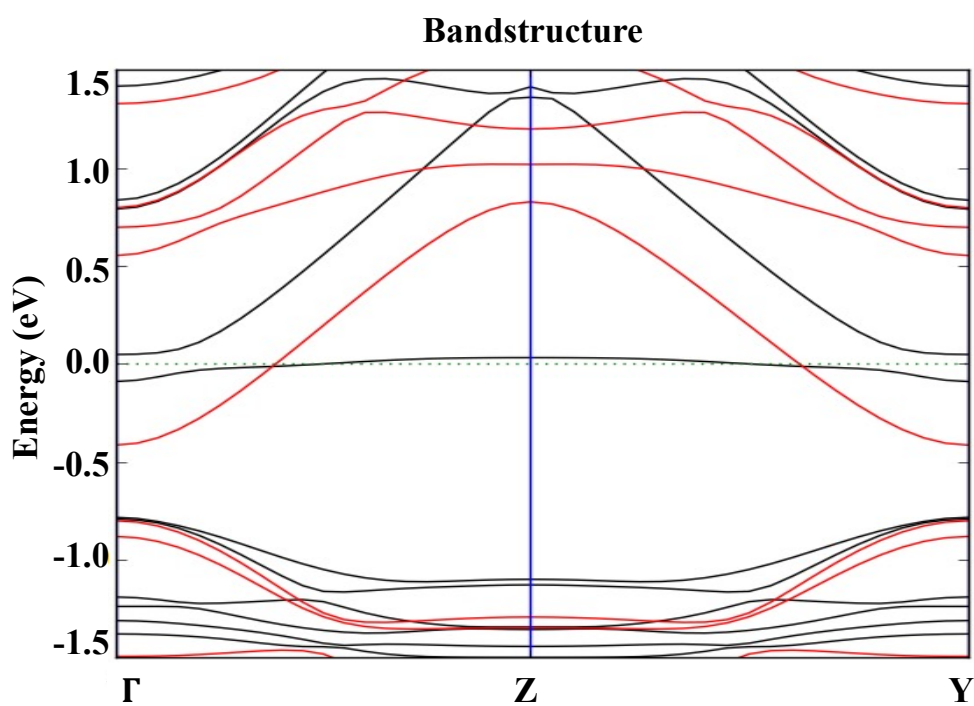
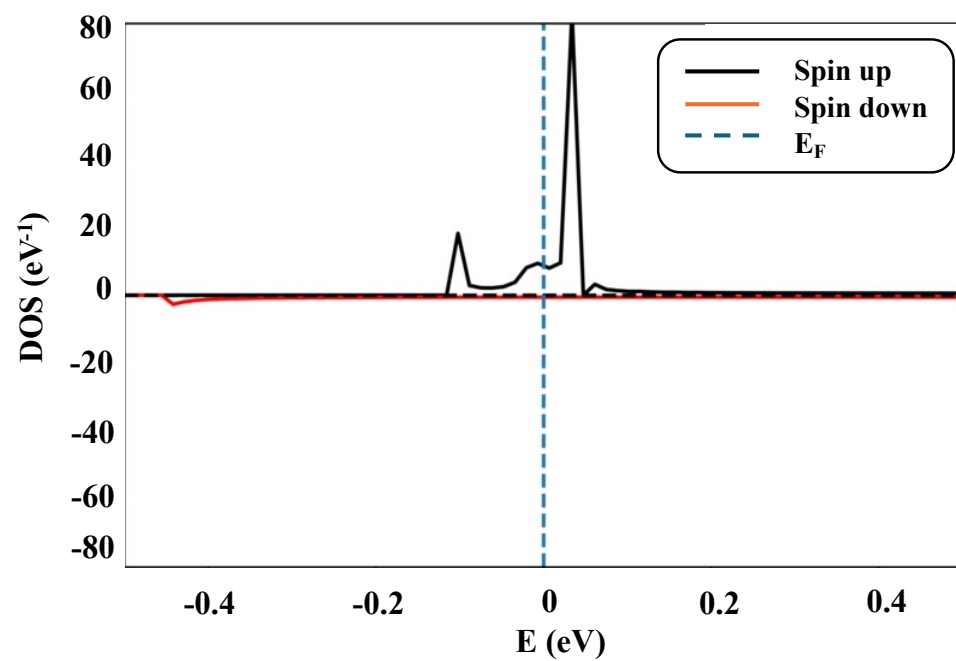


Fig. 3.16 DOS and bandstructure of Cr adsorbed SiCNT(6,0)

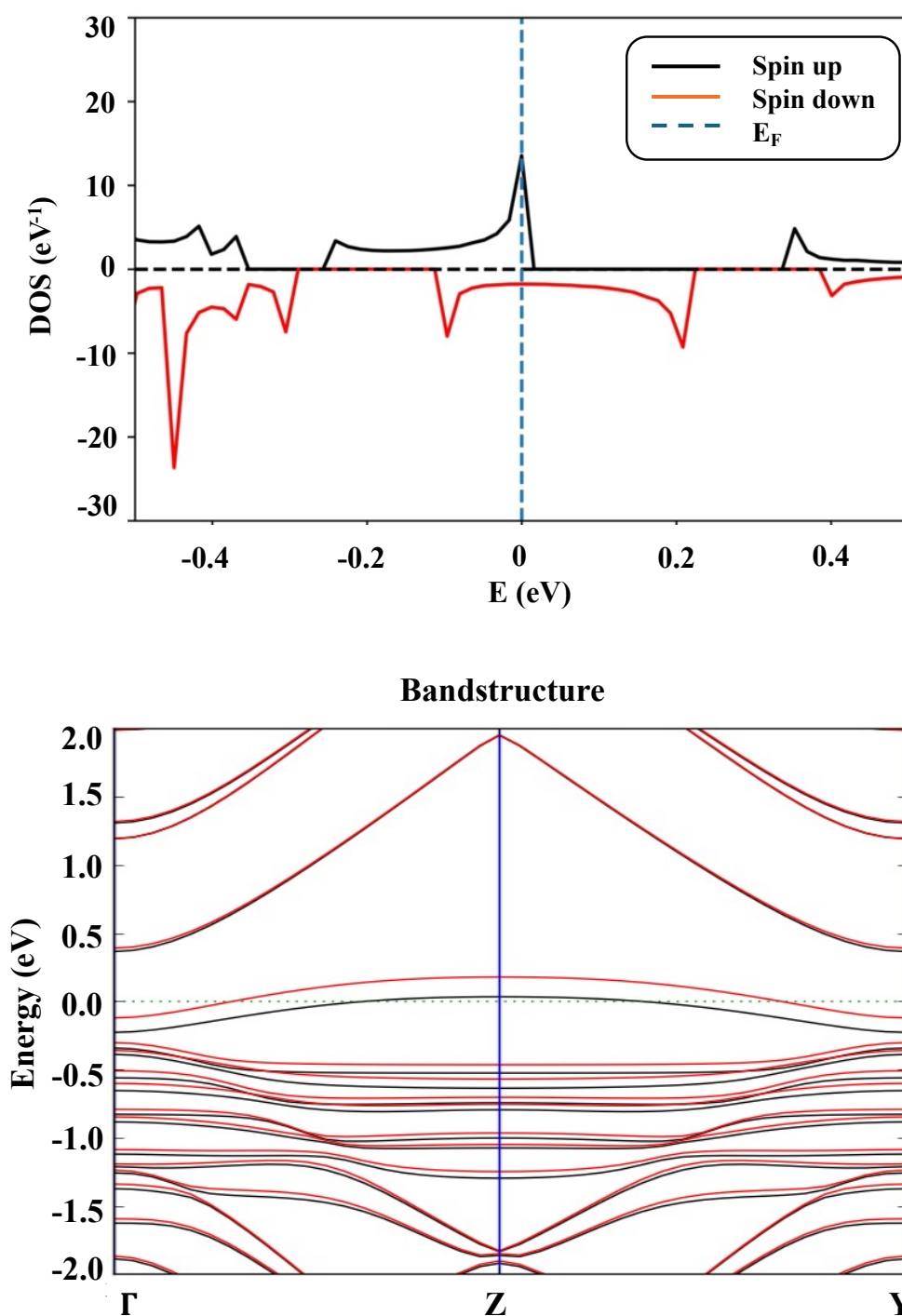


Fig. 3.17 DOS and bandstructure of Cu adsorbed SiCNT(6,0)

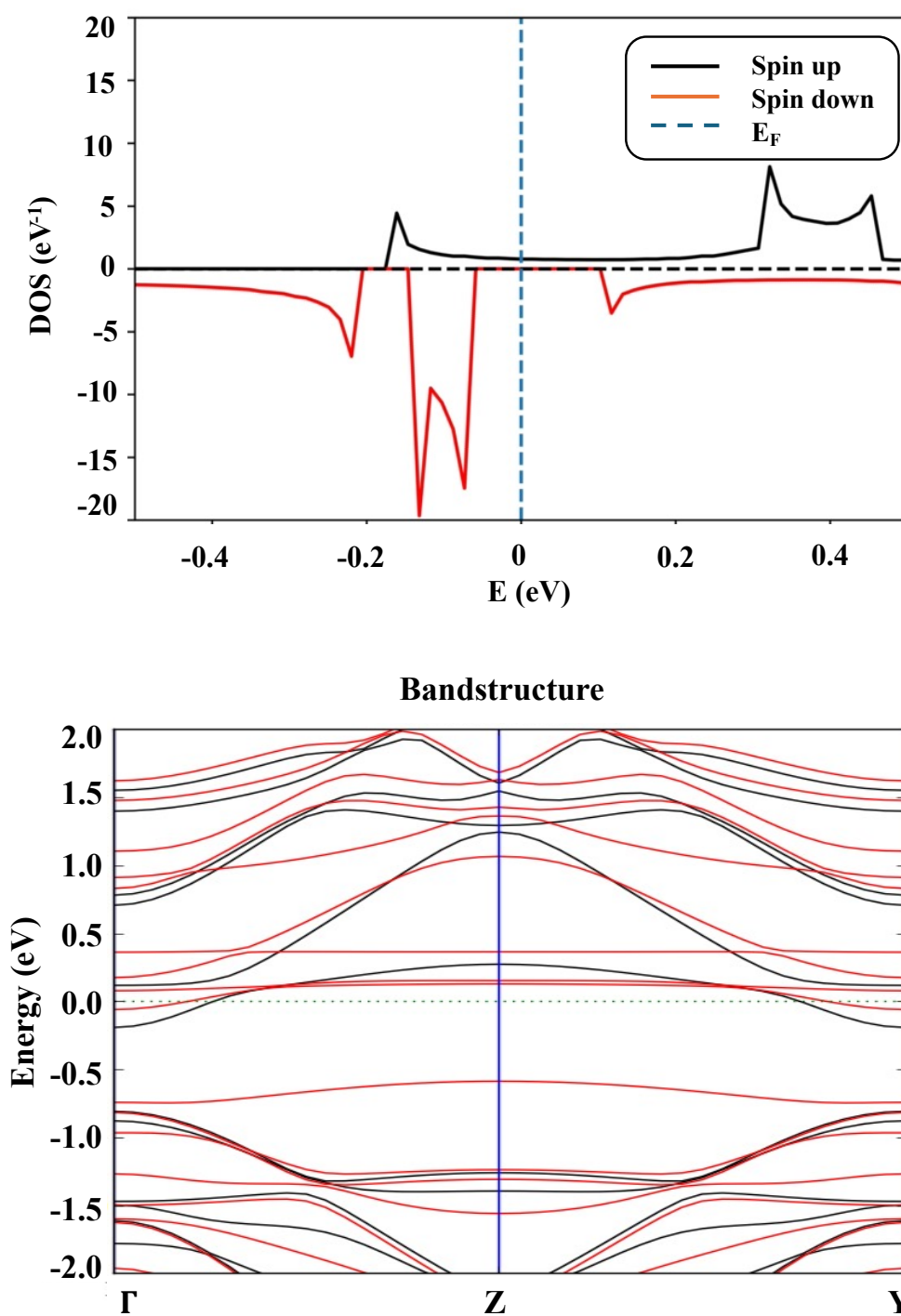


Fig. 3.18 DOS and bandstructure of Fe adsorbed SiCNT(6,0)

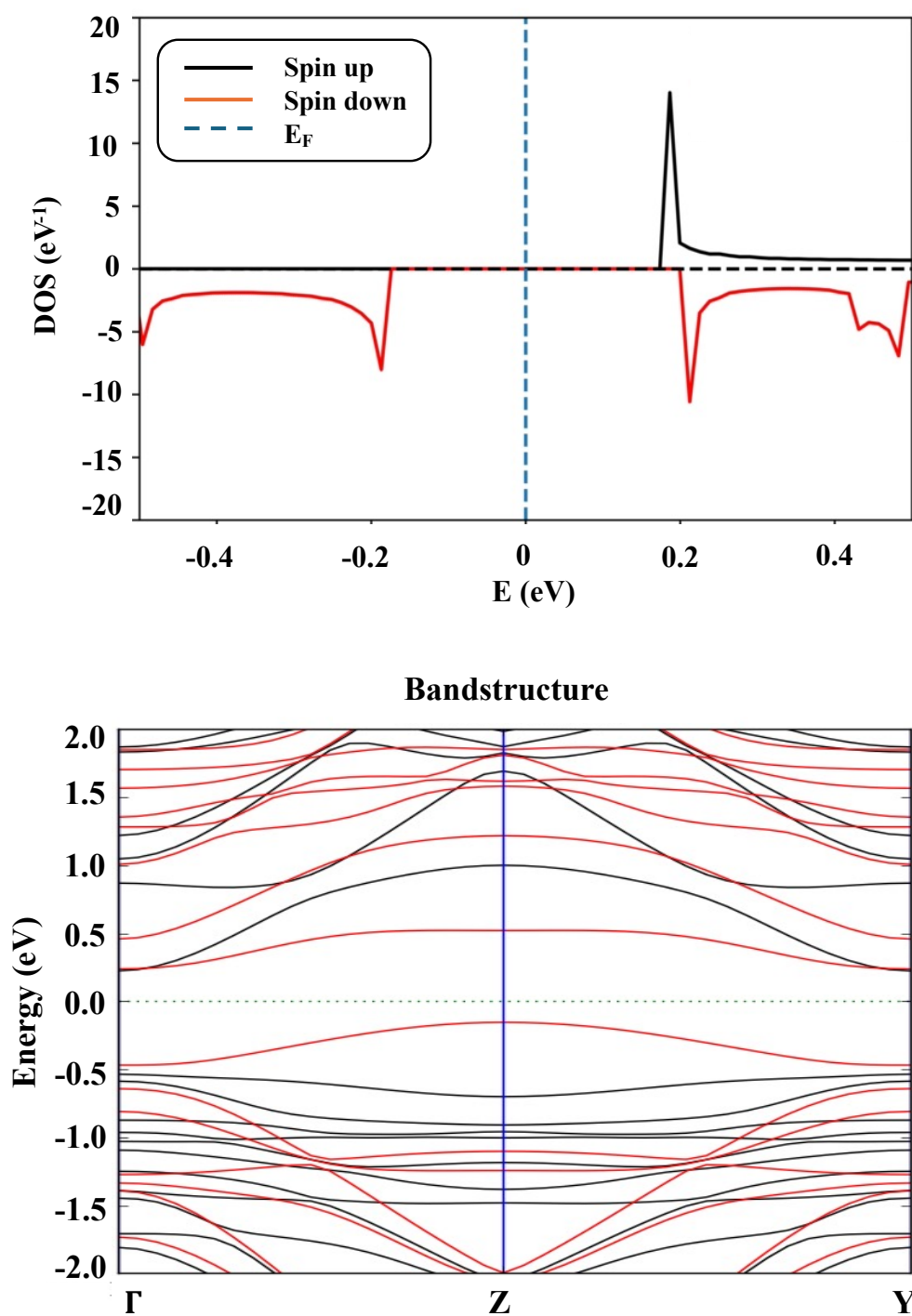


Fig. 3.19 DOS and bandstructure of Mo adsorbed SiCNT(6,0)

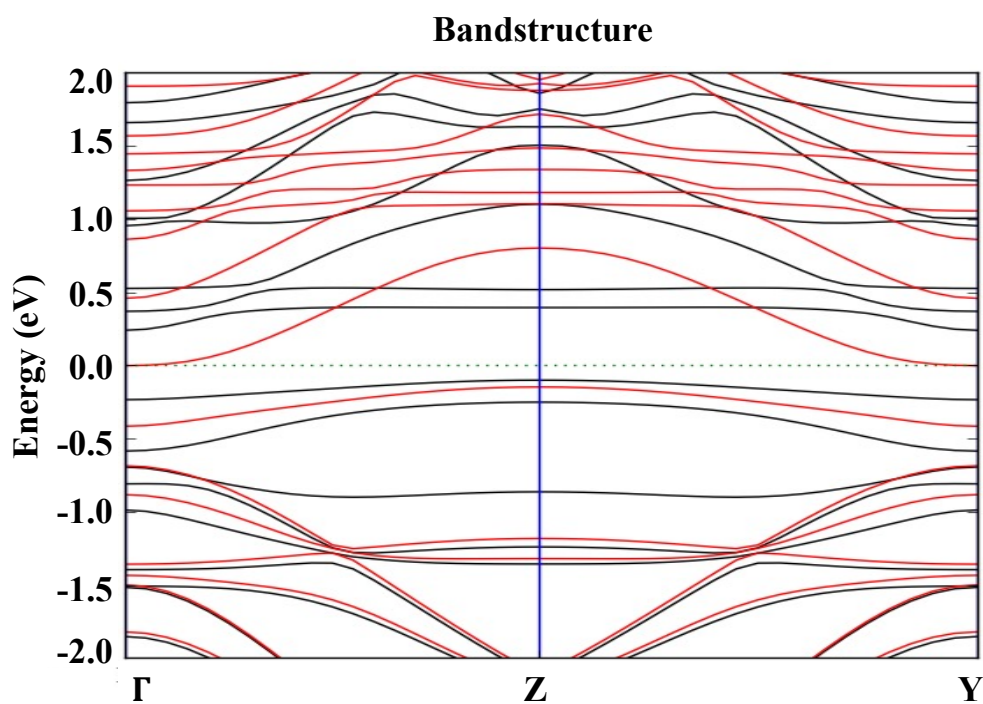
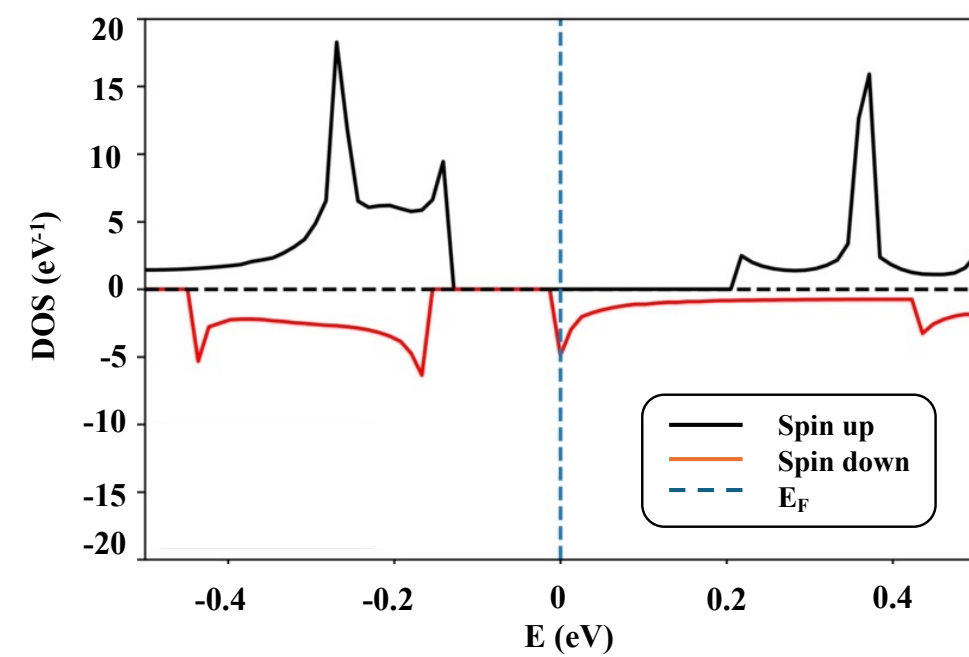


Fig. 3.20 DOS and bandstructure of Ti adsorbed SiCNT(6,0)

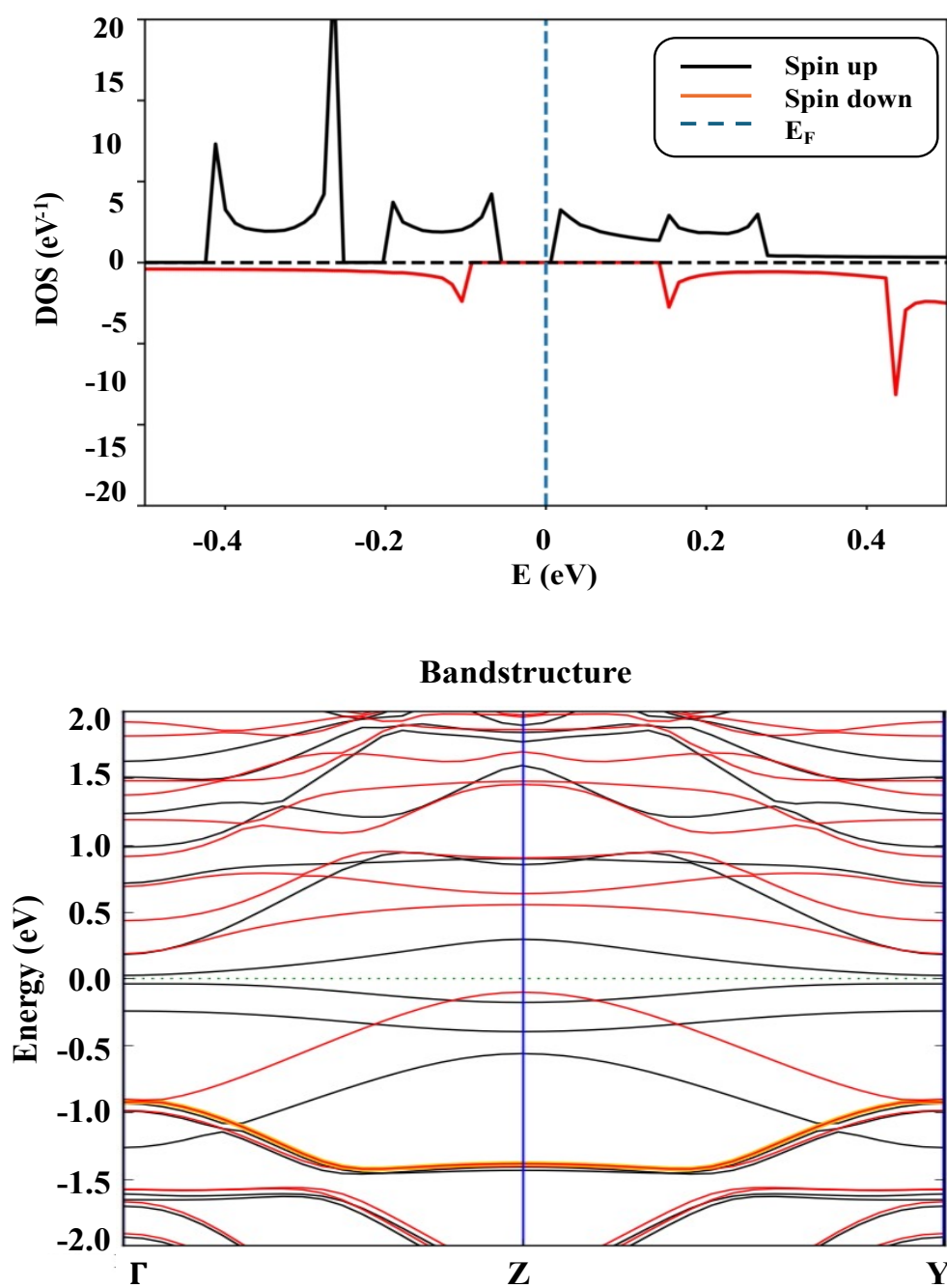


Fig. 3.21 DOS and bandstructure of Zr adsorbed SiCNT(6,0)

Table 3.2 Magnetic Properties of (6,0) SiCNT after adsorption of TM

Simulated structure	Spin- Up	Spin- Down	Magnetic Moment per atom (μ_B)	Magnetic Behaviour
Pristine (6,0)SiCNT	Passed	Passed	NIL	Non- Magnetic
Ag adsorbed (6,0)SiCNT	Passed	Passed	-0.44	FM
Co adsorbed (6,0)SiCNT	Not Passed	Passed	+1.26	HMF
Cr adsorbed (6,0)SiCNT	Passed	Not Passed	+5.33	HMF
Cu adsorbed (6,0)SiCNT	Passed	Passed	+0.28	FM
Fe adsorbed (6,0)SiCNT	Passed	Not Passed	+2.83	HMF
Mo adsorbed (6,0)SiCNT	Not Passed	Not Passed	+4.03	Non- Magnetic
Ti adsorbed (6,0)SiCNT	Not Passed	Passed	+1.76	HMF
Zr adsorbed (6,0)SiCNT	Not Passed	Not Passed	+1.96	Non- Magnetic

However, on adsorption of Mo- atom on SiCNT(6,0), a strong magnetic moment of $4.03 \mu_B$ was observed, but its spin-DOS doesn't show any conducting states in either of the spin channels (Fig. 3.19). Zr- atom also was unable to transform the non-magnetic nature of SiCNT(6,0) to magnetic due to the non-availability of conducting states (see Fig. 3.21) even with a magnetic moment of $1.96 \mu_B$. Therefore, the adsorbed structure can remain non-magnetic even with a high value of calculated magnetic moment. Hence, its correlation with bandstructure and its spin-DOS is necessary to comprehend the impact of adsorption.

3.3.3 SiCNT (8,0)

The pristine SiCNT(8,0) is a semiconductor [97], [98] and the same can be observed from the bandstructure and the DOS of Fig. 3.22. The bandstructure plot shows a significant energy gap at the Fermi level, which signifies its semiconducting nature. The non-availability of conducting states in either channel (spin-up/ spin-down) at the Fermi level in the s-DOS verifies its semiconducting nature. Table 3.3 shows that pristine zigzag (8,0) SiCNT has zero magnetic moment. This verifies that (8,0) SiCNT in pristine form is non-magnetic.

However, when the Co atom is adsorbed on (8,0) SiCNT, it remains semiconducting as its bandstructure in Fig. 3.24 shows a finite energy gap at the Fermi level. Also, its s-DOS, shown in Fig. 3.24 has no available conducting states, which makes it non-magnetic. Table 3.3 shows a negative magnetic moment for Co- adsorbed (8,0) SiCNT, which is primarily due to the unpaired d- orbital electron of the Co atom, but as no conducting states are visible from the spin-DOS, it remains non-magnetic. Similar non-magnetic behaviour can be seen in Fig. 3.27 and Fig. 3.28 for Fe-adsorbed and Mo-adsorbed (8,0) SiCNT structures. They have significant magnetic moments of $2 \mu_B$ and $4 \mu_B$ respectively. This magnetic moment is mainly contributed by the transition Fe and Mo atoms, respectively, but it has no impact on the magnetic nature of the adsorbed structure as no conducting states in either spin-up or spin-down channels are available in the s-DOS, as shown in Fig. 3.27 and Fig. 3.28.

When (8,0) SiCNT is adsorbed with an Ag- atom, its semiconducting nature changes to metallic as its bandstructure shows zero bandgap at the Fermi level (see Fig. 3.23). Although it has conducting states in both spin-up and spin-down channels, it preserves its non-magnetic nature due to negligible magnetic moment (see Table 3.3).

Table 3.3 Magnetic Properties of (8,0) SiCNT after adsorption of TM

Simulated structure	Spin- Up	Spin- Down	Magnetic Moment per atom (μ_B)	Magnetic Behaviour
Pristine (8,0)SiCNT	Not Passed	Not Passed	NIL	Non-Magnetic
Ag adsorbed (8,0)SiCNT	Passed	Passed	NIL	Non-Magnetic
Co adsorbed (8,0)SiCNT	Not Passed	Not Passed	-1.0	Non-Magnetic
Cr adsorbed (8,0)SiCNT	Not Passed	Passed	+5.4	HMF
Cu adsorbed (8,0)SiCNT	Not Passed	Passed	+0.4	HMF
Fe adsorbed (8,0)SiCNT	Not Passed	Not Passed	+2.0	Non-Magnetic
Mo adsorbed (8,0)SiCNT	Not Passed	Not Passed	+4.0	Non-Magnetic
Ti adsorbed (8,0)SiCNT	Passed	Passed	+3.1	HMF
Zr adsorbed (8,0)SiCNT	Passed	Passed	+2.5	HMF

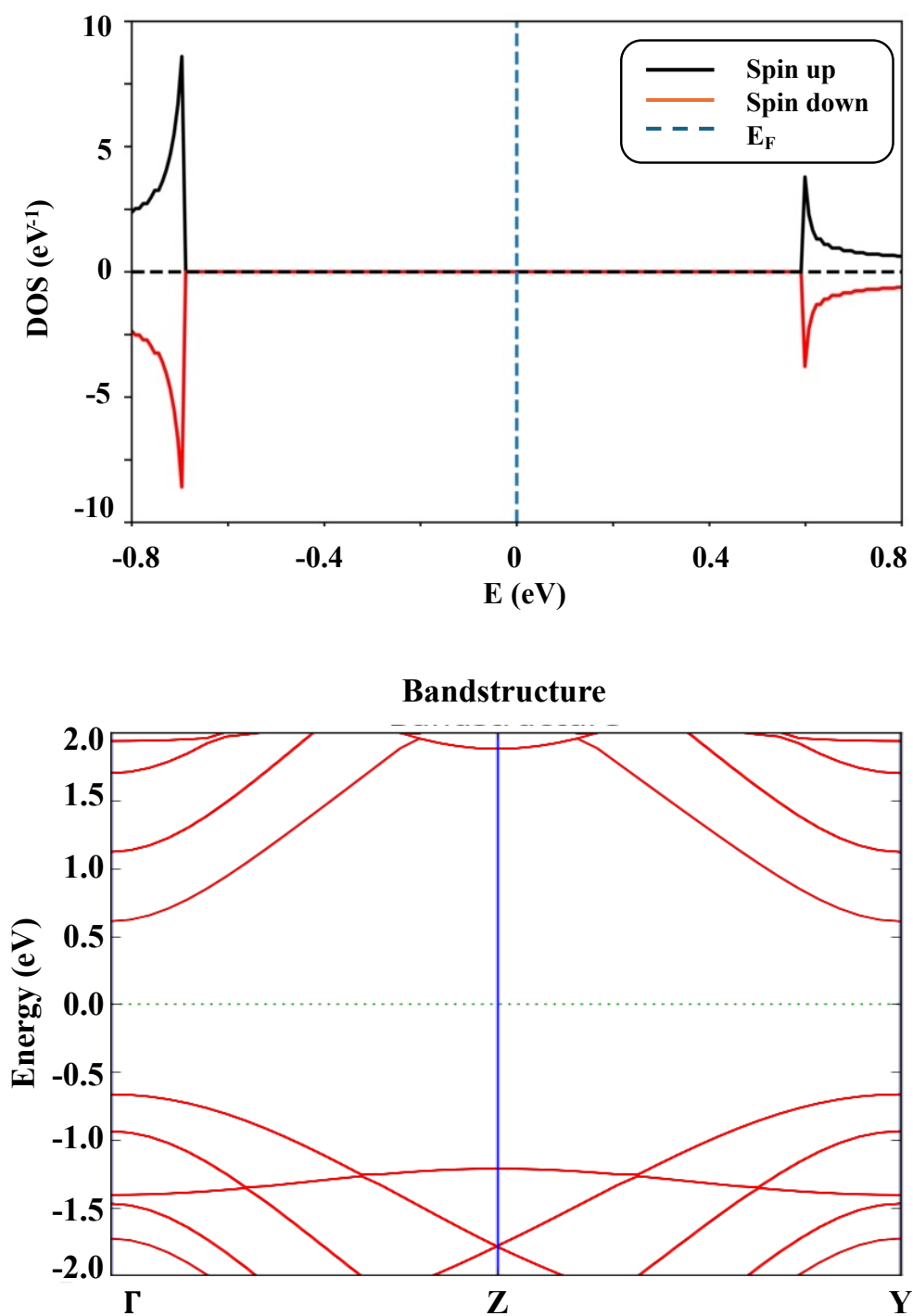


Fig. 3.22 DOS and bandstructure of Pristine SiCNT(8,0)

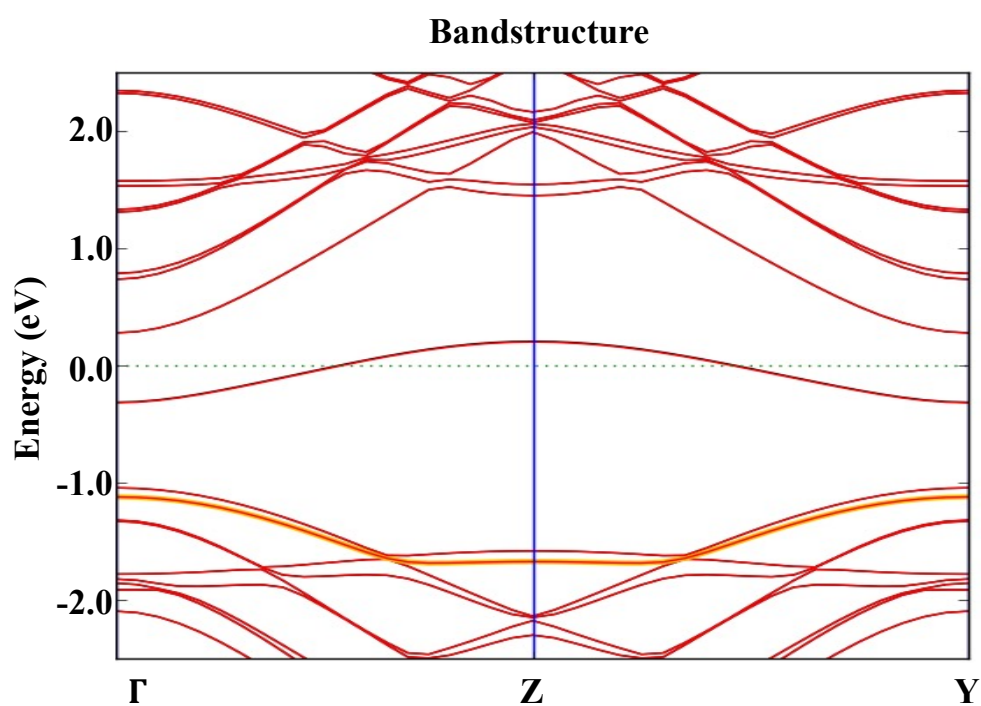
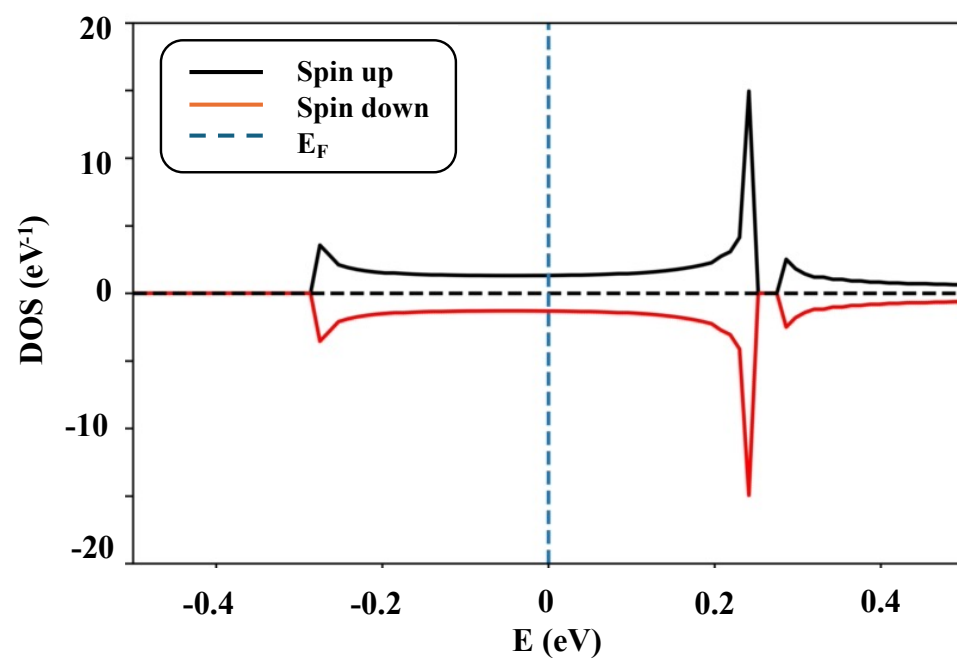


Fig. 3.23 DOS and bandstructure of Ag adsorbed SiCNT(8,0)

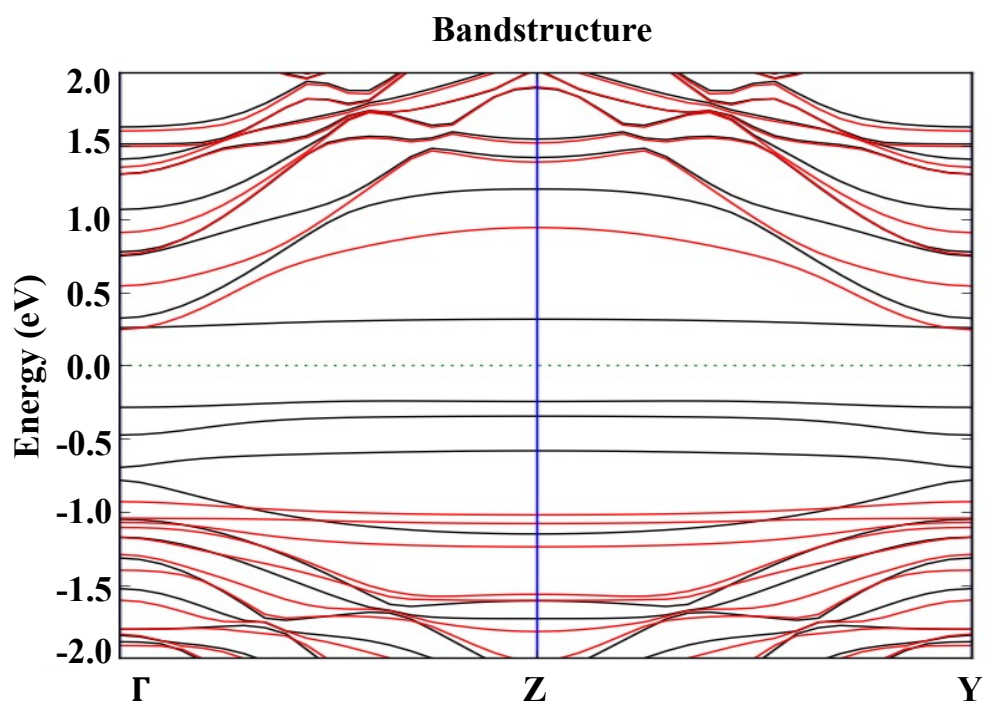
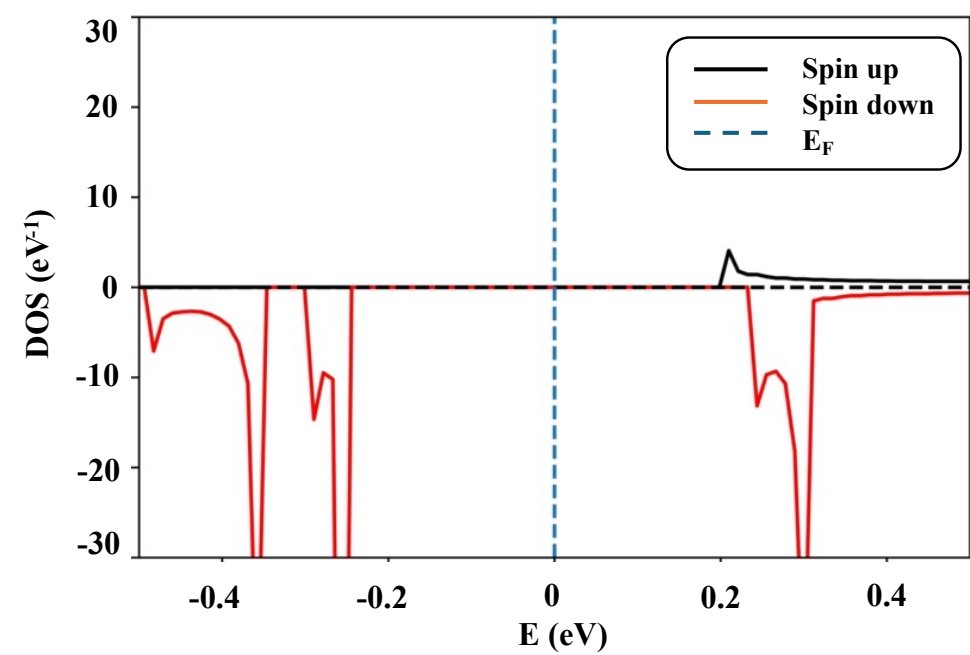


Fig. 3.24 DOS and bandstructure of Co adsorbed SiCNT(8,0)

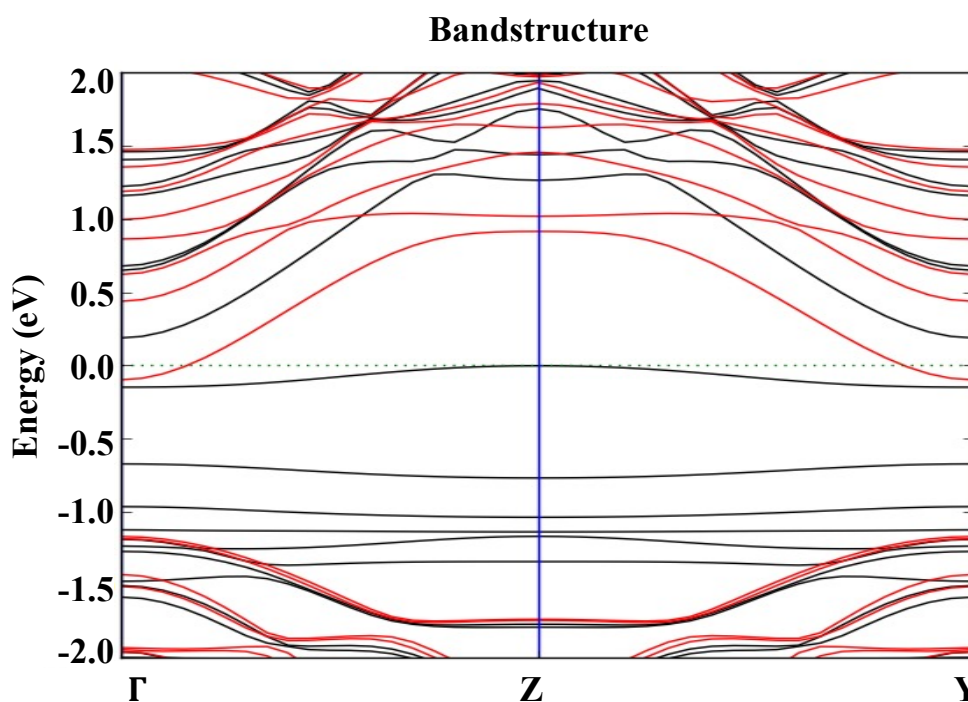
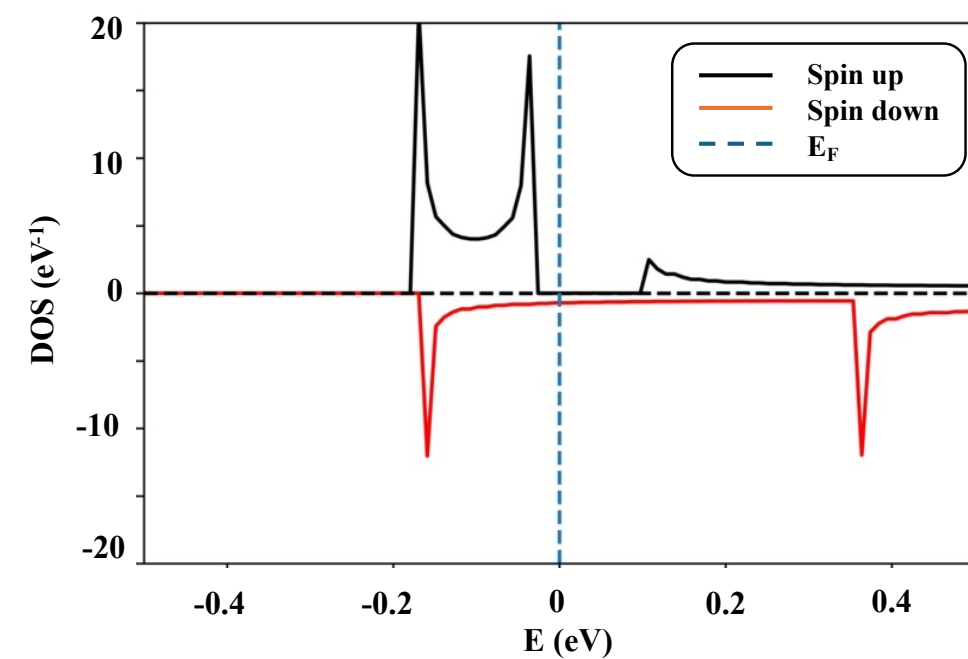


Fig. 3.25 DOS and bandstructure of Cr adsorbed SiCNT(8,0)

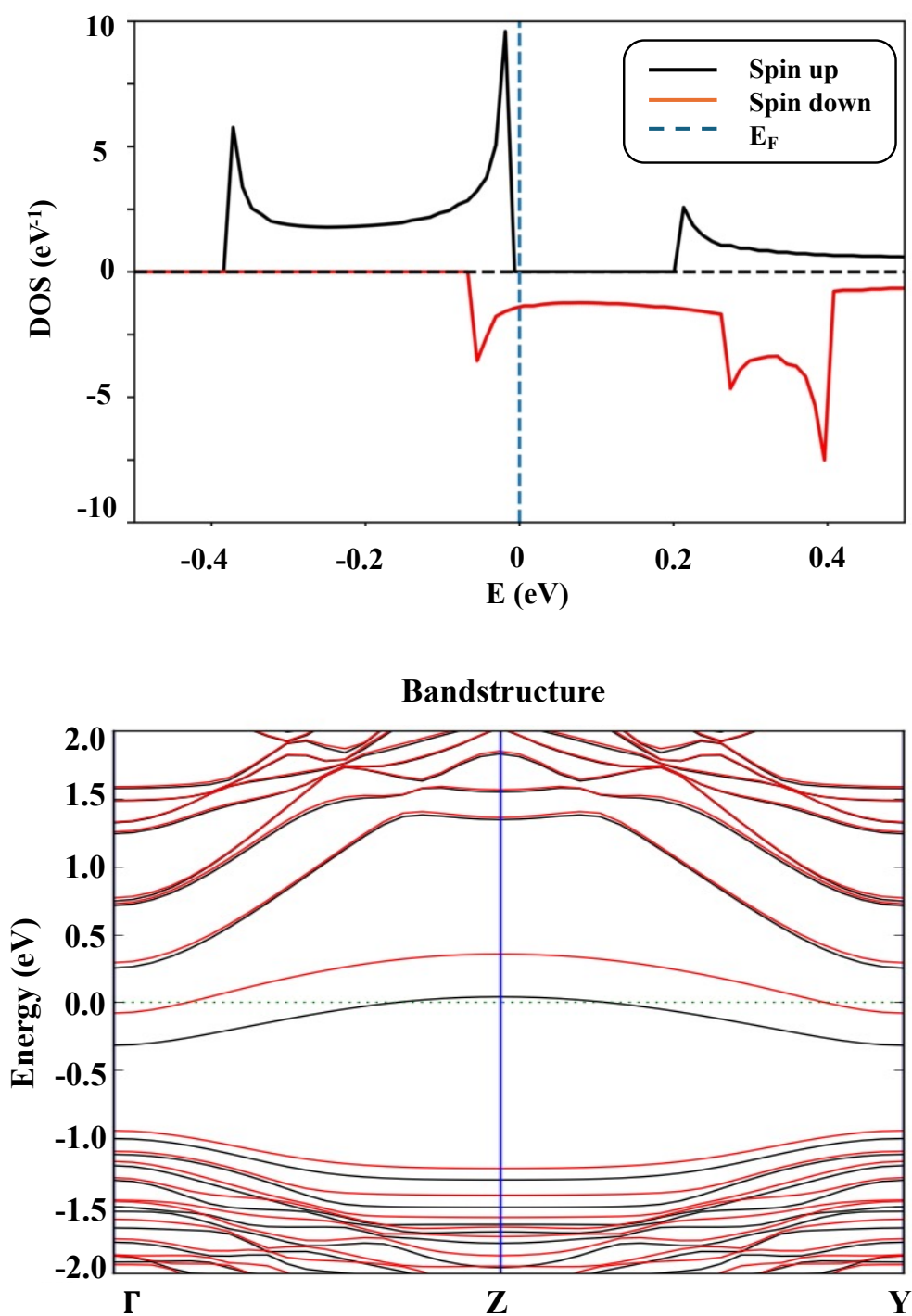


Fig. 3.26 DOS and bandstructure of Cu adsorbed SiCNT(8,0)

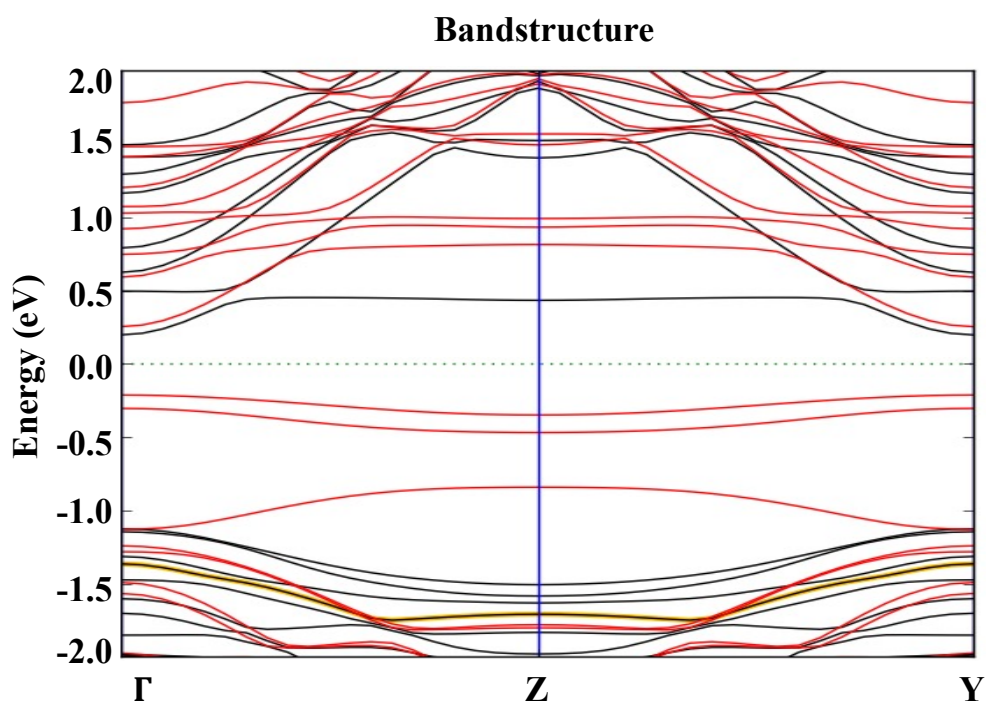
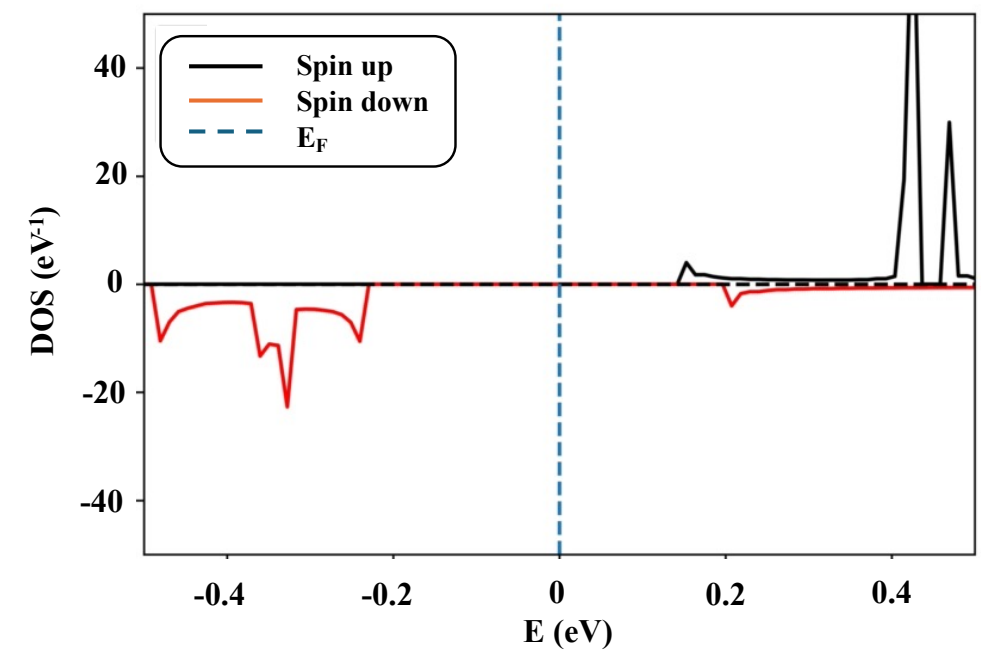


Fig. 3.27 DOS and bandstructure of Fe adsorbed SiCNT(8,0)

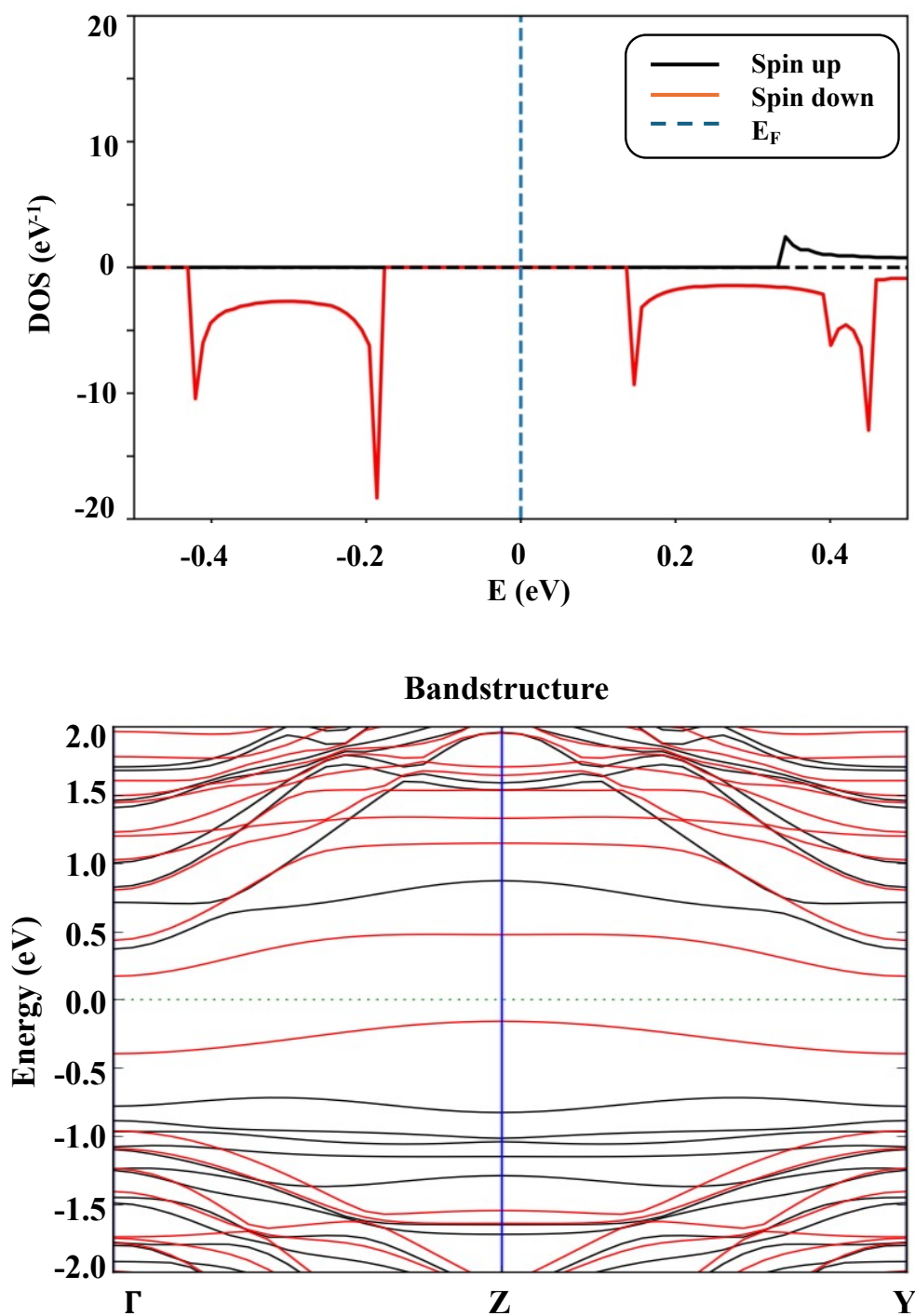


Fig. 3.28 DOS and bandstructure of Mo adsorbed SiCNT(8,0)

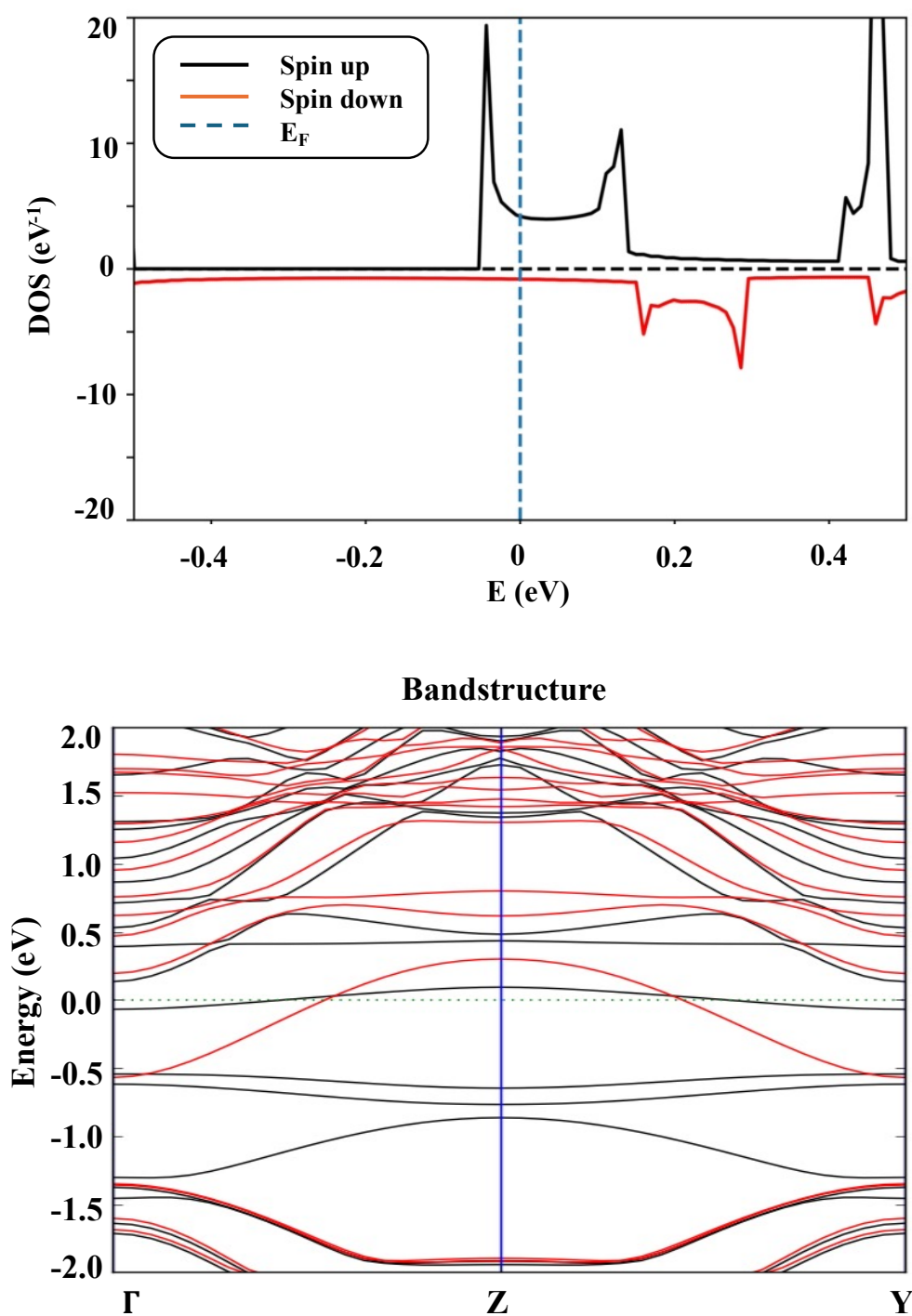


Fig. 3.29 DOS and bandstructure of Ti adsorbed SiCNT(8,0)

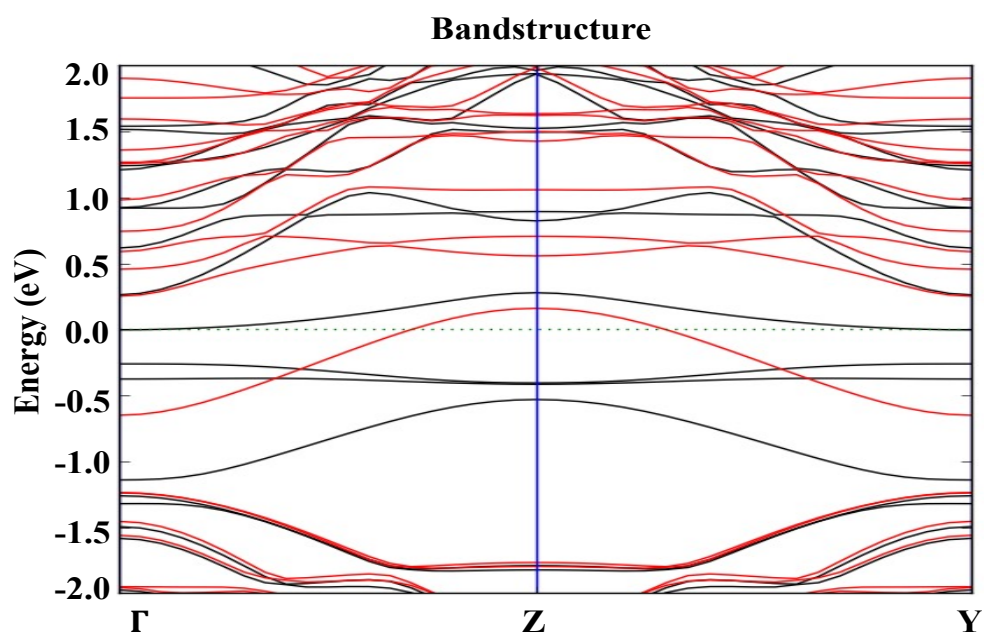
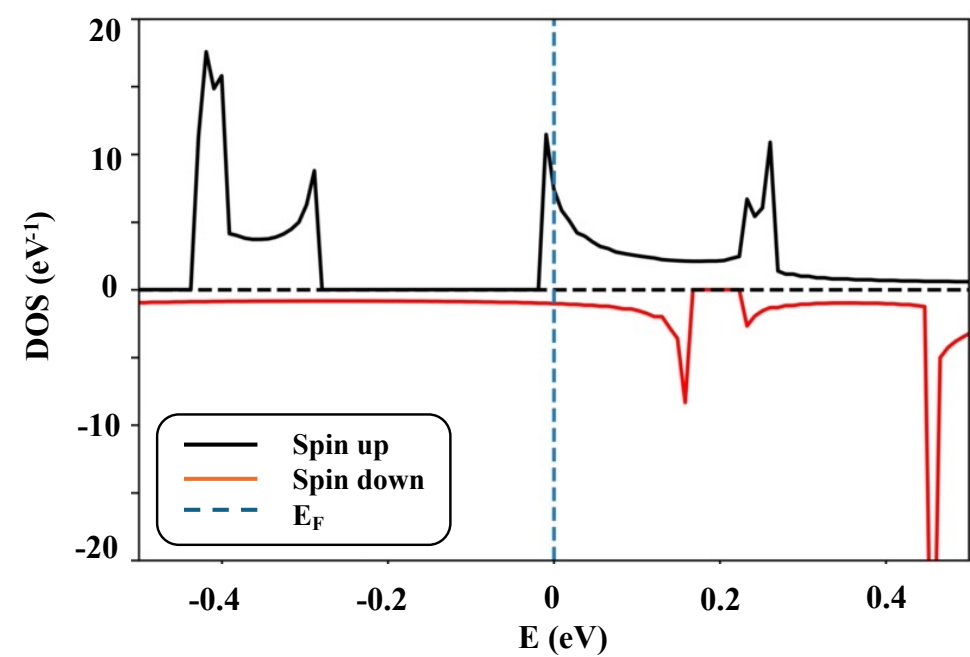


Fig. 3.30 DOS and bandstructure of Zr adsorbed SiCNT(8,0)

However, the Cr-adsorbed (8,0) SiCNT structure is able to change its non-magnetic behaviour to magnetic. It exhibits the highest magnetic moment of $5.47 \mu_B$, which is the highest among all the (8,0) SiCNT simulated structures (see Table 3.3). Its s-DOS, shown in Fig. 3.25 allows conduction in the spin-down channel while simultaneously blocking the spin-down channel, making it an HMF material. Similarly, the Cu-adsorbed (8,0) SiCNT also results in an HMF material, which allows conduction in the spin-down channel, as shown in Fig. 3.26. Its magnetic nature can also be verified by its non-zero magnetic moment of $0.4 \mu_B$. The simulated Ti- adsorbed and Zr- adsorbed (8,0) SiCNT structures also result in magnetic structures. Their s-DOS and bandstructure can be seen in Fig. 3.29 and Fig. 3.30 respectively. Their s-DOS shows that conduction is allowed only in spin-up channels, whereas negligible conduction can be observed in spin-down channels. Ti- on adsorption produces a strong magnetic moment of $3.1 \mu_B$ in the adsorbed structure. Zr- adsorbed (8,0) SiCNT exhibited a strong magnetic nature with a calculated magnetic moment of $2.5 \mu_B$ as seen in Table 3.3. These strong magnetic moments, along with spin-DOS showing conduction in only the spin-up channel, confirm the transformation of non-magnetic SiCNT to HMF structures on adsorption of Ti and Zr.

3.4 Summary

This chapter investigates the transformation of zigzag SiCNTs with varying chiralities from non-magnetic to magnetic materials through the adsorption of various transition metals. Utilizing density functional theory (DFT), the study examines the electronic and magnetic properties of both metallic zigzag (SiCNT(4,0) & SiCNT(6,0)) and semiconducting zigzag (8,0) SiCNTs upon TM adsorption. Pristine zigzag (4,0) SiCNT and (6,0) SiCNT are metallic but non-magnetic, while zigzag (8,0) SiCNTs are semiconducting and non-magnetic.

The investigation reveals that adsorbing TMs like Co, Cr, Fe, Mo, and Ti on (4,0) SiCNTs induces HMF behaviour characterized by significant magnetic moments and spin-selective conduction. Additionally, Cu adsorption on (4,0) SiCNTs results in FM behaviour with notable magnetic moments in both spin channels.

When chirality is changed to (6,0) SiCNT, which is also metallic, then adsorption induces the magnetic moment in the adsorbed structures. Co, Fe, Cr and Ti- adsorbed structures exhibited HMF properties, while Ag and Cu- adsorbed structures exhibited FM properties. Mo and Zr- adsorbed (6,0) SiCNT structures preserved their non-magnetic nature.

Similarly, Cr, Cu, Ti, and Zr adsorption on (8,0) SiCNTs induces HMF properties, transforming their non-magnetic nature. Despite inducing magnetic moments, Fe and Mo adsorbed on (8,0) SiCNTs do not significantly alter their non-magnetic nature. The study employs the Atomistix Toolkit for DFT simulations, confirming changes in

electronic and magnetic properties through s-DOS and bandstructure analysis. Adsorption energy calculations indicate stable and thermodynamically favourable structures.

These findings suggest that TMs are able to induce magnetization in both metallic and semiconducting SiCNTs. The study also shows the impact of change of chirality in SiCNTs as in the case of SiCNT(4,0) and SiCNT(6,0). Also, it confirms that TM-adsorbed SiCNTs are suitable electrode materials for spintronic devices such as MTJs and spin valves, which require efficient spin filtering. The ability to induce magnetization in SiCNTs through TM adsorption enhances their potential for use in advanced spin-based electronic devices.

Chapter 4

TRANSITION METAL INDUCED MAGNETIZATION AND SPIN-POLARIZATION IN BLACK ARSENIC PHOSPHORUS

4.1 Introduction

Spintronics is an emerging field where the electron's spin can be used for current flow in electronic devices and systems. The involvement of spin opens new opportunities for the development of novel electronic devices [16], [99]. The development of these spin-based devices is based on choosing suitable materials which support spin-based characteristics and transport properties. With the advancement in process technology, many spin characteristics like spin-filtering effect (SFE) [100], GMR [101] and Tunnel Magnetoresistance (TMR) have been discovered by theoretical and experimental research on the novel 2D materials [102], [103]. Graphene, black-phosphorus, and silicene are some of the 2D materials of immense interest to both theoretical and experimental research in spintronics [104], [105], [106], [107].

Since the discovery of graphene in 2004, the global scientific community has shown considerable interest in two-dimensional (2D) materials due to their exceptional physical properties. Graphene, with its ultrahigh surface area, mechanical flexibility, and remarkable electrical conductivity, has positioned itself as a high-performance electrode material for energy storage devices [108], [109], [110], [111], [112], [113]. Despite the impressive properties of graphene, the conventional graphite anode in Lithium-Ion Batteries (LIB) faces challenges meeting the growing demands of new storage technologies and the electronic devices market due to its low energy density [114]. Consequently, there is a pressing need to identify advanced electrode materials with enhanced capacities.

In recent years, the study of 2D materials, beyond graphene, has reached new heights, driven by their improved charge carrier ability and higher energy density compared to conventional anode materials [23]. The small volume-to-surface area ratio and exposed surface of a 2D structure allow for controlled manipulation of material properties through impurity doping or defect formation [23], [38], [84], [115], [116]. For instance, the synthesis of 2D phosphorene (Black-P) with a honeycomb structure has garnered attention for its reported ultra-high electron mobility of up to $10^4 \text{ cm}^2/\text{V-s}$ [32], [115].

However, black phosphorus, while promising, is unstable at room temperature and has a fixed band gap, limiting its use in optoelectronics devices. Another notable 2D material, b-AsP, has emerged with higher stability at room temperature and

modulation properties, such as a tunable bandgap compared to black phosphorene [84]. Researchers, including Zhang et al., have proposed the incorporation of AsP in doped atoms, resulting in a transition from semiconductor to metal properties, making it a potential electrode material for Li and Na batteries. Thermodynamically, the composition of b-AsP is most stable when the ratio of As: P is taken as 1:1 [117]. Chemically, AsP has 3 possible configurations: AsP-1, AsP-2 and AsP-3. In AsP-1 configuration, a bond exists only between As and P, while in AsP-2, a bond exists between P-P, As-As and As-P, wherein the top layer consists of only P atoms while only As atoms exist in the bottom layer. AsP-3 configuration consists of in-plane As-P bonds and out-of-plane As-As and P-P bonds [39]. Among all the three chemical configurations, AsP-3 has the maximum bandgap and highest electron mobility of $14380 \text{ cm}^2/\text{V-s}$ [118], [119].

Recent studies indicate that the adsorption or doping of transition metals on non-magnetic materials induces magnetic moment and spin polarization, transforming their nature into magnetic materials. These magnetic materials, exhibiting FM or HMF behaviour upon specific transition metal adsorption, find applications as electrode materials in spin-based devices such as MTJ and spin valves [16], [35], [42], [55], [120]. They offer high spin filtration ($\sim 100\%$) and magnetoresistance ($\sim 103\%$), crucial parameters for evaluating the performance of spin-based devices [29], [71], [120], [121], [122].

Therefore, b-AsP, as a 2D material with high mobility and tunable bandgap, presents an intriguing prospect for transition metal adsorption. This study aims to explore the effects of the adsorption of transition metals on the properties of resulting b-AsP structures. The induced magnetisation and spin polarization in the adsorbed structures could make it a suitable candidate for use as an FM/HMF electrode in the design and synthesis of spin-based devices, such as MTJs and spin-valves.

As AsP is a non-magnetic semiconductor in pristine form, for AsP, it should be made spin-polarized for its applications in spin-dependent transport. In the present study, transition metals (Ti, Cr, Fe, Co, Cu, Zr, Mo and Ag) were adsorbed on pristine AsP-3 configuration to investigate their impact on spin properties. All investigations are performed using first-principles calculations. The selection of AsP-3 among three possible chemical configurations is made owing to the presence of higher mobility in this configuration. Relaxed adsorbed geometry for all transition metal adsorbed structures was obtained before calculating bandstructure, spin-density of states (spin-DOS) and magnetic moment. The results suggest the transition from nonmagnetic semiconducting to magnetic HMF and FM characteristics in transition metal-adsorbed AsP-3 structures.

4.2 Computational Details

The reciprocal effect results in the shifting of electric charge from transition metals to AsP-3, resulting in modified electronic and magnetic properties in AsP-3. The study focused on investigating the electronic and magnetic properties by introducing adsorbed transition metals on the surface of AsP-3. To achieve this, individual atoms of Ag, Co, Ti, Mo, Fe, Cu, Cr and Zr were placed in proximity to the non-magnetic semiconducting AsP-3 surface. The resulting atomic configuration was then relaxed until the forces acting on each atom reached a value of 0.05 eV/Å or lower.



Fig. 4.1 (a) Pristine Semiconducting AsP-3 (b) Co- adsorbed AsP-3

In this study, density functional theory (DFT) simulations were conducted using the Atomistix simulation Toolkit package [123]. The exchange-correlation energy was evaluated based on spin-polarized generalized gradient approximation (SGGA) employing numerical LCAO basis sets. A threshold energy of 130 Rydberg was utilized, and a k -point sampling scheme of (11,11,1) was applied along the x , y , and z axes.

To analyze the electronic properties, spin-polarized density of states (spin-DOS) calculations were performed for semiconducting AsP-3 as well as all the adsorbed structures. Additionally, band structure calculations were performed to confirm the results with the spin-DOS analysis. Furthermore, the magnetic characteristics were examined for all the adsorbed structures through the computation of their overall magnetic moment, confirming their magnetic characteristics.

The density of states (DOS) is a measure of the number of available states within a given energy range, E to $E + dE$. Mathematically, it can be represented as:

$$DOS(E) = \frac{\Delta n}{\Delta E \times L} = \frac{1}{\sqrt{2}\pi A} \left(E - \frac{E_g}{2} \right)^{-\frac{1}{2}} \quad (4.1)$$

In the provided equation, $DOS(E)$ denotes the density of states at a specific energy level E . The energy gap is represented by E_g , and $A = at$ corresponds to the coefficient of the Taylor expansion. The length of the AsP material is denoted by L .

Furthermore, the material's carrier concentration at a specific energy E can be determined by integrating the product of the density of states (DOS) and the probability density function, as expressed by the equation:

$$n(E) = \int DOS(E)f(E)dE \quad (4.2)$$

For confirming the feasibility of transition metals on the AsP-3 surface, the energy of adsorption can be calculated as:

$$E_{ads} = E_{structure} - [E_{TM} + E_{AsP-3}] \quad (4.3)$$

In the above equation, E_{ads} refers to the energy associated with the process of adsorption, $E_{structure}$ represents the total energy of adsorbed structure, E_{AsP-3} represents the total energy of the AsP-3 in intrinsic form, while E_{TM} denotes the total energy of a single transition metal [96].

4.3 Results and Discussions

Fig. 4.1(a) shows the relaxed geometric structure of pristine AsP-3, which is very similar to black phosphorene (b-P) [108]. The geometry has been constructed by substituting 50% of phosphorene (P) atoms in the unit cell of b-P with Arsenic (As) atoms. The geometry of the system was then optimized to ensure stability and suitability for further investigations. The band structure and spin-DOS calculations of pristine AsP-3 are also shown in Fig. 4.2. The calculated bandgap of the pristine AsP-3 is ~ 1.1 eV, confirming its semiconducting nature. The calculated bandgap is very similar to the bandgap reported in [23], [84]. The absence of magnetic properties in pristine AsP-3 can be verified through its spin-density of states (spin-DOS) plot, as illustrated in Fig. 4.2. The spin-DOS plot reveals the absence of conducting states at the Fermi energy level, confirming the non-magnetic nature of pristine AsP-3. Its magnetic moment is also calculated and is shown in Table 4.1. Zero magnetic moment of pristine semiconducting AsP-3 further verifies its non-magnetic nature. Based on these obtained results, it can be concluded that pristine AsP-3 is a non-magnetic semiconductor. These findings align with previous research studies in this field.

To investigate the influence of adsorption, it becomes crucial to examine the magnetic and electronic properties of the structures after the adsorption of transition metals. For the adsorption to take place, pristine AsP-3 surface was utilized as a substrate, and transition metal atoms were placed in close proximity to it. The resulting structure was then optimized through geometry relaxation process. Fig. 4.1(b) depicts the relaxed geometry of the Co atom adsorbed on the non-magnetic semiconducting AsP-3

(highlighted in pink). Similarly, the same procedure was applied to other transition metals individually adsorbed on pristine AsP-3, with subsequent relaxation to optimize the adsorbed structures. It can be observed that the transition metals on adsorption formed bonds with the pristine AsP-3, leading to changes in the electronic and magnetic properties. The adsorption energy was calculated for each structure to assess the feasibility of transition metal adsorption on AsP-3. The calculated adsorption energies were negative for all the structures, indicating that the adsorption process is exothermic and affirming the stability of the adsorbed structures.

As shown in Fig. 4.3, the bandstructure of AsP-3 has zero bandgap after adsorbing Ag. The materials whose bands cross the Fermi level are metallic in nature. This can also be observed from its s-DOS which shows the availability of conducting states at the Fermi level. This confirms its transition from semiconducting to metallic characteristics on adsorption of Ag. Additionally, it can also be observed from its s-DOS (Fig. 4.3) that the Ag-adsorbed structure has states available for conduction in both spin-up as well as spin-down channels. However, its calculated magnetic moment was found to be zero (see Table 4.1). So, Ag- atom on adsorption was unable to induce magnetization in the AsP-3, and it preserved its non-magnetic nature. So, Ag- atom can transform semiconducting AsP-3 to metallic but cannot change its magnetic nature. Similar characteristics were observed when AsP-3 was adsorbed with Cu and Mo. In Fig. 4.6, the bandgap of Cu-adsorbed structure is zero, leading to the transition from semiconducting to metallic nature. Its s-DOS also indicates the presence of conduction states in both spin-up and spin-down channels. However, its negligible magnetic moment (see Table 4.1) indicates its non-magnetic nature. Similarly, for Mo-adsorbed AsP-3, band structure and s-DOS are shown in Fig. 4.8. The resulting adsorbed structure is metallic, as its bandgap is zero. It has states available for conduction in spin-up as well as spin-down channels at the Fermi level, which is confirmed by its s-DOS. The structure, however, remains non-magnetic as its calculated magnetic moment is negligible. Therefore, Ag, Cu and Mo, when adsorbed on the surface of AsP-3, result in the transition of characteristics of AsP-3 from semiconducting to metallic but are unable to induce magnetization and spin-polarization in the adsorbed structures.

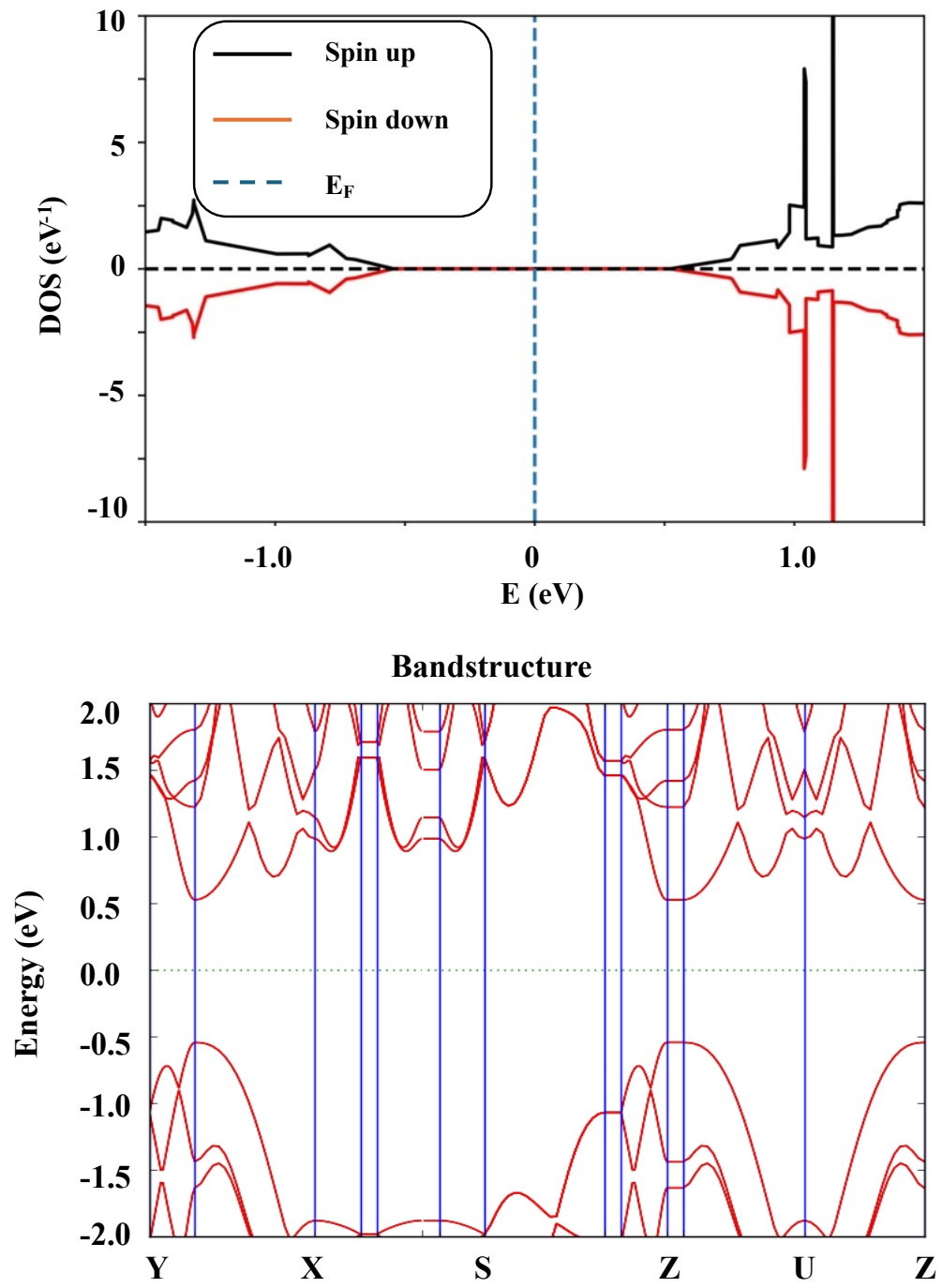


Fig. 4.2 DOS and bandstructure of pristine AsP3

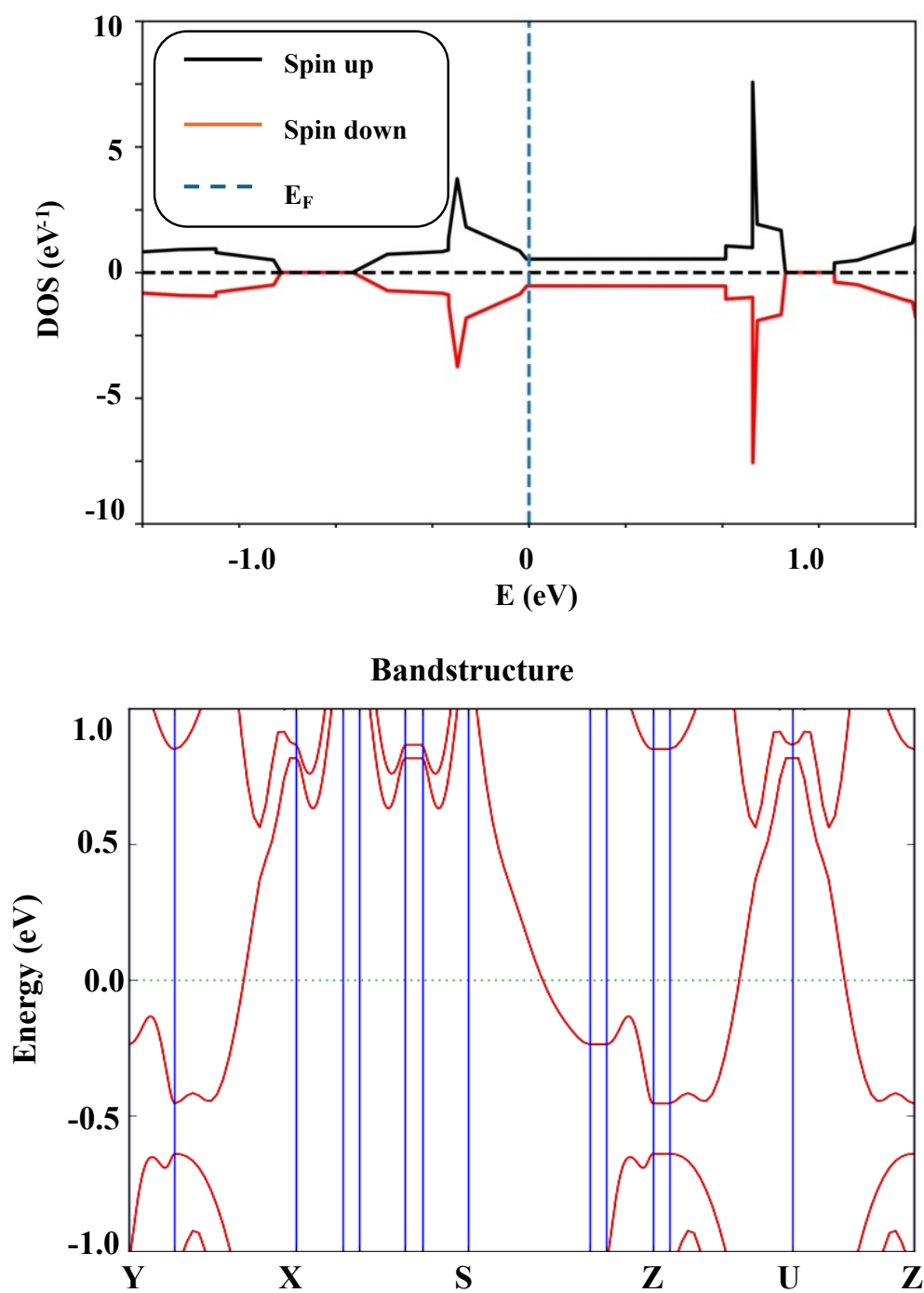


Fig. 4.3 DOS and bandstructure of Ag adsorbed AsP3

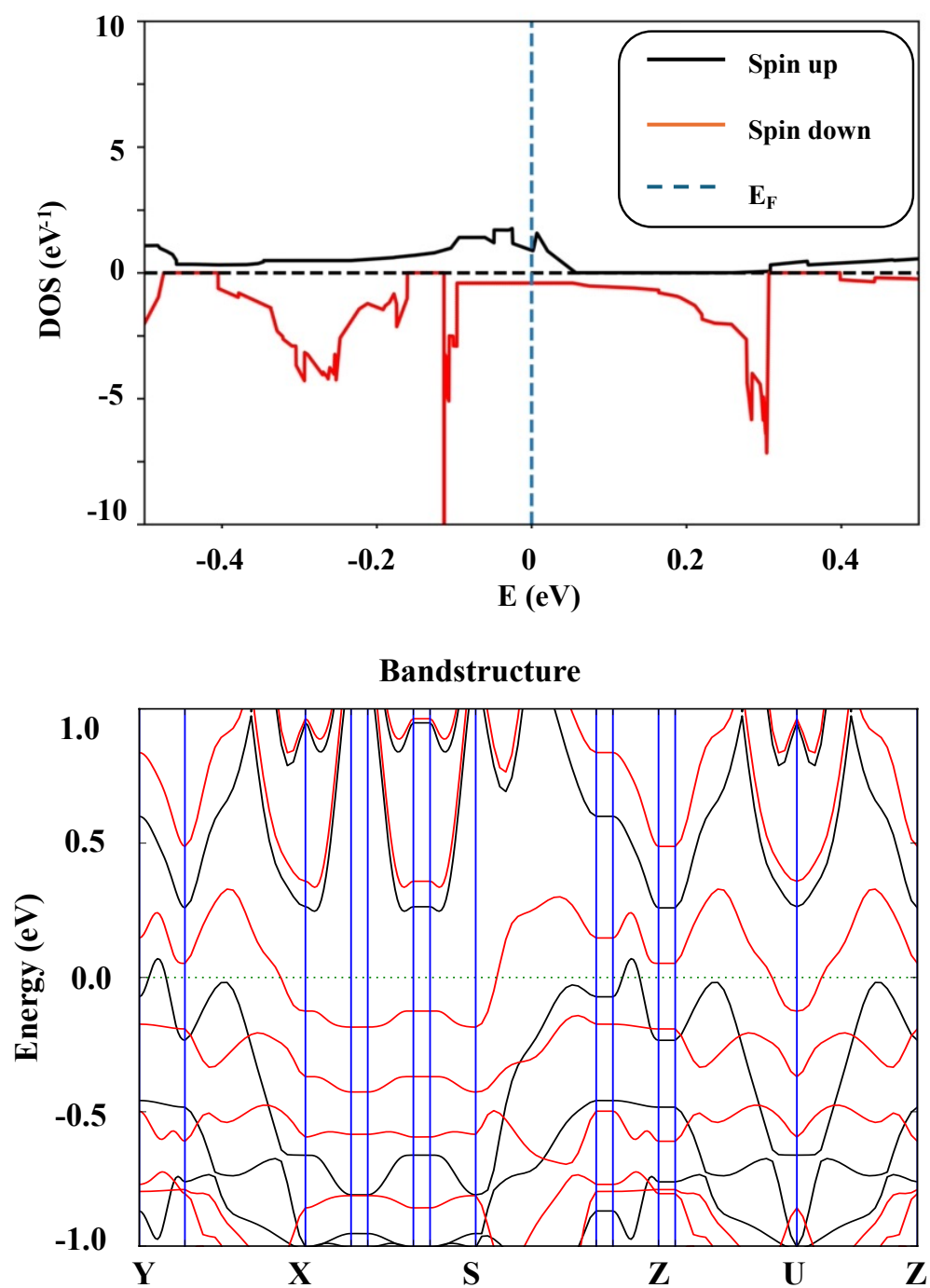


Fig. 4.4 DOS and bandstructure of Co adsorbed AsP3

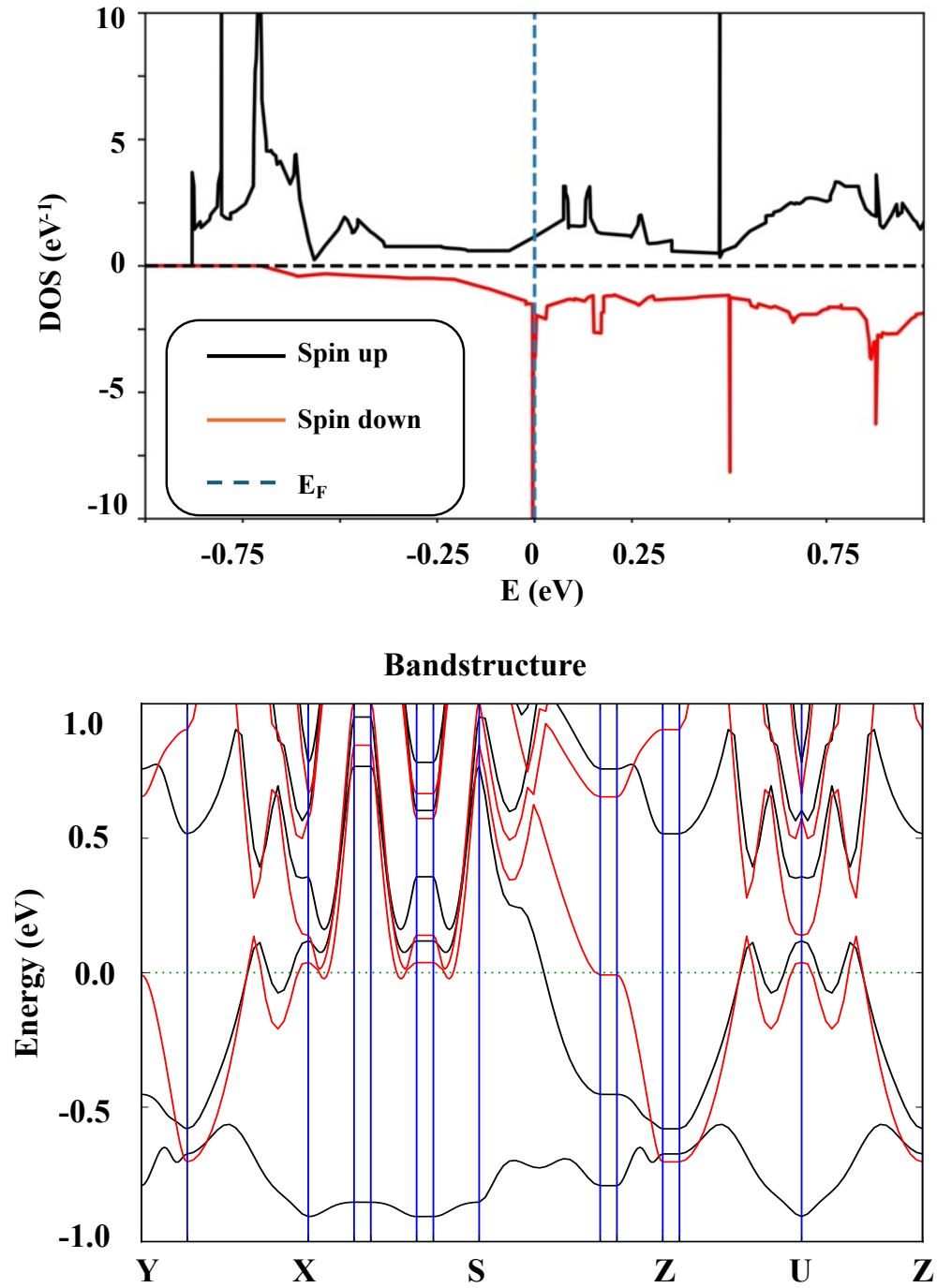


Fig. 4.5 DOS and bandstructure of Cr adsorbed AsP3

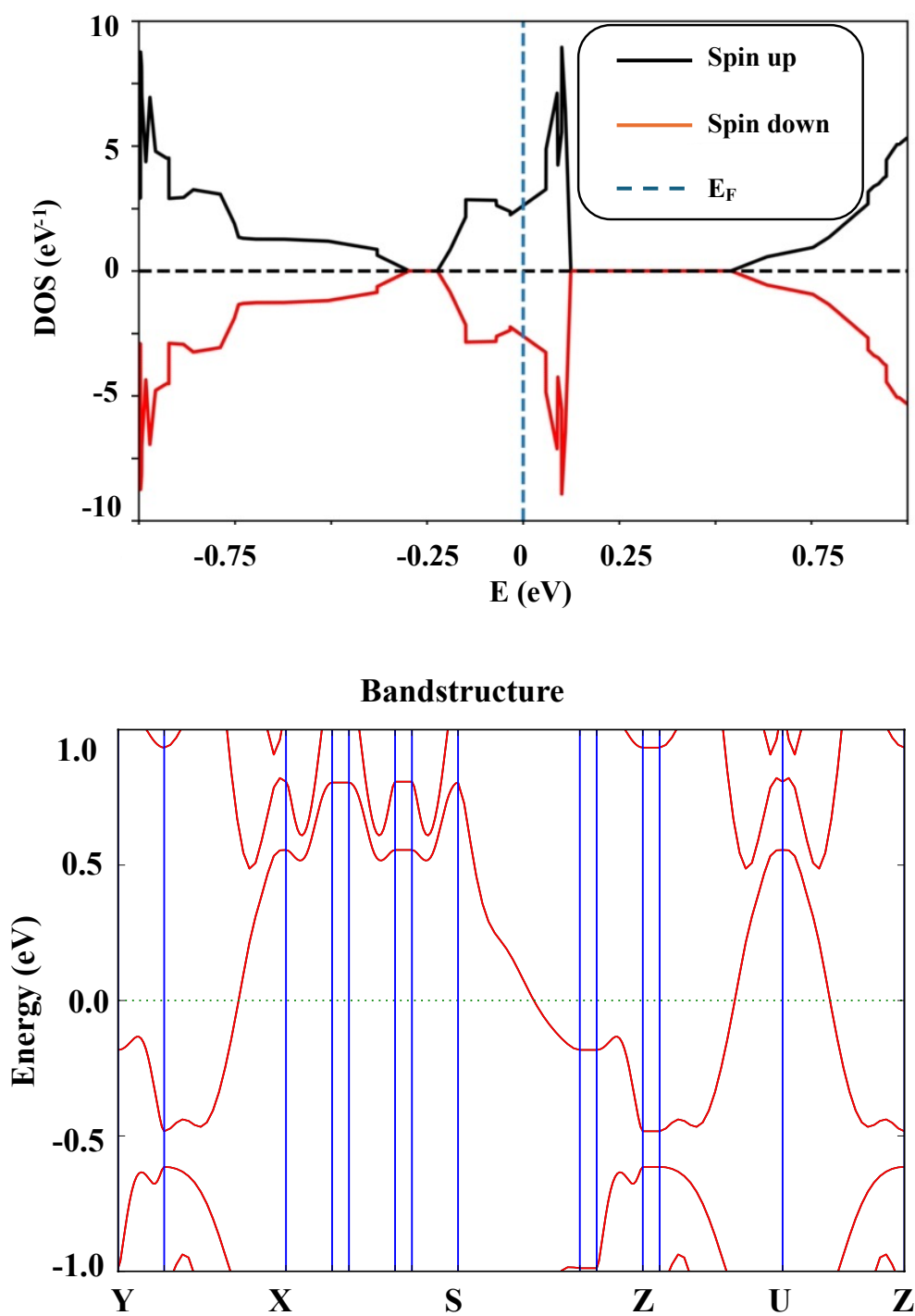


Fig. 4.6 DOS and bandstructure of Cu adsorbed AsP3

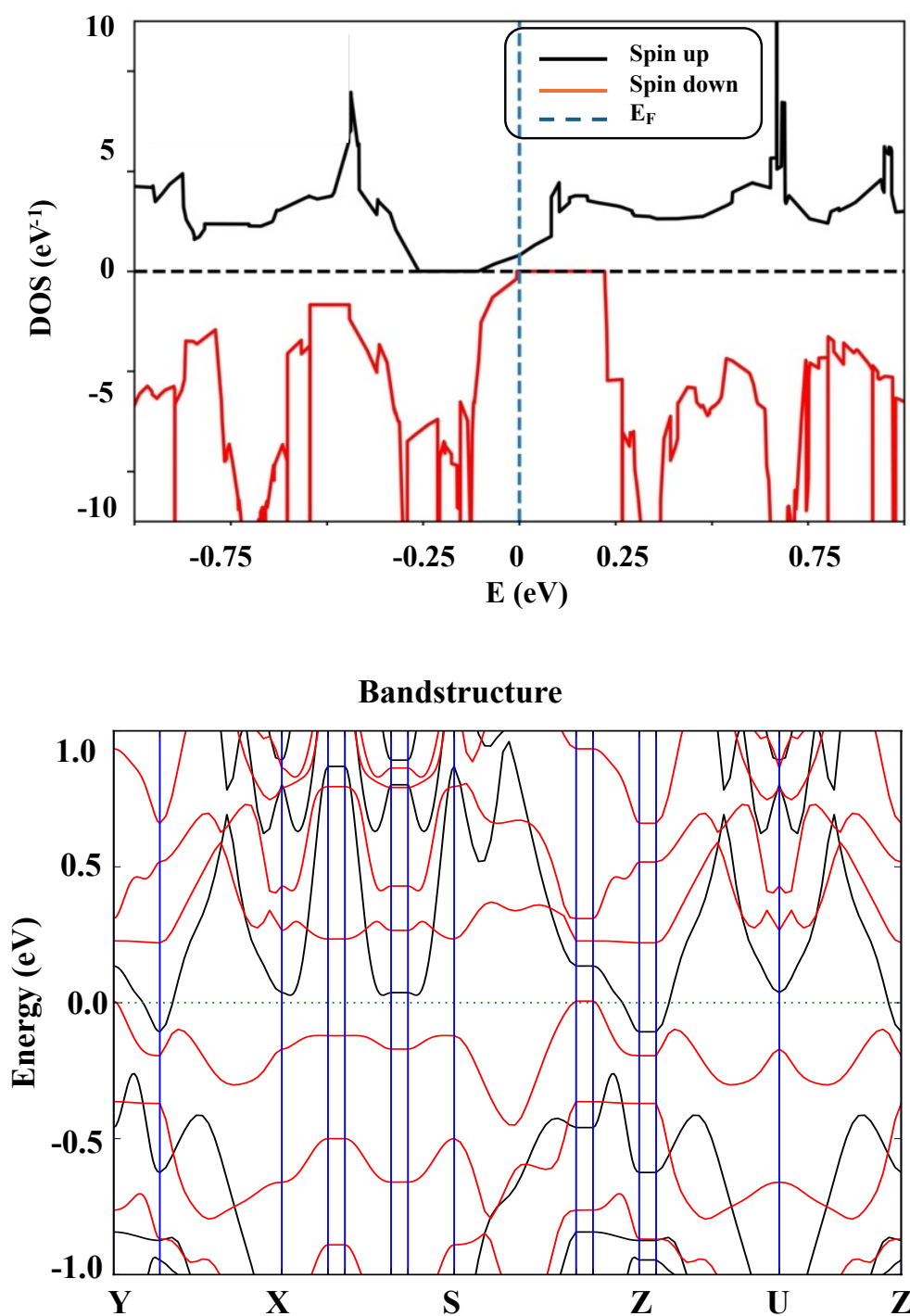


Fig. 4.7 DOS and bandstructure of Fe adsorbed AsP3

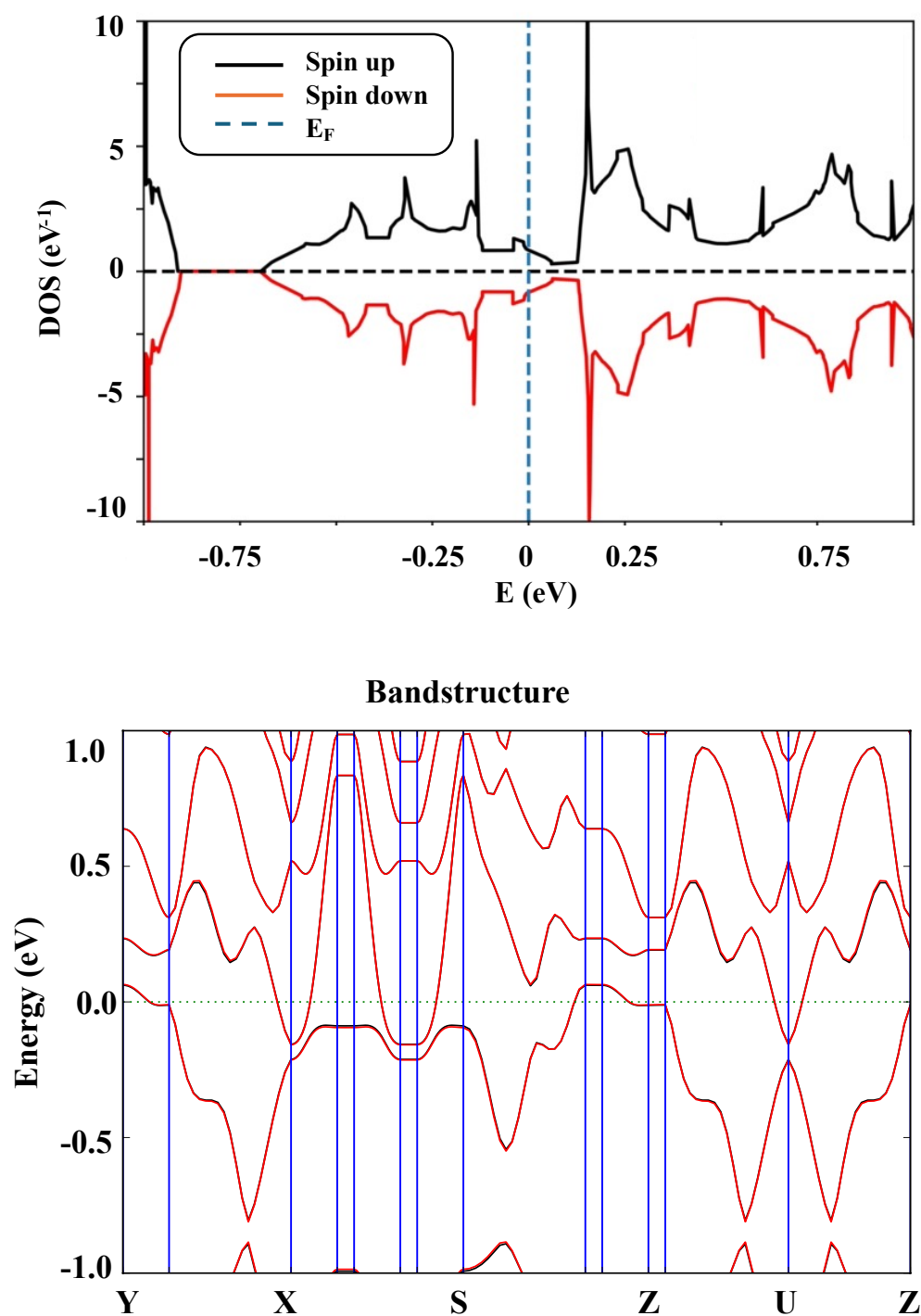


Fig. 4.8 DOS and bandstructure of Mo adsorbed AsP3

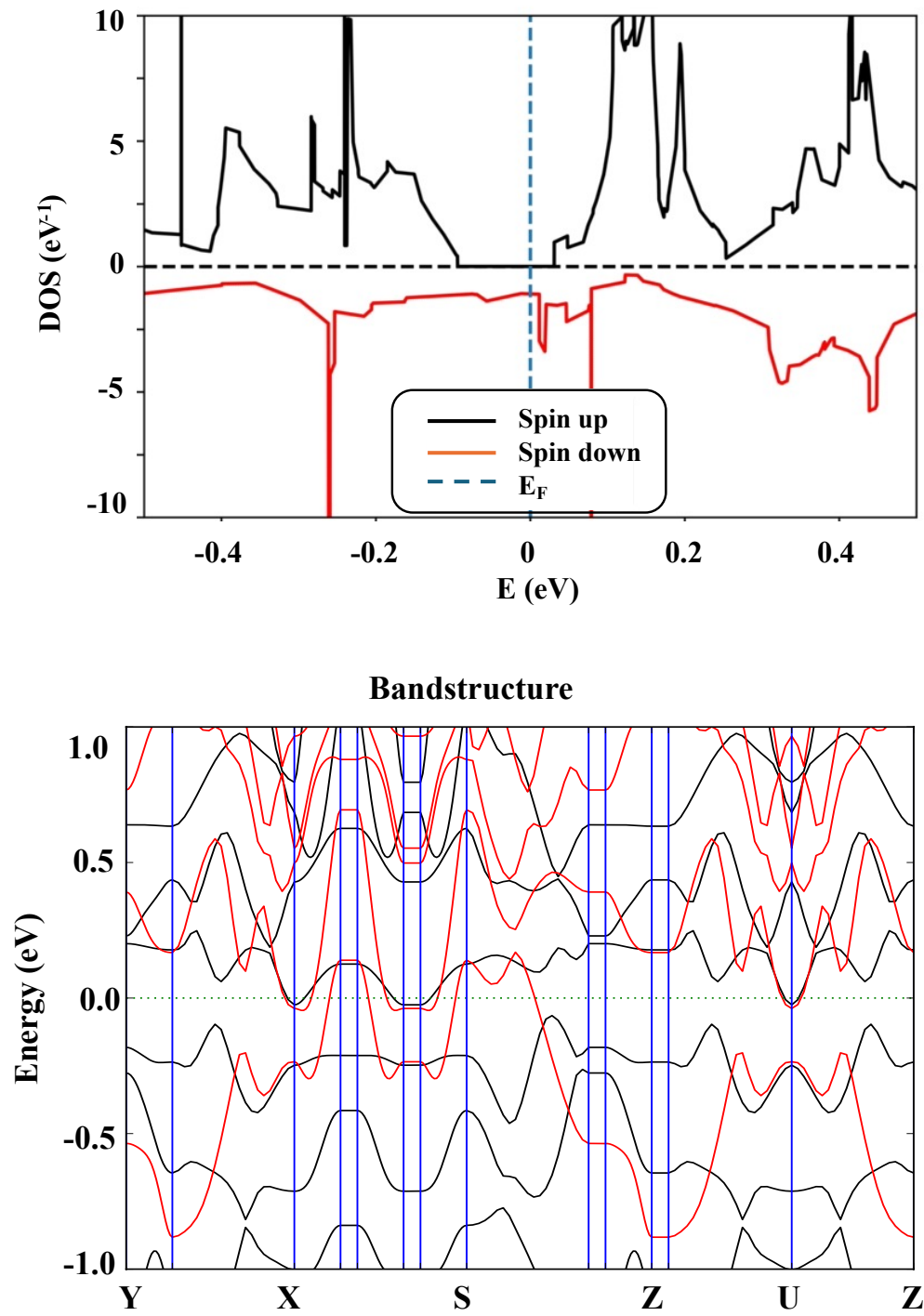


Fig. 4.9 DOS and bandstructure of Ti adsorbed AsP3

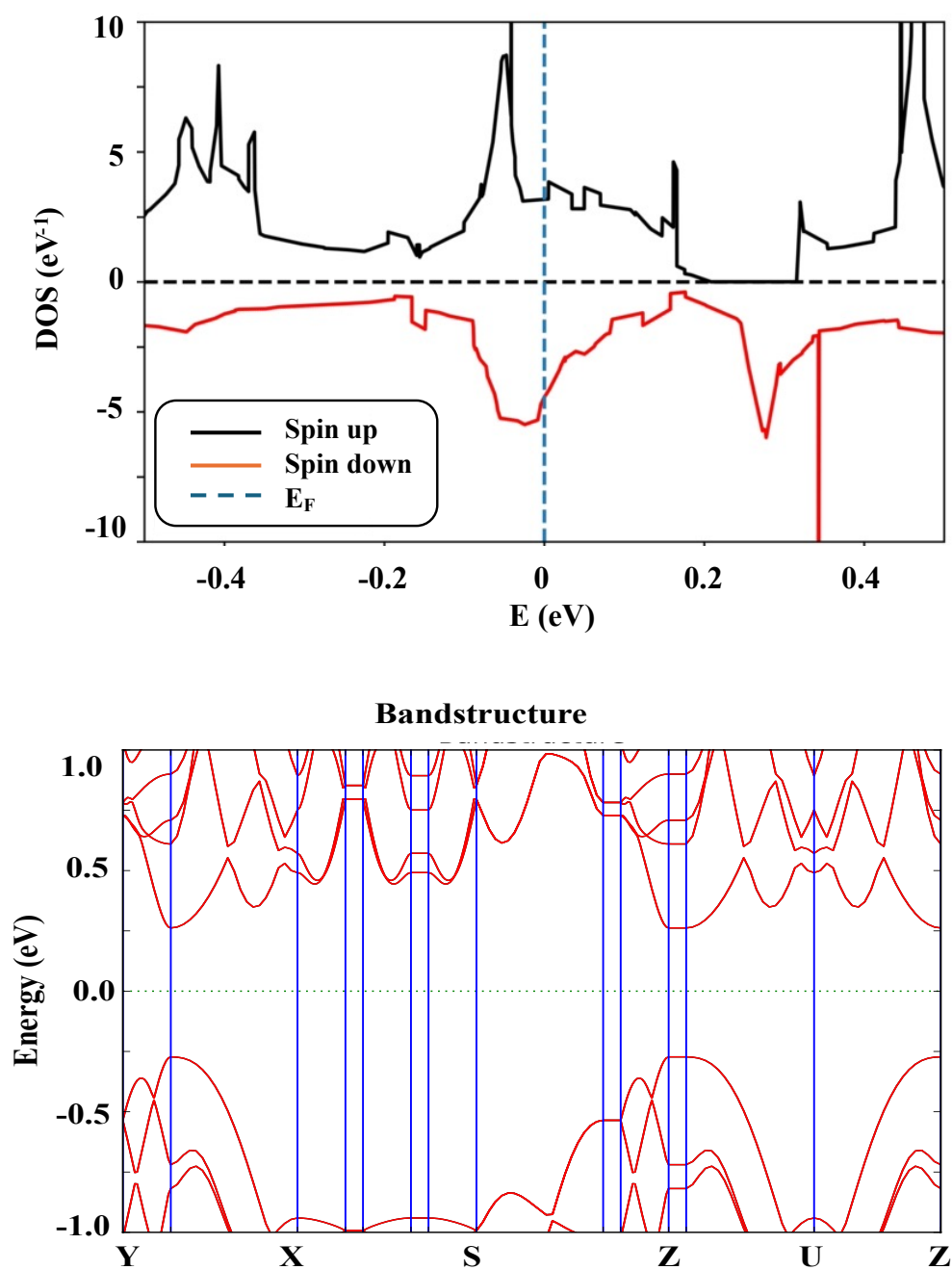


Fig. 4.10 DOS and bandstructure of Zr adsorbed AsP3

Table 4.1 Magnetic Properties of b-AsP-3 after adsorption of TM

Adsorbed structures	Spin-Up	Spin-Down	Magnetic moment /atom (μ_B)	Magnetic Characteristics
Pristine AsP-3	Absent	Absent	NIL	Non- Magnetic
Ag adsorbed AsP-3	Present	Present	NIL	Non- Magnetic
Co adsorbed AsP-3	Present	Absent	0.65	HMF
Cr adsorbed AsP-3	Present	Present	5.09	FM
Cu adsorbed AsP-3	Present	Present	NIL	Non- Magnetic
Fe adsorbed AsP-3	Present	Absent	2.15	HMF
Mo adsorbed AsP-3	Present	Present	NIL	Non- Magnetic
Ti adsorbed AsP-3	Absent	Present	2.21	HMF
Zr adsorbed AsP-3	Present	Present	0.91	FM

However, interesting characteristics were observed when Cr was adsorbed on the surface of AsP-3. The resultant structure transformed from semi-conducting to metallic. The zero bandgap of Cr-adsorbed AsP-3 can be observed in the band structure plot shown in Fig. 4.5. The magnetic moment of the structure was found to be $5.09 \mu_B$, which is highest among all other transition metal adsorbed structures of SiCNT(8,0). It indicates that Cr can induce magnetization very effectively in AsP-3. The spin-DOS of adsorbed structure (see Fig. 4.5) also shows the availability of conducting states in both spin-up and spin-down channels confirming its ferromagnetic nature. Similarly, Zr, when adsorbed on the surface of AsP-3, can transform the nature of AsP-3 from non-magnetic to ferromagnetic. Its band structure in Fig. 4.10 confirms overlapping states with no bandgap. The availability of conducting states, as visible in its s-DOS in both channels confirm its metallic nature. The calculated magnetic moment of $0.91 \mu_B$ although is lower but significant when compared with Cr adsorbed structure. Therefore, Cr and Zr, when adsorbed on the surface of AsP-3, induce ferromagnetism in the adsorbed structure. Hence, Cr and Zr on adsorption were able to transform semiconducting and non- magnetic AsP-3 to metallic and magnetic material. These ferromagnetic materials can be used as electrode materials for spin-based devices like MTJs and spin-based switches.

In the Co adsorbed AsP-3 structure, semiconductor to metallic transition is observed with zero bandgap in the band structure plot shown in Fig. 4.4. Also, the s-DOS of the Co-adsorbed structure shows that the majority of the conducting states are available in spin-up channel than in spin-down channel. This makes the structure half-metallic, as spin-up electrons are the majority carriers. This half-metallicity shows that the material, when used as an electrode, will be allowing only spin-up electrons to pass through the channel while blocking the spin-down electrons which is a highly desirable characteristic of spintronics devices. The non-zero magnetic moment of $0.65 \mu_B$ (see

Table 4.1) also confirms its magnetic nature. HMF characteristics were observed for Fe- adsorbed AsP-3 and Ti- adsorbed AsP-3. Both the adsorbed structures were confirmed to be metallic with zero bandgap, as shown in Fig. 4.7 and Fig. 4.9. For Fe-adsorbed structure, spin-DOS shows the availability of only spin-up states and no spin-down conduction states. Meanwhile, the s-DOS of Ti-adsorbed structure in Fig. 4.9 shows the opposite behaviour, where conducting states are available only in spin-down channel. The availability of conducting states in only one of the channels (spin-up or spin-down) makes these adsorbed structures HMF. The calculated magnetic moments of $2.14 \mu_B$ and $2.21 \mu_B$ for Fe-adsorbed and Ti-adsorbed AsP-3 in Table 4.1 confirms their magnetic behaviour. Therefore, when Co, Fe and Ti are adsorbed on the surface of non-magnetic AsP-3, in addition to the transition from semiconducting to metallic characteristic of AsP-3, induced magnetization and spin- polarization are also observed. Such structures can be used to design electrodes for spin-based devices. When the device is fabricated using HMF materials as electrodes, it allows the electrons of only one spin type (spin-up or spin-down) to pass through the channel and blocks the electrons of opposite spin and therefore the majority of the spin current is composed of only one type of spin-electrons. This characteristic of a spin-based device where only one type of spin electron (up/down) is allowed while blocking the other spin type (down/up) electron is expressed in the form of magnetoresistance such as TMR or GMR.

The efficiency of a spin-based device is determined based on the value of magnetoresistance ratio. Higher values of magnetoresistance ratio indicate better spin-filtration and spin-selectivity. Spin-based devices exploit this property of magnetoresistance to conduct current from the left electrode to the right electrode through a non-magnetic channel [16]. Hence, these findings confirm that transition metals, on adsorption, can induce the transition of semiconducting AsP-3 to a metallic state. Also, specific transition metals like Cr, Zr, Co, Fe and Ti are able to induce magnetization and spin- polarization in the adsorbed structures.

4.4 Summary

This chapter investigates the transformation of 2D b-AsP from a non-magnetic semiconductor to materials with magnetic properties through the adsorption of various transition metals. Using DFT, the study explores the electronic and magnetic properties of b-AsP when adsorbed with TMs such as Co, Fe, Ti, Cr, Zr, Ag, Cu, and Mo. The results reveal that while pristine b-AsP exhibits semiconducting behaviour with a bandgap of ~ 1.1 eV, adsorption of Co, Fe, and Ti converts it into an HMF and adsorption of Cr and Zr results in FM behaviour. In contrast, adsorption of Ag, Cu, and Mo are not able to transform the magnetic nature of b-AsP. The study employs DFT simulations using the Atomistix Toolkit, calculating s-DOS and band structures to confirm these transformations. Adsorption energy calculations indicate stable and

thermodynamically favourable structures. The induced magnetization and spin-polarization in b-AsP through TM adsorption suggest its potential as an electrode material in spintronic devices like MTJs and spin valves. These findings demonstrate the versatility of b-AsP for spintronic applications, offering high spin filtration and magnetoresistance critical for advanced electronics. The results promises that b-AsP, with its tunable electronic and magnetic properties, holds promise for future spin-based devices.

Chapter 5

IMPLEMENTATION OF FAULT TOLERANT ARITHMETIC

LOGIC UNIT USING MCELL

5.1 Introduction

It has been observed that the continuous downscaling in integrated circuits using CMOS technology has warranted the integration of a significant number of transistors in a smaller area, hence providing more computing power. Although technologies like Chip Multi-Processors (CMPs) highly increase computational power, factors like temperature and power consumption limit their use in the long run. Higher power consumption is directly related to on-chip temperatures, which could further lead to hardware failures [124], [125] in the long run of the device. One way to tackle this problem is to use lower operating voltages [126], but it's only an option when a tradeoff with computational speed is an option due to the reduced current drivers of the transistors. One way to counter this is to reduce the threshold voltage for transistors, but this, in turn, produces high amounts of transistor leakage currents [127]. Leakage power consumption is a major issue as it possesses a similar contribution in switching/dynamic power in complete circuit power consumption in nano-scale technologies[128].

An attractive tradeoff that has come forward in recent years is the use of spintronic devices because they have features such as non-volatility, low static power consumption and lesser area discussed thoroughly in [129]. Spintronic devices utilize not only the charge of electrons but also their up and down spins, unlike traditional electronic devices that solely rely on electronic charge. In spintronic devices, the term "digital state" refers to the orientation of magnetization in a ferromagnetic material that has uniaxial anisotropy. This type of material can have only two stable states, namely "up" and "down." Unlike traditional electronic devices that require electrical power to store information, spintronic devices store information as a magnetization direction, which means that it is non-volatile and does not need an electrical power supply to maintain its state [3].

Modelling logic gates can be done using either the MTJ [130] device or the mCell [131]. The characteristics of MTJs, which have the capacity to change their magnetic state in response to an external magnetic field, provide the basis for the model. This method depends on using MTJs as tiny fundamental building blocks for logic gates, which can then be merged into much bigger circuits. The mCell, on the other hand, takes a very different approach and models the behaviour of individual molecules and

their interactions. This method sacrifices efficiency in favour of a more thorough modelling of the physical and chemical mechanisms that govern the behaviour of logic gates. The MTJ model has a smaller set of logic gates, but it performs better in terms of simulation times and design simplicity. The mCell device, in comparison, provides a more flexible approach that enables the modelling of a considerably wider choice of logic gates. mCells can further be used in the future for synthesizing hybrid Field Programmable Gate Arrays (FPGA) [132], [133], non-volatile flip-flops [134], [134], full – adders, arithmetic logic units (ALU), etc.

As we know the major challenges associated with current ALU circuits, it has been recognized that they suffer from significant power consumption and lack of error detection capabilities. Therefore, to mitigate these drawbacks, we use the Parity Preserving Reversibility Gate (PPRG) for the implementation of ALU [135] because PPRG is a concept in reversible computing. It emphasizes maintaining the parity (even or odd) of bits during computational operations. In PPRG logic, reversible gates and circuits are designed to ensure that the number of set bits in the input matches the number of set bits in the output, preserving parity. This property is crucial in reducing energy dissipation, making PPRG logic relevant in quantum computing and low-power electronic circuits [136]. It aims to create more energy-efficient and information-preserving computational processes by minimizing irreversible transformations [137].

In this study, a fault-tolerant ALU that uses PPRG has been designed. For the implementation of PPRG [138] we use the mCell logic. The use of mCells in the implementation of the ALU offers several benefits, including non-volatility, high-speed operation, and high-density integration. The use of mCell also offers the potential for novel digital circuit designs, which are primarily constructed from logical gates that have several advantages over CMOS technology.

5.2 Structure of The Proposed Logic Gates

An MTJ-based device, also known as a mCell, has been used as shown in Fig. 5.1 [10]. It has four terminals, namely W+, W- (write path), and R, R* (read path).

Spintronic devices operate by using a magnetic domain wall that is present in the write path. It is pushed to and fro due to an electric current. The free layer of an MTJ is magnetically linked to the write path, and the tunnelling magnetoresistance of the element changes the state of the resistance of the read path. This resistance across the read path (R and R*) is high when positive current is flowing across the write path (W- to W+), and the resistance is low when the direction of current is reversed. Measuring the resistance across the read-path terminals, which can be either high or low, determines the state of the device.

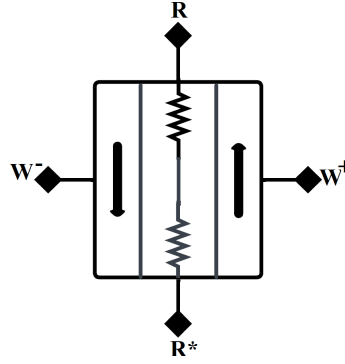


Fig. 5.1 Schematic diagram of an mCell

Our investigation includes the implementation of a range of logic gates like NAND, NOR, AND, OR, using the mCell on Cadence Virtuoso. The gates used are made by clubbing two magnetic cells together, named the Upper mCell (UmC) and the Lower mCell (LmC) [139]. They form a complementary pair, meaning when one is high, the other will be low. Only one of the two mCells is used at a time for giving input; the other one remains grounded. The inputs are given to the W pins of one of the mCells. The state of the gate depends on the net current flowing through the write path.

The operation of these gates is based on the comparison of the resistance of UmC and LmC. If the LmC has higher resistance than the UmC, $I_{LmC} < I_{UmC}$, thus resulting in a positive output current obtained across the '+V' and 'Output' terminal, giving high logic ('1'). Similarly, if the LmC has lower resistance than the UmC, $I_{LmC} > I_{UmC}$, thus resulting in a negative output current obtained across the 'Output' terminal and '-V', giving low logic ('0').

Overall, the gates use complementary mCell pairs in order to control the output current based on resistance comparisons between the UmC and the LmC. We obtained an accurate transient response of the gates, wherein +ve current represents high state (logic 1) and -ve current represents low state (logic 0). The circuits were operated at +50mV and -50mV.

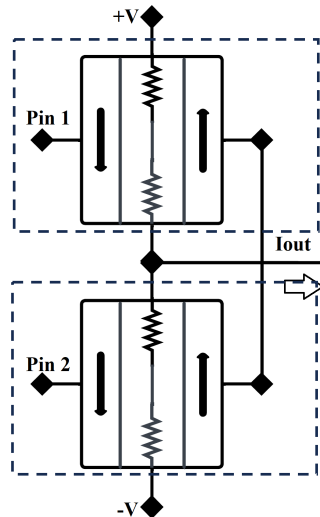


Fig. 5.2 General structure of logic gates

For making logic gates using mCell, some assumptions should be made [139]:

- (i) $W+$ pin is on the right side of the mCell and $W-$ pin is on the left side of the mCell.
- (ii) The current flowing from $W-$ to $W+$ is considered positive while that flowing from $W+$ to $W-$ is considered negative.
- (iii) $+I(1)$ indicates current entering mCell from $W-$ to $W+$. $-I(1)$ indicates current entering mCell from $W+$ to $W-$.
- (iv) $+I(0)$ indicates current drawn from $W+$ terminal of mCell and $-I(0)$ indicates current drawn from $W-$ terminal of mCell.
- (v) If a current of magnitude I enters mCell from $W-$ terminal or current of magnitude I is drawn from $W+$ terminal of mCell then mCell enters the high resistance (R_H) state. If a current of magnitude I enters mCell from $W+$ terminal or current of magnitude I is drawn from $W-$ terminal of mCell then mCell enters the low resistance (R_L) state.

5.3 Implementation of Basic Logic Gates Using mCell

5.3.1 Not Gate / Inverter

Fig. 5.3 shows the block diagram of a mCell inverter. Input is given to the LmC. When input is logic 1 the UmC is said to be in the R_H state and the LmC is said to be in the R_L state, which represents an output current denoting logic 0. When the input is logic 0, the UmC is said to be in the R_L state and the LmC is said to be in the R_H state, resulting in an output current denoting logic 1.

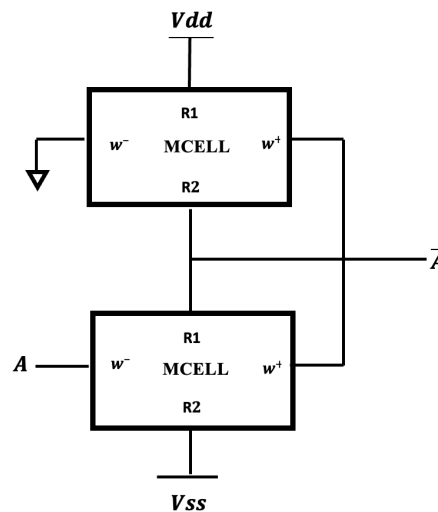


Fig. 5.3 mCell Based NOT Gate

5.3.2 NOR and NAND Gates

The NOR gate shown in Fig. 5.4 is created by furnishing a control current (I_c) of $-I$ (denoted as I_\downarrow), and the output is dependent on the inputs A and B that are applied at the LmC. When both A and B are $-I$ (denotes as I_\downarrow), a net negative current flow through LmC ($R_{UmC} < R_{LmC}$), resulting in '1' output, as explained above. In rest all cases the net input current is positive hence obtaining '0' output. The NAND gate shown in Fig. 5.5 is created by furnishing control current (I_c) of I_\uparrow . The NAND gate produces logic '1' when either of A or B are I_\uparrow . This produces a net positive current through LmC ($R_{LmC} > R_{UmC}$), hence a logic high state.

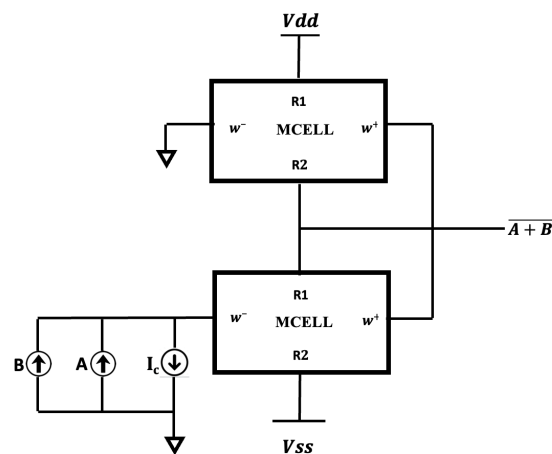


Fig. 5.4 mCell Based NOR Gate

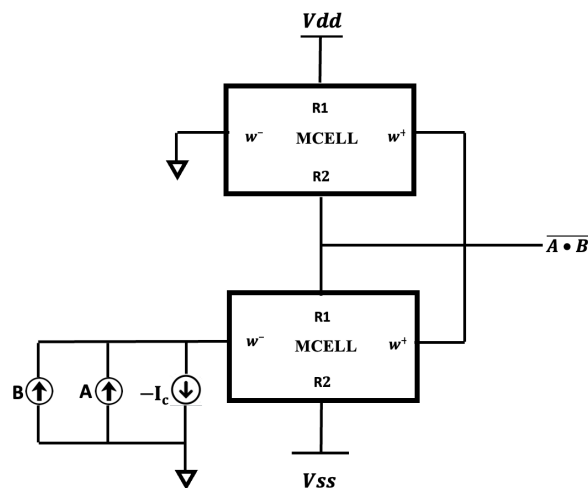


Fig. 5.5 mCell Based NAND Gate

5.3.3 OR and AND Gates

AND and OR gates can be created by using NAND and NOR gates with a little modification in the connection of the inputs. This can be done by changing the input pins from LmC to UmC. The truth table for various gates implemented using mCell is shown in Table 5.1.

Table 5.1 Truth Table of Implemented Logic Gates

Input A	Input B	Control Input (I _c)	Total Input (I _{net})	Output (I _{out}) using LmC		Output (I _{out}) using UmC	
I_{\uparrow}	I_{\uparrow}	I_{\uparrow}	$3I_{\uparrow}$	0	NAND	1	AND
I_{\uparrow}	I_{\downarrow}	I_{\uparrow}	I_{\uparrow}	1		0	
I_{\downarrow}	I_{\uparrow}	I_{\uparrow}	I_{\uparrow}	1		0	
I_{\downarrow}	I_{\downarrow}	I_{\uparrow}	I_{\downarrow}	1		0	
I_{\uparrow}	I_{\uparrow}	I_{\downarrow}	I_{\uparrow}	0	NOR	1	OR
I_{\uparrow}	I_{\downarrow}	I_{\downarrow}	I_{\downarrow}	0		1	
I_{\downarrow}	I_{\uparrow}	I_{\downarrow}	I_{\downarrow}	0		1	
I_{\downarrow}	I_{\downarrow}	I_{\downarrow}	$3I_{\downarrow}$	1		0	

5.4 Implementation of Complex Logic Circuits Using mCell

5.4.1 Parity Preserving Reversible Gate

We create a logic circuit that is both fault tolerant and reversible. Parity check method is used to discover errors. A reversible gate must fulfill certain requirements in order to be parity-preserving [135]:

- (i) One-to-one correspondence mapping must be used for input and output.
- (ii) XOR of inputs = XOR of output

Schematic of (PPRG) used is shown in Fig. 5.6 and its truth table is shown in Table 5.2. It has 3 inputs 'A', 'B' and 'C' and 3 output 'P', 'Q', and 'R'. The outputs for the PPRG are given as

$$P = A \oplus B$$

$$Q = AC + \bar{B}\bar{C}$$

$$R = \bar{B}\bar{C} + C\bar{A}$$

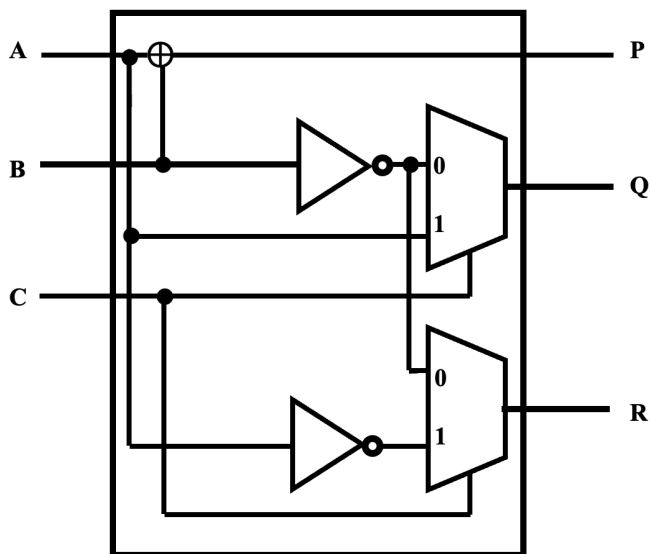


Fig. 5.6 Schematic Diagram of PPRG

Table 5.2 Truth Table of PPRG

A	B	C	P	Q	R
0	0	0	0	1	1
0	0	1	0	0	1
0	1	0	1	0	0
0	1	1	1	0	1
1	0	0	1	1	1
1	0	1	1	1	0
1	1	0	0	0	0
1	1	1	0	1	0

5.4.2 Double Feynman Gate

It is a 3*3 reversible logic gate, as shown in Fig. 5.7 [140]. There are 3 inputs and 3 outputs on it. The 3 outputs are given as

$$P = A$$

$$Q = A \oplus B$$

$$R = A \oplus C$$

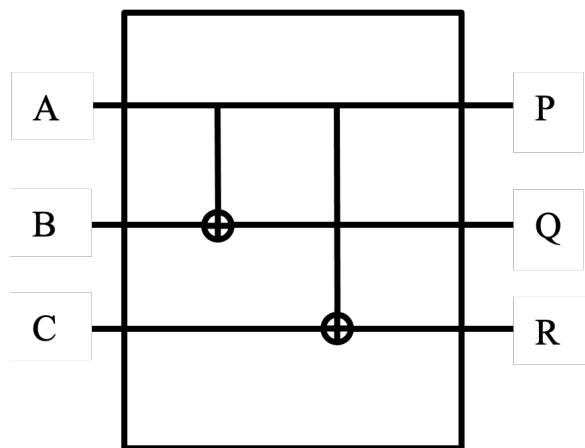


Fig. 5.7 Double Feynman Gate

5.4.3 Design of Full Adder

A PPRG-based full adder is designed as shown in Fig. 5.8. The overall design consists of 3 PPRG gates. It has 3 inputs and 6 outputs. Out of the 6 outputs, 4 are garbage output and of the two remaining one of the outputs represents the sum (S) and other output represents the carry out (C_{out}).

$$S = A \oplus B \oplus C_{in}$$

$$C_{out} = AB + BC_{in} + AC_{in}$$

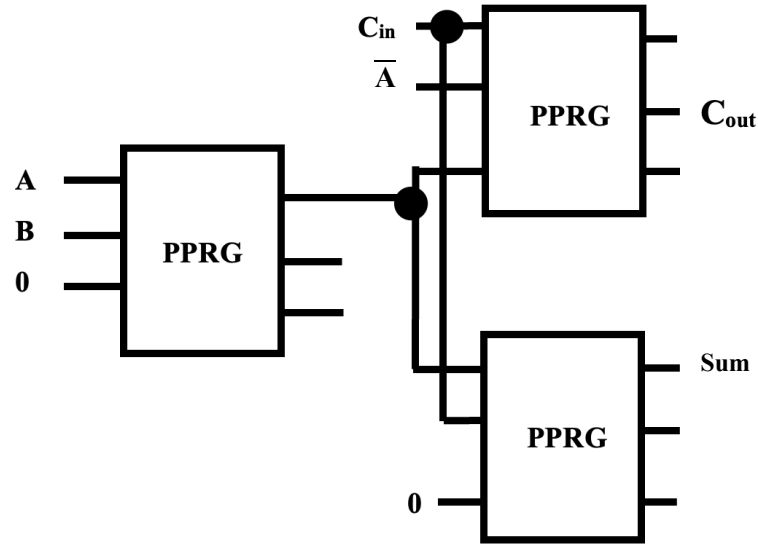


Fig. 5.8 PPRG based Full Adder

5.5 Proposed Arithmetic Logic Unit

For developing the ALU, we have designed an operation selector using the PPRG and DFG as shown in Fig. 5.9. The operation selector is used to decide the operation to be performed in the ALU. It is connected in cascade with the Full-Adder. The block diagram of the ALU is shown in Fig. 5.10. The operation selector has 3 outputs which are given as inputs to the full adder. The functionality of operation selector is given as [141]:

$$X = A_i + \bar{S}_0(S_1 \oplus B_i)$$

$$Y = S_0 B_i + \bar{S}_1 \bar{B}_i$$

$$Z = \bar{S}_2 C_i$$

The final output of ALU is decided by the output of Full-Adder which are given as

$$A_i = X_i \oplus Y_i \oplus Z_i$$

$$B_i = X_i Y_i + Y_i Z_i + X_i Z_i$$

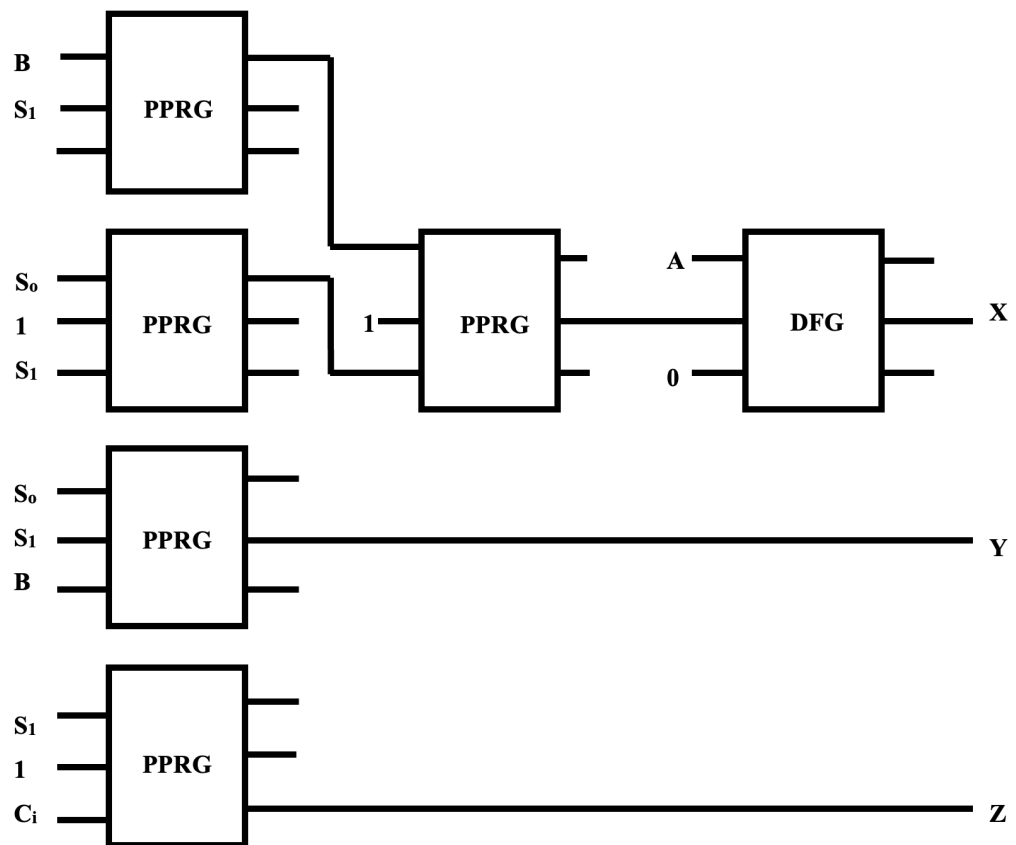


Fig. 5.9 Operation Selector Circuit of ALU

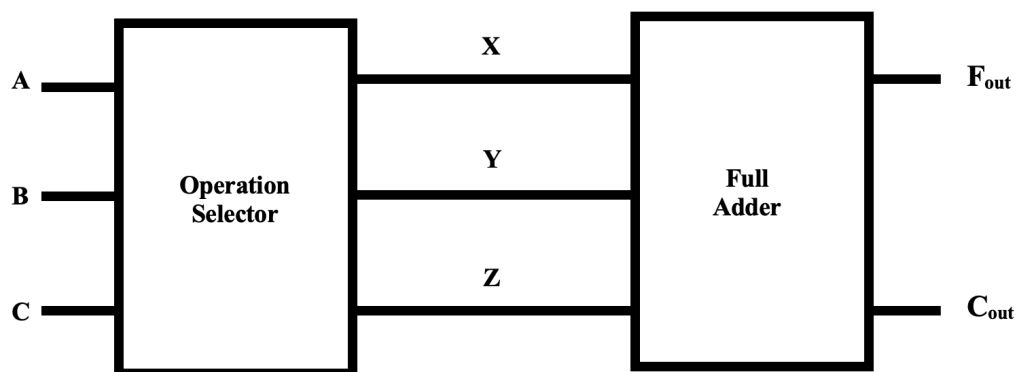


Fig. 5.10 Block Diagram of ALU

5.6 Setup and Simulation

All the circuits implemented using the mCell have been simulated in the Cadence® Virtuoso® environment. For all the simulations we have taken value of V_{DD} as +50 mV and that of V_{SS} as -50 mV. Value of current input is taken as 1.5 uA. The functionalities performed by the proposed ALU can be seen from Table 5.3. The transient response of the ALU can be seen in Fig. 5.11.

Table 5.3 Functional Table of ALU

Selection				Output		Operation(s)	
S_2	S_1	S_0	C_i	F	C	F	C
0	0	0	1	-	\overline{AB}	-	Logical NAND
0	0	1	0	\overline{A}	-	Logical NOT	-
0	0	1	1	A	-	Transfer input A	-
0	1	0	0	$A \odot B$	-	Logical XNOR	-
0	1	0	1	$A \oplus B$	$A - B$	Logical XOR	Subtract
0	1	1	0	-	AB	-	AND
0	1	1	1	$A + B + 1$	$A + B$	Addition including carry	Logical OR
1	0	1	X	$A + 1$	-	Increment input A	-
1	1	0	X	$A - B - 1$	-	Subtraction including Borrow	-
1	1	1	X	$A + B$	AB	Half Adder	

5.7 Results and Discussions

Table 5.4 shows the results obtained in terms of the propagation delay product of different components used in the construction of the ALU. The propagation delay of the NOT Gate/Inverter obtained is the least among all the components and is equal to 4.6 nsec. The delay obtained in case of NAND and NOR Gates are 28.06 nsec and 30.2 nsec, respectively, which is more compared to the inverter due to the presence of current I_c . The final propagation delay of the ALU obtained through the output pins F_{out} & C_{out} are 565 nsec & 728 nsec, respectively. The reason for the higher propagation delay is the cascading effect, which comes into play due to the architecture used.

The calculated average power delay product can be observed in Table 5.4 of the different components used in the construction of the ALU. It is to be noted that the calculated power delay product here increases with the number of components used or the number of cascading stages between the input and the output pin. This result was accomplished by designing the architecture of the circuit which would drive the

resulting output current being the same in all the modules involved in the circuit. The current used as input to switch the mCell is same in all the gates and modules and the power supply used and the resistance provided by the mCell for the output current is same in all the cases. Thus, the same output current is obtained for all the cases.

The different power-delay products obtained corresponding to the different components constructed using mCell based logic can also be seen in Table 5.4. The Power Delay Product (PDP) of proposed ALU using mCell logic is 80.56 fJ through F_{out} pin and 103.81 fJ through C_{out} pin.

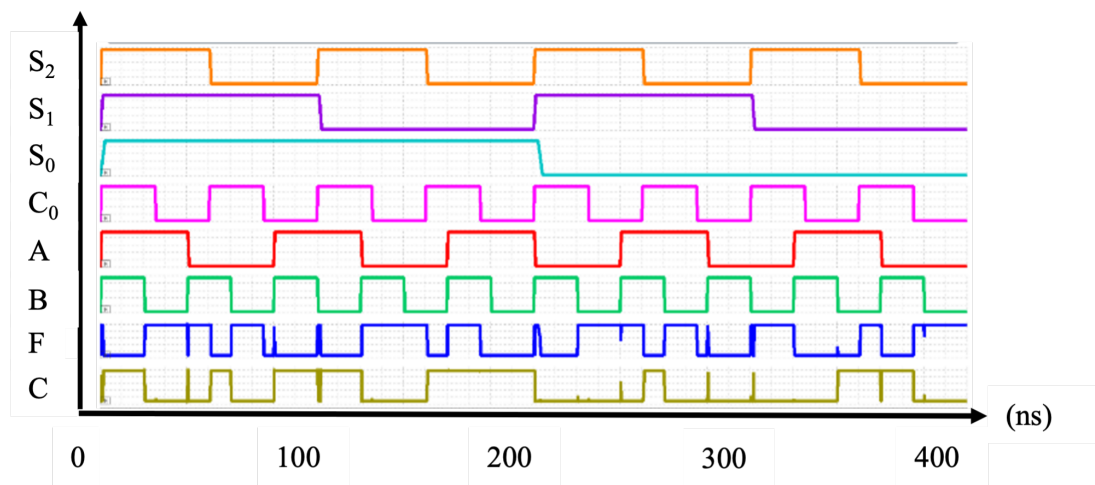


Fig. 5.11 Transient Response of ALU

Table 5.4 Power Delay Product of ALU and its Subcomponents

ALU subcomponents	Power Delay Product (PDP) (fJ)
Inverter	0.65
NAND	4.00
NOR	4.30
ALU (F_{out})	80.56
ALU (C_{out})	103.81

The output waveform obtained (Fig. 5.11) shows the single-bit binary inputs A & B along with the carry input C_{in} and the results obtained in the waveform of F_{out} (Sum) and C_{out} (Carry out) corresponding to the opcode ($S_2 S_1 S_0$) which can be observed according to the Functional Table (Table 5.3) of ALU. The output obtained is also represented in the binary format.

5.8 Summary

In this chapter, a novel design for a fault-tolerant ALU using mCell-based logic has been proposed and simulated. The mCell technology, which leverages spintronic devices, offers significant advantages in terms of reduced area, non-volatility, and negligible static power consumption. These characteristics make mCell an attractive alternative to traditional CMOS technology, which faces limitations due to high power consumption and on-chip temperature issues.

The proposed ALU design integrates PPRG logic, which ensures energy-efficient and error-detection capabilities by maintaining parity during computational operations. This feature is crucial in reducing energy dissipation and enhancing the reliability of the ALU.

The paper details the implementation of ALU using various basic and complex logic gates using mCell, including NOT, NAND, NOR, AND, OR, and PPRG-based full adders. The mCell-based NOT gate demonstrates lowest power delay product of approximately 0.65 fJ, highlighting the efficiency of mCell technology in maintaining low power requirements of the proposed circuits.

Simulation results show that the proposed ALU design achieves a power delay product of 80.56 fJ through the F_{out} pin and 103.81 fJ through the C_{out} pin, indicating significant improvements over conventional designs. The study concludes that mCell-based logic circuits, with their non-volatility, low power consumption, and high-density integration, hold promise for future applications in spintronic devices, including magnetic memories, hybrid FPGAs, and non-volatile flip-flops.

Chapter 6

CONCLUSION, FUTURE SCOPE AND SOCIAL IMPACT

6.1 Conclusion

The research conducted on the adsorption of transition metals on zigzag SiCNT and b-AsP, along with the implementation of fault-tolerant ALU using mCell technology, reveals significant findings in the field of spintronics. The primary goal was to explore the magnetic properties induced by transition metals in non-magnetic materials to potentially enhance the performance of spintronic devices such as MTJ and spin valves.

6.1.1 Zigzag SiCNTs

In the case of zigzag SiCNTs, the DFT simulations are performed based on the first principles study to analyze the induced magnetic behaviour of TM when adsorbed on metallic zigzag (4,0) SiCNT and semiconducting zigzag (8,0) SiCNT. The SiCNTs, otherwise non-magnetic, showed a strong FM and HMF nature when adsorbed with transition metals, suggesting their capability to induce magnetization in non-magnetic (both metallic and semiconducting) zigzag SiCNTs. The (4,0) SiCNT, when adsorbed with Co, Cr, Fe, Mo and Ti, exhibited the HMF nature. The (8,0) SiCNT, which is semiconducting, when adsorbed with Cr, Cu, Ti and Zr, is also found to exhibit an HMF nature. The results also showed that Cr and Ti are able to transform both metallic and semiconducting zigzag SiCNTs into HMF and are promising candidates for inducing magnetization in both metallic as well as semiconducting zigzag SiCNT structures. The FM and HMF materials are the most used materials for constructing the electrodes in spin-based devices. Thus, the TM-adsorbed SiCNTs can play a significant role in designing magnetic devices like magnetic storage devices, MTJs, and spin valves for applications in the field of spintronics.

6.1.2 Black Arsenic Phosphorus

For b-AsP, the adsorption of transition metals similarly induced significant spin polarization, making these materials promising candidates for spintronic applications. DFT investigation delineates the impact of transition metal adsorption on the electronic and magnetic properties of semiconducting AsP-3. Utilizing Spin-DOS analysis, distinct alterations in response to the adsorption of Ag, Co, Mo, Cr, Cu, Zr, Fe, and Ti have been elucidated.

The adsorption of Ag, Cu, and Mo induces non-magnetic metallic characteristics in AsP-3, as discerned through spin-DOS analysis. This departure from the intrinsic semiconducting behavior of AsP-3 holds potential for applications in unconventional electronic devices. In contrast, Cr and Zr adsorption yields a substantial magnetic moment, indicative of strong ferromagnetic behavior. Notably, the Cr-adsorbed structure exhibits a remarkable magnetic moment of $5.09 \mu_B$.

Further examination of Co, Fe, and Ti adsorption reveals pronounced HMF characteristics. This positions AsP-3 as a promising candidate for two-dimensional spintronic devices, capitalizing on the nuanced interplay between electronic and magnetic features.

In conclusion, the DFT investigations provide insights into the tunability of AsP-3 through transition metal adsorption, elucidating its responsive behaviour. The results established that AsP-3 is a material of interest for tailored applications in the field of spintronics.

6.1.3 ALU Design using mCell

The research also includes the implementation of a fault-tolerant ALU using mCell technology, demonstrating the potential of mCell-based logic circuits in spintronic applications. The proposed design showcases the significant advantages of mCell-based logic circuits over traditional CMOS technology, particularly in terms of power consumption, area efficiency, and non-volatility. By incorporating PPRG logic, the design ensures efficient error detection and energy conservation, making it highly suitable for advanced computational applications.

The experimental results highlight the low power consumption by the ALU and its subcomponents. The ALU design achieves impressive power delay products of 80.56 fJ through the F_{out} pin and 103.81 fJ through the C_{out} pin, marking a considerable improvement compared to conventional designs.

The successful implementation and simulation of various basic and complex logic gates using mCell underscore the potential of this technology for future advancements. mCell-based circuits, with their high-speed operation, non-volatility, and reduced power requirements, are poised to play a crucial role in the development of next-generation spintronic devices, magnetic memories, hybrid FPGAs, and non-volatile flip-flops.

In conclusion, this research establishes mCell as a viable and efficient alternative to CMOS technology for constructing larger and more complex digital circuits, paving the way for innovative designs in low-power, high-performance computational systems.

6.2 Future Scope

The findings from this research open up numerous opportunities for further exploration and development in the field of spintronics. One significant area of future work involves the experimental validation of the computational results presented in this study. While the density functional theory calculations provide a strong theoretical foundation, experimental verification is essential to confirm the practical applicability of transition metal adsorbed Zigzag SiCNT and AsP in real-world devices. This would involve synthesizing these materials, characterizing their magnetic properties, and integrating them into prototype spintronic devices such as MTJ and spin valves.

Another promising direction for future research is the investigation of other transition metals and their potential to induce magnetic properties in non-magnetic materials. While this study focused on Ag, Co, Cr, Fe, Mo, Ti, Cu, and Zr, there may be other transition metals or combinations of metals that could produce even more favourable magnetic characteristics. Exploring these possibilities could lead to the discovery of new materials with optimized properties for specific spintronic applications.

Additionally, the scalability and stability of these materials under different environmental conditions and operational stresses need to be thoroughly examined. For spintronic devices to be commercially viable, it is crucial to ensure that the materials maintain their magnetic properties over time and under varying temperatures, pressures, and other external influences. This includes studying the effects of long-term use, thermal cycling, and exposure to different chemical environments.

Furthermore, the integration of transition metal adsorbed SiCNT and AsP into more complex device architectures could be explored. This includes the development of multi-layered structures, hybrid devices combining different materials, and the incorporation of these materials into existing semiconductor technologies. The potential to create multifunctional devices that leverage both the electronic and magnetic properties of these materials could revolutionize the design and functionality of future electronic devices. Collaborative efforts between computational scientists, experimentalists, and device engineers will be crucial in advancing this field and bringing these innovative materials from the lab to practical applications.

Building on the advancements made in this research, the implementation of fault-tolerant ALUs using mCell technology, as demonstrated in this thesis, represents a significant step forward. Future work can extend the application of mCell-based logic circuits, which demonstrate low power consumption, non-volatility, and high-density integration, into broader areas of digital and spintronic devices. Exploring the combination of mCell technology with TM-adsorbed materials could lead to even more efficient and versatile spintronic components. Additionally, expanding the

research into developing other components, such as hybrid FPGAs and non-volatile flip-flops using mCell technology, could provide further advancements in the field.

6.3 Social Impact

The development and implementation of advanced spintronic devices using transition metal adsorbed zigzag SiCNT and b-AsP have the potential to bring about significant positive impacts on society. One of the most notable impacts is the enhancement of data storage technology. Spintronic devices, such as MTJ and spin valves, offer higher data density, faster read and write speeds, and lower power consumption compared to traditional electronic devices. This can lead to more efficient data centres, reduced energy consumption, and a smaller carbon footprint, which are critical for addressing the growing demands of the digital age and mitigating the environmental impact of technology.

Additionally, the use of these advanced materials in spintronic devices can lead to the development of more secure and robust data storage solutions. The inherent properties of spintronics, such as non-volatility and resistance to external magnetic fields, make these devices ideal for applications where data integrity and security are paramount. This can have profound implications for sectors such as finance, healthcare, and national security, where the protection of sensitive information is crucial.

In the realm of consumer electronics, the integration of spintronic technology can result in the creation of faster, smaller, and more efficient devices. Smartphones, laptops, and other personal gadgets can benefit from the enhanced performance and energy efficiency offered by spintronic components, leading to longer battery life and improved user experiences. Moreover, the advancement of spintronic technology can drive innovation in emerging fields such as quantum computing and artificial intelligence, where the ability to manipulate and store information at the quantum level can unlock new computational capabilities.

The social impact of this research extends beyond technology and into the economic domain. The commercialization of spintronic devices using materials like zigzag SiCNT and AsP can stimulate economic growth by creating new markets and job opportunities. Industries focused on the production, design, and maintenance of spintronic components will emerge, fostering economic development and contributing to the knowledge economy. Furthermore, advancements in spintronics can enhance the competitiveness of nations that invest in this technology, positioning them at the forefront of the next technological revolution.

On a broader scale, the environmental benefits of spintronic technology cannot be overlooked. The reduction in power consumption and increased efficiency of electronic devices can contribute to global sustainability efforts. As societies move

towards greener and more sustainable practices, the adoption of energy-efficient technologies like spintronics will be pivotal in achieving environmental goals and combating climate change.

In addition to these benefits, the implementation of fault-tolerant ALUs using mCell technology can further enhance the reliability and efficiency of electronic devices. The non-volatility, low power consumption, and high-speed operation of mCell-based circuits can significantly reduce the energy footprint of digital devices, contributing to environmental sustainability. Moreover, the fault-tolerant nature of the ALU design can improve the resilience of critical systems in sectors such as aerospace, healthcare, and defence, where reliability and error detection are paramount.

In conclusion, the research on transition metal adsorbed Zigzag SiCNT and AsP not only advances the field of spintronics but also holds the promise of substantial social benefits. From enhancing data storage and security to driving economic growth and promoting environmental sustainability, the potential applications of these advanced materials underscore the importance of continued research and development in this area.

REFERENCES

- [1] I. Z. ˇ Utic´*utic´*, J. Fabian, and S. Das Sarma, ‘Spintronics: Fundamentals and applications’.
- [2] S. M. Yakout, ‘Spintronics: Future Technology for New Data Storage and Communication Devices’, *J. Supercond. Nov. Magn.*, vol. 33, no. 9, pp. 2557–2580, Sep. 2020, doi: 10.1007/S10948-020-05545-8/TABLES/5.
- [3] S. A. Wolf *et al.*, ‘Spintronics: A spin-based electronics vision for the future’, *Science*, vol. 294, no. 5546, pp. 1488–1495, Nov. 2001, doi: 10.1126/SCIENCE.1065389.
- [4] M. N. Baibich *et al.*, ‘Giant Magnetoresistance of (001)Fe(001) Cr Magnetic Snperlattices’, *Phys Rev Lett*, vol. 61, no. 21, pp. 2472–2475, Nov. 1988, doi: 10.1103/PhysRevLett.61.2472.
- [5] S. Yuasa, T. Nagahama, A. Fukushima, Y. Suzuki, and K. Ando, ‘Giant room-temperature magnetoresistance in single-crystal Fe/MgO/Fe magnetic tunnel junctions’, *Nat. Mater.* 2004 312, vol. 3, no. 12, pp. 868–871, Oct. 2004, doi: 10.1038/nmat1257.
- [6] G. Binasch, P. Grünberg, F. Saurenbach, and W. Zinn, ‘Enhanced magnetoresistance in layered magnetic structures with antiferromagnetic interlayer exchange’, *Phys. Rev. B*, vol. 39, no. 7, p. 4828, Mar. 1989, doi: 10.1103/PhysRevB.39.4828.
- [7] B. Irfan, ‘Spintronics: Overview on Spin Based Electronics and Its Potential Applications’, *Int. J. Mater. Sci. Appl.*, vol. 10, no. 5, Art. no. 5, Sep. 2021, doi: 10.11648/j.ijmsa.20211005.11.
- [8] J. S. Moodera, L. R. Kinder, T. M. Wong, and R. Meservey, ‘Large Magnetoresistance at Room Temperature in Ferromagnetic Thin Film Tunnel Junctions’, vol. 74, p. 16, 1995.
- [9] ‘Observation of the Spin Hall Effect in Semiconductors | Science’. Accessed: Jul. 29, 2024. [Online]. Available: <https://www.science.org/doi/abs/10.1126/science.1105514>
- [10] M. Z. Hasan and C. L. Kane, ‘Colloquium: Topological insulators’, 2010, doi: 10.1103/RevModPhys.82.3045.
- [11] S. Manzeli, D. Ovchinnikov, D. Pasquier, O. V. Yazyev, and A. Kis, ‘2D transition metal dichalcogenides’, *Nat. Rev. Mater.* 2017 28, vol. 2, no. 8, pp. 1–15, Jun. 2017, doi: 10.1038/natrevmats.2017.33.
- [12] A. D. Kent and D. C. Worledge, ‘A new spin on magnetic memories’, *Nat. Nanotechnol.* 2015 103, vol. 10, no. 3, pp. 187–191, Mar. 2015, doi: 10.1038/nnano.2015.24.
- [13] D. D. Awschalom, L. C. Bassett, A. S. Dzurak, E. L. Hu, and J. R. Petta, ‘Quantum spintronics: Engineering and manipulating atom-like spins in semiconductors’, *Science*, vol. 339, no. 6124, pp. 1174–1179, Mar. 2013, doi: 10.1126/science.1231364.
- [14] C. Chappert, A. Fert, and F. N. Van Dau, ‘The emergence of spin electronics in data storage’, *Nat. Mater.* 2007 611, vol. 6, no. 11, pp. 813–823, 2007, doi: 10.1038/nmat2024.

- [15] S. Choudhary, N. Singh, and P. Ranjan, 'Journal of Magnetism and Magnetic Materials Induced magnetization in armchair and Zig-zag CNTs on adsorbing transition metals', *J. Magn. Magn. Mater.*, vol. 538, no. July, p. 168287, 2021, doi: 10.1016/j.jmmm.2021.168287.
- [16] S. Choudhary and A. Chauhan, 'First-principles study of spin transport in CrO₂-SiCNT-CrO₂ magnetic tunnel junction', *J. Comput. Electron.*, pp. 2–6, 2015, doi: 10.1007/s10825-015-0725-x.
- [17] F. Xia, H. Wang, and Y. Jia, 'ARTICLE Rediscovering black phosphorus as an anisotropic layered material for optoelectronics and electronics', 2014, doi: 10.1038/ncomms5458.
- [18] Y. Luo *et al.*, 'Adsorption of Transition Metals on Black Phosphorene: a First-Principles Study', *Nanoscale Res. Lett.*, vol. 13, no. 1, pp. 1–9, Sep. 2018, doi: 10.1186/S11671-018-2696-X/FIGURES/5.
- [19] D. Morris, D. Bromberg, J.-G. (Jimmy) Zhu, and L. Pileggi, 'mLogic: ultra-low voltage non-volatile logic circuits using STT-MTJ devices', in *Proceedings of the 49th Annual Design Automation Conference*, in DAC '12. New York, NY, USA: Association for Computing Machinery, Jun. 2012, pp. 486–491. doi: 10.1145/2228360.2228446.
- [20] D. M. Bromberg, 'Current-Driven Magnetic Devices for Non-Volatile Logic and Memory'.
- [21] S. Ikeda *et al.*, 'Tunnel magnetoresistance of 604% at 300 K by suppression of Ta diffusion in CoFeBMgOCoFeB pseudo-spin-valves annealed at high temperature', *Appl. Phys. Lett.*, vol. 93, no. 8, p. 82508, Aug. 2008, doi: 10.1063/1.2976435/923250.
- [22] F. Ahmad *et al.*, 'Advances in graphene-based electrode materials for high-performance supercapacitors: A review', *J. Energy Storage*, vol. 72, p. 108731, Nov. 2023, doi: 10.1016/J.EST.2023.108731.
- [23] X. Zhang, P. Gong, F. Liu, K. Yao, S. Zhu, and Y. Lu, 'Half-metallic of non-metal-adsorbed AsP and multifunctional two-dimensional spintronic device of impure AsP from first-principles calculations', *Phys. E Low-Dimens. Syst. Nanostructures*, vol. 137, p. 115016, Mar. 2022, doi: 10.1016/j.physe.2021.115016.
- [24] M. Luo, Y. H. Shen, and T. L. Yin, 'Electronic and magnetic properties of TM atoms adsorption on 2D silicon carbide by first-principles calculations', *Solid State Commun.*, vol. 252, pp. 1–5, Feb. 2017, doi: 10.1016/j.ssc.2017.01.003.
- [25] A. V. Papavasileiou, M. Menelaou, K. J. Sarkar, and Z. Sofer, 'Ferromagnetic Elements in Two-Dimensional Materials: 2D Magnets and Beyond', vol. 2309046, 2024, doi: 10.1002/adfm.202309046.
- [26] P. Gu *et al.*, 'Multi-state data storage in a two-dimensional stripy antiferromagnet implemented by magnetoelectric effect', doi: 10.1038/s41467-023-39004-4.
- [27] M. Menon, E. Richter, A. Mavrandonakis, G. Froudakis, and A. N. Andriotis, 'Structure and stability of SiC nanotubes', *Phys. Rev. B - Condens. Matter Mater. Phys.*, vol. 69, no. 11, pp. 45–48, 2004, doi: 10.1103/PhysRevB.69.115322.
- [28] M. Saini and S. Choudhary, 'Understanding the Spin Transport in H₂O-Adsorbed CNT-Based Magnetic Tunnel Junction', *J. Supercond. Nov. Magn.*

- 2018 324, vol. 32, no. 4, pp. 925–929, Jun. 2018, doi: 10.1007/S10948-018-4783-8.
- [29] C. K. Yang, J. Zhao, and J. P. Lu, ‘Magnetism of Transition-Metal/Carbon-Nanotube Hybrid Structures’, *Phys. Rev. Lett.*, vol. 90, no. 25, p. 4, Jun. 2003, doi: 10.1103/PhysRevLett.90.257203.
 - [30] A. K. Geim and I. V. Grigorieva, ‘Van der Waals heterostructures’, *Nature*, vol. 499, no. 7459, pp. 419–425, 2013, doi: 10.1038/nature12385.
 - [31] B. Meshginqalam and S. Alaei, ‘Transition metals adsorption and conductivity modification in carbon nanotubes: analytical modeling and DFT study’, *Adsorption*, vol. 24, no. 6, pp. 575–583, Aug. 2018, doi: 10.1007/s10450-018-9964-z.
 - [32] S. Z. Butler *et al.*, ‘Progress, challenges, and opportunities in two-dimensional materials beyond graphene’, *ACS Nano*, vol. 7, no. 4, pp. 2898–2926, Apr. 2013.
 - [33] S. Sugahara and M. Tanaka, ‘A spin metal-oxide-semiconductor field-effect transistor using half-metallic-ferromagnet contacts for the source and drain’, *Appl. Phys. Lett.*, vol. 84, no. 13, pp. 2307–2309, 2004, doi: 10.1063/1.1689403.
 - [34] P. Barla, V. K. Joshi, and S. Bhat, ‘Spintronic devices: a promising alternative to CMOS devices’, *J. Comput. Electron.* 2021 202, vol. 20, no. 2, pp. 805–837, Jan. 2021, doi: 10.1007/S10825-020-01648-6.
 - [35] S. Choudhary and S. Qureshi, ‘Theoretical study on the effect of dopant positions and dopant density on transport properties of a BN co-doped SiC nanotube’, *Phys Lett A*, vol. 377, no. 5, pp. 430–435, Jan. 2013, doi: 10.1016/j.physleta.2012.12.007.
 - [36] S. Choudhary and M. Varshney, ‘First-Principles Study of Spin Transport in CrO₂–CNT–CrO₂ Magnetic Tunnel Junction’, *J. Supercond. Nov. Magn.* 2015 2810, vol. 28, no. 10, pp. 3141–3145, Jun. 2015, doi: 10.1007/S10948-015-3142-2.
 - [37] S. Choudhary and M. Kumar, ‘Enhanced magnetoresistance in hydrogen- and fluorine-passivated zigzag aluminium nitride’, *Eur. Phys. J. Plus*, vol. 123, 2020, doi: 10.1140/epjp/s13360-020-00945-0.
 - [38] Y. Sun, Z. Shuai, and D. Wang, ‘Lattice thermal conductivity of monolayer AsP from first-principles molecular dynamics’, *Phys. Chem. Chem. Phys.*, vol. 20, no. 20, pp. 14024–14030, May 2018, doi: 10.1039/c8cp01840e.
 - [39] J. L. Zhang *et al.*, ‘Epitaxial Growth of Single Layer Blue Phosphorus: A New Phase of Two-Dimensional Phosphorus’, *Nano Lett.*, vol. 16, no. 8, pp. 4903–4908, Aug. 2016, doi: 10.1021/acs.nanolett.6b01459.
 - [40] G. E. W. Bauer, E. Saitoh, and B. J. Van Wees, ‘Spin caloritronics’, *Nat. Mater.*, vol. 11, no. 5, pp. 391–399, 2012, doi: 10.1038/nmat3301.
 - [41] S. Tripathi, S. Choudhary, and P. K. Misra, ‘A Novel STT-SOT MTJ-Based Nonvolatile SRAM for Power Gating Applications’, *IEEE Trans. Electron Devices*, vol. 69, no. 3, pp. 1058–1064, 2022, doi: 10.1109/TED.2022.3140407.
 - [42] S. Choudhary and S. Singla, ‘Thermally Assisted Magneto Resistance and Spin-Filtration in Single Layer MoS₂’, *IEEE Trans. Nanotechnol.*, vol. 18, p. 467, 2019, doi: 10.1109/TNANO.2019.2911324.
 - [43] S. Ikeda *et al.*, ‘A perpendicular-anisotropy CoFeB–MgO magnetic tunnel junction’, *Nat. Mater.*, vol. 9, no. 9, pp. 721–724, 2010, doi: 10.1038/NMAT2804.

- [44] S. Datta and B. Das, 'Electronic analog of the electro-optic modulator', *Appl. Phys. Lett.*, vol. 56, no. 7, pp. 665–667, Feb. 1990, doi: 10.1063/1.102730.
- [45] A. Fert and H. Jaffrès, 'Conditions for efficient spin injection from a ferromagnetic metal into a semiconductor', *Phys. Rev. B - Condens. Matter Mater. Phys.*, vol. 64, no. 18, 2001, doi: 10.1103/PHYSREVB.64.184420.
- [46] H. C. Koo, J. H. Kwon, J. Eom, J. Chang, S. H. Han, and M. Johnson, 'Control of spin precession in a spin-injected field effect transistor', *Science*, vol. 325, no. 5947, pp. 1515–1518, 2009, doi: 10.1126/SCIENCE.1173667.
- [47] B. Dieny *et al.*, 'Opportunities and challenges for spintronics in the microelectronics industry', *Nat. Electron.*, vol. 3, no. 8, pp. 446–459, Aug. 2020, doi: 10.1038/s41928-020-0461-5.
- [48] S. Ahn, H. Lim, H. Shin, and S. Lee, 'Analytic model of spin-torque oscillators (STO) for circuit-level simul', *J. Semicond. Technol. Sci.*, vol. 13, no. 1, pp. 28–33, Feb. 2013, doi: 10.5573/JSTS.2013.13.1.028.
- [49] J. V. Kim, 'Spin-Torque Oscillators', *Solid State Phys. - Adv. Res. Appl.*, vol. 63, pp. 217–294, 2012, doi: 10.1016/B978-0-12-397028-2.00004-7.
- [50] H. P. Bartling *et al.*, 'Universal high-fidelity quantum gates for spin-qubits in diamond', Mar. 2024, Accessed: Jul. 23, 2024. [Online]. Available: <https://arxiv.org/abs/2403.10633v1>
- [51] K. Uchida *et al.*, 'Observation of the spin Seebeck effect', *Nature*, vol. 455, no. 7214, pp. 778–781, 2008, doi: 10.1038/nature07321.
- [52] T. da C. Santa Clara Gomes, F. Abreu Araujo, and L. Piraux, 'Making flexible spin caloritronic devices with interconnected nanowire networks', *Sci. Adv.*, vol. 5, no. 3, 2019, doi: 10.1126/SCIADV.AAV2782.
- [53] 'Iijima, S. (1991) Synthesis of Carbon Nanotubes. Nature, 354, 56-58. - References - Scientific Research Publishing'. Accessed: Dec. 28, 2021. [Online]. Available: [https://www.scirp.org/\(S\(i43dyn45teexjx455qlt3d2q\)\)/reference/ReferencesPapers.aspx?ReferenceID=1241661](https://www.scirp.org/(S(i43dyn45teexjx455qlt3d2q))/reference/ReferencesPapers.aspx?ReferenceID=1241661)
- [54] S. Choudhary and S. Qureshi, 'Theoretical study on effect of radial and axial deformation on electron transport properties in a semiconducting Si – C nanotube', *Bull Mater Sci*, vol. 35, no. 5, pp. 713–718, 2012.
- [55] S. Choudhary and S. Qureshi, 'Theoretical study on transport properties of a BN co-doped SiC nanotube', *Phys Lett A*, vol. 375, no. 38, pp. 3382–3385, Sep. 2011, doi: 10.1016/j.physleta.2011.08.001.
- [56] 'Physical properties of layer structures: optical properties and photoconductivity of thin crystals of molybdenum disulphide', *Proc. R. Soc. Lond. Ser. Math. Phys. Sci.*, vol. 273, no. 1352, pp. 69–83, Apr. 1963, doi: 10.1098/RSPA.1963.0075.
- [57] K. S. Novoselov *et al.*, 'Electric field in atomically thin carbon films', *Science*, vol. 306, no. 5696, pp. 666–669, Oct. 2004, doi: 10.1126/SCIENCE.1102896.
- [58] C. Tan *et al.*, 'Recent Advances in Ultrathin Two-Dimensional Nanomaterials', *Chem. Rev.*, vol. 117, no. 9, pp. 6225–6331, May 2017, doi: 10.1021/ACS.CHEMREV.6B00558.
- [59] B. Anasori and Y. Gogotsi, '2D Metal carbides and nitrides (MXenes): Structure, properties and applications', *2D Met. Carbides Nitrides MXenes Struct. Prop. Appl.*, pp. 1–534, Oct. 2019, doi: 10.1007/978-3-030-19026-2.

- [60] M. Ghambarian, Z. Azizi, and M. Ghashghaee, 'Phosphorene defects for high-quality detection of nitric oxide and carbon monoxide: A periodic density functional study', *Chem. Eng. J.*, vol. 396, Sep. 2020, doi: 10.1016/J.CEJ.2020.125247.
- [61] N. B. Singh and S. K. Shukla, 'Properties of two-dimensional nanomaterials', *Two-Dimens. Nanostructures Biomed. Technol. Bridge Mater. Sci. Bioeng.*, pp. 73–100, Jan. 2019, doi: 10.1016/B978-0-12-817650-4.00003-6.
- [62] Y. Pei *et al.*, 'Recent progress in the synthesis and applications of 2D metal nanosheets', *Nanotechnology*, vol. 30, no. 22, Mar. 2019, doi: 10.1088/1361-6528/AB0642.
- [63] M. Isa khan, S. Khalid, A. Majid, and S. S. Alarfaji, 'Empowering spintronics performance of 3d transition metal adsorbed B4C3 monolayer: A DFT outlook', *J. Phys. Chem. Solids*, vol. 187, no. August 2023, p. 111599, Apr. 2024, doi: 10.1016/j.jpcs.2023.111599.
- [64] M. Luo, Y. H. Shen, and T. L. Yin, 'Tunable magnetism in 2D silicon carbide doped with Co and Fe dopants: Ab initio study', *Optik*, vol. 130, pp. 589–593, Feb. 2017, doi: 10.1016/j.ijleo.2016.10.086.
- [65] X. Zhao, C. Xia, T. Wang, and X. Dai, 'Effect of structural defects on electronic and magnetic properties of pristine and Mn-doped MoS2 monolayer', *Solid State Commun.*, vol. 220, pp. 31–35, Jul. 2015, doi: 10.1016/j.ssc.2015.07.003.
- [66] Y. Wang *et al.*, 'Manipulating electronic and magnetic properties of black phosphorene with 4d series transition metal adsorption', *Phys. Lett. Sect. Gen. At. Solid State Phys.*, vol. 383, no. 23, pp. 2765–2771, Aug. 2019, doi: 10.1016/j.physleta.2019.05.057.
- [67] Z. Cui, K. Yang, K. Ren, S. Zhang, and L. Wang, 'Adsorption of metal atoms on MoSi2N4 monolayer: A first principles study', *Mater. Sci. Semicond. Process.*, vol. 152, Dec. 2022, doi: 10.1016/j.mssp.2022.107072.
- [68] K. S. Novoselov *et al.*, 'Two-dimensional gas of massless Dirac fermions in graphene', *Nat. 2005 4387065*, vol. 438, no. 7065, pp. 197–200, Nov. 2005, doi: 10.1038/nature04233.
- [69] X. Han, J. Yang, P. Yuan, B. Bian, H. Shi, and Y. Ding, 'Spin-dependent transport in a multifunctional spintronic device with graphene nanoribbon electrodes', *J. Comput. Electron.*, vol. 17, no. 2, pp. 604–612, Jun. 2018, doi: 10.1007/s10825-018-1148-2.
- [70] J. Deb and U. Sarkar, 'Boron-nitride and boron-phosphide doped twin-graphene: Applications in electronics and optoelectronics', *Appl. Surf. Sci.*, vol. 541, no. December 2020, p. 148657, 2021, doi: 10.1016/j.apsusc.2020.148657.
- [71] O. M. J. Van 't Erve *et al.*, 'Graphene and monolayer transition-metal dichalcogenides: properties and devices', *J. Mater. Res. 2016 317*, vol. 31, no. 7, pp. 845–877, Apr. 2016, doi: 10.1557/JMR.2015.397.
- [72] K. Tarawneh and Y. Al-Khatatbeh, 'Adsorption of 3d transition-metal atoms on two-dimensional penta-graphene: A first-principles study', *J. Saudi Chem. Soc.*, p. 101611, Mar. 2023, doi: 10.1016/j.jscs.2023.101611.
- [73] W. Hu *et al.*, 'Embedding atomic cobalt into graphene lattices to activate room-temperature ferromagnetism', *Nat. Commun. 2021 121*, vol. 12, no. 1, pp. 1–8, Mar. 2021, doi: 10.1038/s41467-021-22122-2.

- [74] R. Nandee, M. A. Chowdhury, A. Shahid, N. Hossain, and M. Rana, 'Band gap formation of 2D material in graphene: Future prospect and challenges', *Results Eng.*, vol. 15, p. 100474, Sep. 2022, doi: 10.1016/J.RINENG.2022.100474.
- [75] J. H. Garcia, M. Vila, A. W. Cummings, and S. Roche, 'Spin transport in graphene/transition metal dichalcogenide heterostructures', *Chem. Soc. Rev.*, vol. 47, no. 9, pp. 3359–3379, Apr. 2018, doi: 10.1039/C7CS00864C.
- [76] Q. H. Wang, K. Kalantar-Zadeh, A. Kis, J. N. Coleman, and M. S. Strano, 'Electronics and optoelectronics of two-dimensional transition metal dichalcogenides', *Nat. Nanotechnol.* 2012 711, vol. 7, no. 11, pp. 699–712, Nov. 2012, doi: 10.1038/nnano.2012.193.
- [77] S. Shirvani, M. Ghashghaee, and K. J. Smith, 'Two-dimensional Nanomaterials in Thermocatalytic Reactions: Transition Metal Dichalcogenides, Metal Phosphorus Trichalcogenides and MXenes', *Catal. Rev. - Sci. Eng.*, vol. 65, no. 1, pp. 1–51, Jan. 2023, doi: 10.1080/01614940.2021.1899605.
- [78] V. Musle, A. Kumar, and S. Choudhary, 'Temperature dependent spin transport investigations in single layer VTe₂', *J. Alloys Compd.*, vol. 770, pp. 345–349, Jan. 2019, doi: 10.1016/J.JALLCOM.2018.08.170.
- [79] F. Yang *et al.*, 'Emerging Enhancement and Regulation Strategies for Ferromagnetic 2D Transition Metal Dichalcogenides', *Adv. Sci.*, vol. 10, no. 21, p. 2300952, Jul. 2023, doi: 10.1002/ADVS.202300952.
- [80] A. A. Tedstone, D. J. Lewis, and P. O'Brien, 'Synthesis, Properties, and Applications of Transition Metal-Doped Layered Transition Metal Dichalcogenides', *Chem. Mater.*, vol. 28, no. 7, pp. 1965–1974, Apr. 2016, doi: 10.1021/acs.chemmater.6b00430.
- [81] K. S. Novoselov, A. Mishchenko, A. Carvalho, and A. H. Castro Neto, '2D materials and van der Waals heterostructures', *Science*, vol. 353, no. 6298, 2016, doi: 10.1126/science.aac9439.
- [82] M. Fang¹ and E.-H. Yang¹, '2D Magnetic Semiconductors via Substitutional Doping of Transition Metal Dichalcogenides'.
- [83] M. Fang and E.-H. Yang, 'Advances in Two-Dimensional Magnetic Semiconductors via Substitutional Doping of Transition Metal Dichalcogenides', *Materials*, vol. 16, no. 10, p. 3701, May 2023, doi: 10.3390/ma16103701.
- [84] F. Shojaei and H. S. Kang, 'Electronic Structure and Carrier Mobility of Two-Dimensional α Arsenic Phosphide', *J. Phys. Chem. C*, vol. 119, no. 34, pp. 20210–20216, Aug. 2015, doi: 10.1021/acs.jpcc.5b07323.
- [85] A. Loiseau, F. Willaime, N. Demoncy, G. Hug, and H. Pascard, 'Boron Nitride Nanotubes with Reduced Numbers of Layers Synthesized by Arc Discharge', *Phys. Rev. Lett.*, vol. 76, no. 25, p. 4737, Jun. 1996, doi: 10.1103/PhysRevLett.76.4737.
- [86] N. G. Chopra *et al.*, 'Boron Nitride Nanotubes', *Science*, vol. 269, no. 5226, pp. 966–967, Aug. 1995, doi: 10.1126/SCIENCE.269.5226.966.
- [87] B. Yan, G. Zhou, J. Wu, W. Duan, and B. L. Gu, 'Bonding modes and electronic properties of single-crystalline silicon nanotubes', *Phys. Rev. B - Condens. Matter Mater. Phys.*, vol. 73, no. 15, 2006, doi: 10.1103/PHYSREVB.73.155432.

- [88] S. Behzad, R. Moradian, and R. Chegel, 'Structural and Electronic Properties of Silicon Carbide Nanotubes', pp. 1860–1869, 2012, doi: 10.1166/jctn.2012.2597.
- [89] M. Zhao, Y. Xia, F. Li, R. Q. Zhang, and S. T. Lee, 'Strain energy and electronic structures of silicon carbide nanotubes: Density functional calculations', *Phys. Rev. B - Condens. Matter Mater. Phys.*, vol. 71, no. 8, pp. 1–6, 2005, doi: 10.1103/PhysRevB.71.085312.
- [90] B. Peng, M. Annamalai, S. Mothes, and M. Schröter, 'Device design and optimization of CNTFETs for high-frequency applications', *J. Comput. Electron.*, vol. 20, no. 6, pp. 2492–2500, Dec. 2021, doi: 10.1007/s10825-021-01805-5.
- [91] E. V. Larina, V. I. Chmyrev, V. M. Skorikov, P. N. D'yachkov, and D. V. Makaev, 'Band structure of silicon carbide nanotubes', *Inorg. Mater.*, vol. 44, no. 8, pp. 823–834, 2008, doi: 10.1134/S0020168508080086.
- [92] C. K. Yang, J. Zhao, and J. P. Lu, 'Complete spin polarization for a carbon nanotube with an adsorbed atomic transition-metal chain', *Nano Lett.*, vol. 4, no. 4, pp. 561–563, 2004, doi: 10.1021/nl035104x.
- [93] H. Cui, G. Zhang, X. Zhang, and J. Tang, 'Rh-doped MoSe₂ as a toxic gas scavenger: a first-principles study', *Nanoscale Adv.*, vol. 1, no. 2, pp. 772–780, Feb. 2019, doi: 10.1039/C8NA00233A.
- [94] A. Srivastava, S. K. Jain, and P. S. Khare, 'Ab-initio study of structural, electronic, and transport properties of zigzag GaP nanotubes', *J. Mol. Model.*, vol. 20, no. 3, 2014, doi: 10.1007/s00894-014-2171-2.
- [95] A. Chauhan, A. Maahich, and J. Pal, 'First-principles calculations of the electronic and optical properties of WSe₂/Cd_{0.9}Zn_{0.1}Te van der Waals heterostructure', *J. Comput. Electron.*, vol. 20, no. 1, pp. 13–20, Feb. 2021, doi: 10.1007/s10825-021-01659-x.
- [96] D. Bahamon, M. Khalil, A. Belabbes, Y. Alwahedi, L. F. Vega, and K. Polychronopoulou, 'A DFT study of the adsorption energy and electronic interactions of the SO₂ molecule on a CoP hydrotreating catalyst', *RSC Adv.*, vol. 11, no. 5, pp. 2947–2957, Jan. 2021, doi: 10.1039/C9RA10634K.
- [97] T. Lei, I. Pochorovski, and Z. Bao, 'Separation of Semiconducting Carbon Nanotubes for Flexible and Stretchable Electronics Using Polymer Removable Method', *Acc. Chem. Res.*, vol. 50, no. 4, pp. 1096–1104, 2017, doi: 10.1021/acs.accounts.7b00062.
- [98] T. Dürkop, S. A. Getty, E. Cobas, and M. S. Fuhrer, 'Extraordinary Mobility in Semiconducting Carbon Nanotubes', *Nano Lett.*, vol. 4, no. 1, pp. 35–39, 2004, doi: 10.1021/nl034841q.
- [99] M. R. Kumar and S. Singh, 'Ab Initio Analysis of Li Adsorption on Beryllium-Doped Zigzag Graphene Nanoribbon for Lithium-Ion Batteries (LIBs)', *J. Electron. Mater.*, vol. 51, no. 11, pp. 6134–6144, Nov. 2022, doi: 10.1007/s11664-022-09807-0.
- [100] Z. L. Li, X. X. Fu, G. P. Zhang, and C. K. Wang, 'Effect of Gate Electric Field on Single Organic Molecular Devices', *Chin. J. Chem. Phys.*, vol. 26, no. 2, p. 185, May 2013, doi: 10.1063/1674-0068/26/02/185-190.

- [101] D. Ma *et al.*, ‘Electronic Transport Properties of an Anthraquinone-Based Molecular Switch with Carbon Nanotube Electrodes’, *Chin. Phys. Lett.*, vol. 29, no. 4, p. 047302, Apr. 2012, doi: 10.1088/0256-307X/29/4/047302.
- [102] M. Ouyang and D. D. Awschalom, ‘Coherent Spin Transfer Between Molecularly Bridged Quantum Dots’, *Science*, vol. 301, no. 5636, pp. 1074–1078, 2003, doi: 10.1126/science.1086963.
- [103] Y. Ni, X. Wang, W. Tao, S. C. Zhu, and K. L. Yao, ‘The spin-dependent transport properties of zigzag α -graphyne nanoribbons and new device design’, *Sci. Rep. 2016 61*, vol. 6, no. 1, pp. 1–10, May 2016, doi: 10.1038/srep25914.
- [104] P. Vogt *et al.*, ‘Silicene: Compelling Experimental Evidence for Graphenelike Two-Dimensional Silicon’, *Phys Rev Lett*, vol. 108, no. 15, p. 155501, Apr. 2012, doi: 10.1103/PhysRevLett.108.155501.
- [105] M. Buscema, D. J. Groenendijk, S. I. Blanter, G. A. Steele, H. S. J. van der Zant, and A. Castellanos-Gomez, ‘Fast and Broadband Photoresponse of Few-Layer Black Phosphorus Field-Effect Transistors’, *Nano Lett.*, vol. 14, no. 6, pp. 3347–3352, Jun. 2014, doi: 10.1021/nl5008085.
- [106] H. Liu *et al.*, ‘Phosphorene: An Unexplored 2D Semiconductor with a High Hole Mobility’, *ACS Nano*, vol. 8, no. 4, pp. 4033–4041, Apr. 2014, doi: 10.1021/nl501226z.
- [107] W. Lu *et al.*, ‘Plasma-assisted fabrication of monolayer phosphorene and its Raman characterization’, *Nano Res. 2014 76*, vol. 7, no. 6, pp. 853–859, May 2014, doi: 10.1007/S12274-014-0446-7.
- [108] A. Castellanos-Gomez, ‘Black Phosphorus: Narrow Gap, Wide Applications’, *J. Phys. Chem. Lett.*, vol. 6, no. 21, pp. 4280–4291, Nov. 2015, doi: 10.1021/acs.jpcllett.5b01686.
- [109] Z. Y. Zhang *et al.*, ‘Indirect-direct band gap transition through electric tuning in bilayer MoS₂’, *J. Chem. Phys.*, vol. 140, no. 17, p. 174707, May 2014, doi: 10.1063/1.4873406.
- [110] V. Shukla, R. B. Araujo, N. K. Jena, and R. Ahuja, ‘The curious case of two dimensional Si₂BN: A high-capacity battery anode material’, *Nano Energy*, vol. 41, pp. 251–260, Nov. 2017, doi: 10.1016/J.NANOEN.2017.09.026.
- [111] A. S. Nair, R. Ahuja, R. Ahuja, and B. Pathak, ‘Unraveling the single-atom electrocatalytic activity of transition metal-doped phosphorene’, *Nanoscale Adv.*, vol. 2, no. 6, pp. 2410–2421, Jun. 2020, doi: 10.1039/D0NA00209G.
- [112] Y. Pan *et al.*, ‘Graphdiyne–metal contacts and graphdiyne transistors’, *Nanoscale*, vol. 7, no. 5, pp. 2116–2127, Jan. 2015, doi: 10.1039/C4NR06541G.
- [113] J. Xu *et al.*, ‘2D Frameworks of C₂N and C₃N as New Anode Materials for Lithium-Ion Batteries’, *Adv. Mater.*, vol. 29, no. 34, p. 1702007, Sep. 2017, doi: 10.1002/ADMA.201702007.
- [114] J. Zhang *et al.*, ‘Blue-AsP monolayer as a promising anode material for lithium- and sodium-ion batteries: a DFT study’, *Phys. Chem. Chem. Phys.*, vol. 23, no. 9, pp. 5143–5151, Mar. 2021, doi: 10.1039/D0CP05879C.
- [115] Y. Xu, G. Liu, S. Xing, G. Zhao, and J. Yang, ‘Tuning the mechanical and electronic properties and carrier mobility of phosphorene via family atom doping: a first-principles study’, *J. Mater. Chem. C*, vol. 8, no. 42, pp. 14902–14909, Nov. 2020, doi: 10.1039/D0TC04024J.

- [116] X. Zhang *et al.*, ‘Stable high efficiency two-dimensional perovskite solar cells via cesium doping’, *Energy Environ. Sci.*, vol. 10, no. 10, pp. 2095–2102, Oct. 2017, doi: 10.1039/C7EE01145H.
- [117] Z. Zhu, J. Guan, and D. Tománek, ‘Structural Transition in Layered As_{1-x}P_x Compounds: A Computational Study’, *Nano Lett.*, vol. 15, no. 9, pp. 6042–6046, Sep. 2015, doi: 10.1021/acs.nanolett.5b02227.
- [118] M. Xie *et al.*, ‘A promising two-dimensional solar cell donor: Black arsenic–phosphorus monolayer with 1.54 eV direct bandgap and mobility exceeding 14,000 cm² V⁻¹ s⁻¹’, *Nano Energy*, vol. 28, pp. 433–439, Oct. 2016, doi: 10.1016/J.NANOEN.2016.08.058.
- [119] D. M. Rowe, V. S. Shukla, and N. Savvides, ‘Phonon scattering at grain boundaries in heavily doped fine-grained silicon–germanium alloys’, *Nat.* 1981 2905809, vol. 290, no. 5809, pp. 765–766, 1981, doi: 10.1038/290765a0.
- [120] S. Saini and S. Choudhary, ‘A DFT study of transition metal doped two-dimensional Bismuth (Bismuthene) for spintronics applications’, *Adv. Nat. Sci. Nanosci. Nanotechnol.*, vol. 13, no. 1, p. 015005, Feb. 2022, doi: 10.1088/2043-6262/AC53FE.
- [121] K. Zhang, X. Wu, and J. Yang, ‘Transition Metal Dichalcogenides Magnetic Atomic Chains’, *Nanoscale Adv.*, 2022, doi: 10.1039/D2NA00543C.
- [122] Z. G. majd, S. F. Taghizadeh, P. Amiri, and B. Vaseghi, ‘Half-metallic properties of transition metals adsorbed on WS₂ monolayer: A first-principles study’, *J. Magn. Magn. Mater.*, vol. 481, pp. 129–135, 2019, doi: <https://doi.org/10.1016/j.jmmm.2019.01.063>.
- [123] ‘Atomistic Simulation Software | QuantumATK - Synopsys’. Accessed: Jun. 16, 2023. [Online]. Available: <https://www.synopsys.com/silicon/quantumatk.html>
- [124] N. H. E. Weste, *CMOS VLSI Design: A Circuits and Systems Perspective*. Pearson Education, 2006. [Online]. Available: <https://books.google.co.in/books?id=Wqlo0P3doKoC>
- [125] N. S. Kim *et al.*, ‘Leakage current: Moore’s law meets static power’, *Computer*, vol. 36, no. 12, pp. 68–75, Dec. 2003, doi: 10.1109/MC.2003.1250885.
- [126] M. Dolatshahi, O. Hashemipour, and K. Navi, ‘A new systematic design approach for low-power analog integrated circuits’, *AEU - Int. J. Electron. Commun.*, vol. 66, no. 5, pp. 384–389, May 2012, doi: 10.1016/j.aeue.2011.09.005.
- [127] K. Roy, S. Mukhopadhyay, and H. Mahmoodi-Meimand, ‘Leakage current mechanisms and leakage reduction techniques in deep-submicrometer CMOS circuits’, *Proc. IEEE*, vol. 91, no. 2, pp. 305–327, Feb. 2003, doi: 10.1109/JPROC.2002.808156.
- [128] P. Gupta, A. B. Kahng, P. Sharma, and D. Sylvester, ‘Gate-length biasing for runtime-leakage control’, *IEEE Trans. Comput.-Aided Des. Integr. Circuits Syst.*, vol. 25, no. 8, pp. 1475–1485, Aug. 2006, doi: 10.1109/TCAD.2005.857313.
- [129] G. Prenat *et al.*, ‘CMOS/Magnetic Hybrid Architectures’, in *2007 14th IEEE International Conference on Electronics, Circuits and Systems*, Dec. 2007, pp. 190–193. doi: 10.1109/ICECS.2007.4510962.
- [130] J.-G. (Jimmy) Zhu and C. Park, ‘Magnetic tunnel junctions’, *Mater. Today*, vol. 9, no. 11, pp. 36–45, Nov. 2006, doi: 10.1016/S1369-7021(06)71693-5.

- [131] David M. Bromberg and Daniel H. Morris, ‘mCell Model’. Jan. 2015. doi: doi:/10.4231/D3CR5ND3Q.
- [132] N. Bruchon, L. Torres, G. Sassatelli, and G. Cambon, ‘Magnetic tunnelling junction based FPGA’, in *Proceedings of the 2006 ACM/SIGDA 14th international symposium on Field programmable gate arrays*, in FPGA ’06. New York, NY, USA: Association for Computing Machinery, Feb. 2006, pp. 123–130. doi: 10.1145/1117201.1117220.
- [133] W. Zhao, E. Belhaire, Q. Mistral, E. Nicolle, T. Devolder, and C. Chappert, ‘Integration of Spin-RAM technology in FPGA circuits’, in *2006 8th International Conference on Solid-State and Integrated Circuit Technology Proceedings*, Oct. 2006, pp. 799–802. doi: 10.1109/ICSICT.2006.306511.
- [134] K. Ryu, J. Kim, J. Jung, J. P. Kim, S. H. Kang, and S.-O. Jung, ‘A Magnetic Tunnel Junction Based Zero Standby Leakage Current Retention Flip-Flop’, *IEEE Trans. Very Large Scale Integr. VLSI Syst.*, vol. 20, no. 11, pp. 2044–2053, Nov. 2012, doi: 10.1109/TVLSI.2011.2172644.
- [135] L. Mahor, A. Chauhan, and P. Tiwari, ‘Parity Preserving Reversible Design Using FinFETs’, in *2019 1st International Conference on Signal Processing, VLSI and Communication Engineering (ICSPVCE)*, Mar. 2019, pp. 1–6. doi: 10.1109/ICSPVCE46182.2019.9092779.
- [136] C. H. Bennett, ‘Logical Reversibility of Computation’, *IBM J. Res. Dev.*, vol. 17, no. 6, pp. 525–532, Nov. 1973, doi: 10.1147/rd.176.0525.
- [137] A. Roohi, R. Zand, S. Angizi, and R. F. DeMara, ‘A Parity-Preserving Reversible QCA Gate with Self-Checking Cascadable Resiliency’, *IEEE Trans. Emerg. Top. Comput.*, vol. 6, no. 4, pp. 450–459, Oct. 2018, doi: 10.1109/TETC.2016.2593634.
- [138] S. M. R. Taha, *Reversible Logic Synthesis Methodologies with Application to Quantum Computing*, vol. 37. in *Studies in Systems, Decision and Control*, vol. 37. Cham: Springer International Publishing, 2016. doi: 10.1007/978-3-319-23479-3.
- [139] V. Jamshidi and M. Fazeli, ‘Design of ultra low power current mode logic gates using magnetic cells’, *AEU - Int. J. Electron. Commun.*, vol. 83, pp. 270–279, Jan. 2018, doi: 10.1016/j.aeue.2017.09.009.
- [140] M. Rajeshwari, Rohini. S. Hongal, and Rajashekar. B. Shettar, ‘Design and Implementation of 8 Bit Shift Register using Reversible Logic’, in *2018 International Conference on Current Trends towards Converging Technologies (ICCTCT)*, Mar. 2018, pp. 1–4. doi: 10.1109/ICCTCT.2018.8551165.
- [141] T. R. Rakshith and R. Saligram, ‘Parity preserving logic based fault tolerant reversible ALU’, in *2013 IEEE Conference on Information & Communication Technologies*, Apr. 2013, pp. 485–490. doi: 10.1109/CICT.2013.6558144.

LIST OF PUBLICATIONS AND THEIR PROOFS

Journals

1. **Anurag Chauhan**, Kapil Sharma, and Sudhanshu Choudhary, Transition metal induced-magnetization in zigzag SiCNTs. J Comput Electron 22, 964–970 (2023). <https://doi.org/10.1007/s10825-023-02030-y> (IF: 2.1)
2. **Anurag Chauhan**, Kapil Sharma, and Sudhanshu Choudhary, “Transition metal induced- magnetization and spin-polarisation in black arsenic Phosphorus,” Ain Shams Eng. J., p. 102632, 2024, doi:<https://doi.org/10.1016/j.asej.2024.102632>. (IF: 6.0)

International Conferences:

1. **Anurag Chauhan**, Kapil Sharma, and Sudhanshu Choudhary “Transition Metal-induced Magnetization in (6,0) SiCNT” in the 2nd International Conference on Recent Advances in Functional Materials (RAFM-2024).
2. **Anurag Chauhan**, Kapil Sharma, and Sudhanshu Choudhary “Implementation of Fault Tolerant Arithmetic Logic Unit Using mCell” in the 2nd International Conference on Atomic, Molecular, Material, Nano and Optical Physics with Applications (ICAMNOP- 2023)

1. **Anurag Chauhan**, Kapil Sharma, and Sudhanshu Choudhary, Transition metal induced-magnetization in zigzag SiCNTs. *J Comput Electron* 22, 964–970 (2023). <https://doi.org/10.1007/s10825-023-02030-y> (IF: 2.1)

Journal of Computational Electronics
<https://doi.org/10.1007/s10825-023-02030-y>



Transition metal induced-magnetization in zigzag SiCNTs

Anurag Chauhan¹ · Kapil Sharma¹ · Sudhanshu Choudhary²

Received: 29 September 2022 / Accepted: 16 March 2023
 © The Author(s), under exclusive licence to Springer Science+Business Media, LLC, part of Springer Nature 2023

Abstract

In this paper, we report the induced magnetization in metallic and semiconducting SiCNTs on the adsorption of transition metals. The resultant adsorbed SiCNTs structures showed half-metal-ferromagnetic and ferromagnetic behaviour verifying the induced magnetization. The spin-density of states and bandstructure have also been studied, confirming the induced magnetic behaviour. The strength of the induced ferromagnetic behaviour is varied with the various transition metals and is then related to the calculated magnetic moment in the adsorbed structure. The Cr adsorbed (8,0) SiCNT indicated strong half-metal-ferromagnetic behaviour with a magnetic moment of $5.4 \mu_B$. Only Cu-adsorbed (6,0) metallic SiCNT showed ferromagnetic behaviour among all the simulated structures indicating the impact of transition metal on the SiCNT structures. These promising results will be helpful in designing of devices like spin-valves, MTJs, and MRAMs in the field of spintronics.

Keywords Silicon carbide nanotube · Ferromagnetism · Density functional theory · Adsorption · Transition metals · Magnetic moment

1 Introduction

In the last 2 decades, carbon nanotubes have opened a new world of possibilities for researchers and the semiconductor industry. They are considered as one of the promising candidates for designing of nanodevices like nanosensors due to their high stability, unique electronic and mechanical properties and high frequency response [1, 2].

The successful synthesis of the Boron-Nitride nanotube showed that nanotubes synthesized from other materials are also feasible [3, 4]. Later, silicon carbide nanotubes were also reported to be grown using the self-assembling technique [5]. These nanostructures showed very different and unique properties compared to their bulk forms due to their small size and tubular structure. The nanotubes could behave metallic or semiconducting based on their chirality and diameter dimensions. Compared to carbon nanotubes

(CNTs), silicon carbide nanotubes (SiCNTs) are more suitable in the electronics industry field due to their unique physical and electronic properties. Therefore, SiCNTs are more suitable for higher power, temperature, and frequency operations [6–9]. The studies report that the nature of SiCNTs depends on the value of (n, m) , where n and m are the chirality vectors. The $(n, 0)$ nanotubes are identified as zigzag nanotubes, whereas (n, n) nanotubes are identified as armchair nanotubes. It also states that $(n, 0)$ i.e., zigzag SiCNTs for $n = (7, 9)$ are semiconducting in nature, and their bandgap increases with the value of the chiral vector n , whereas they are metallic for $n \leq 6$ [10, 11]. For the case of (n, n) , i.e., armchair nanotubes, SiCNTs are metallic for $n = 5$ and 6 but semiconducting in the range $n = (7, 10)$ with their bandgap decreasing with an increasing value of n . Due to these properties of SiCNTs, they make a very suitable material to be used as the channel in developing spintronic devices [12, 13].

Spintronic devices find their applications in designing of programmable logic elements, magnetic sensors, Magnetic Tunnel Junctions (MTJ) and magnetic random-access memory (MRAM). While choosing an electrode material for designing of spintronic device, half-metallicity is the most important characteristic. Materials possessing half-metallicity are highly selective to the spin orientation of the electron and hence are used as electrode material in the designing of


✉ Anurag Chauhan
 anuragchauhan@dtu.ac.in
 Kapil Sharma
 kapil@ieee.org
 Sudhanshu Choudhary
 sudhanshu.choudhary@und.edu

¹ Delhi Technological University, New Delhi, India

² University of North Dakota, Grand Forks, ND, USA

2. **Anurag Chauhan**, Kapil Sharma, and Sudhanshu Choudhary, “Transition metal induced- magnetization and spin-polarisation in black arsenic Phosphorus,” *Ain Shams Eng. J.*, p. 102632, 2024, doi:<https://doi.org/10.1016/j.asej.2024.102632>. (IF: 6.0)


Ain Shams Engineering Journal 15 (2024) 102632



Contents lists available at ScienceDirect

Ain Shams Engineering Journal

journal homepage: www.sciencedirect.com



Full Length Article

Transition metal induced- magnetization and spin-polarisation in black arsenic phosphorous

Anurag Chauhan^{a,*}, Kapil Sharma^a, Sudhanshu Choudhary^b

^a Delhi Technological University, India
^b University of North Dakota, North Dakota, United States

ARTICLE INFO

Keywords:
Spintronics
Half metallic
Black arsenic phosphorus
Density Functional Theory
2D materials
Adsorption
Transition Metals
Magnetization

ABSTRACT

The electronic and magnetic properties of two-dimensional black Arsenic Phosphorus (b-AsP) on adsorption of Transition Metals (TM) on its surface are investigated using density functional theory (DFT) based on first principles calculations. Spin-density of states (S-DOS) and the bandstructure of all the transition metals adsorbed structures have been plotted which reveals their change from non-magnetic to magnetic behaviour. The results suggest that pristine b-AsP which is a non-magnetic semiconductor turns into a half metal ferromagnet (HMF) on adsorption of Co, Fe and Ti, and it turns into a ferromagnet (FM) on adsorption of Cr and Zr. The total magnetic moments were also calculated to further support our results and findings. Strong magnetic moments were observed for Cr, Fe and Ti adsorbed b-AsP structures. Ag, Cu and Mo adsorption over b-AsP results into non-magnetic metallic characteristics with very weak magnetic moments. This transformation from a non-magnetic semiconductor to a magnetic HMF or FM material demonstrates the potential use of b-AsP in designing spin magnetic devices for various spin-based applications.

1. Introduction

Spintronics is an emerging field where the electron's spin can be used for current flow in electronic devices and systems. The involvement of spin opens new opportunities for development of novel electronic devices [1,2]. The development of these spin-based devices is based on choosing suitable materials which support spin-based characteristics and transport properties. With the advancement in process technology, many spin characteristics like spin-filtering effect (SFE) [3,4] Giant Magnetoresistance (GMR), and Tunnel Magnetoresistance (TMR) have been discovered by theoretical and experimental research on the novel 2D materials [5,6]. Graphene, black- phosphorus, and silicene are some of the 2D materials of immense interest to both theoretical and experimental research in spintronics [7–12].

Since the discovery of graphene in 2004, the global scientific community has shown considerable interest in two-dimensional (2D) materials due to their exceptional physical properties. Graphene, with its ultrahigh surface area, mechanical flexibility, and remarkable electrical conductivity, has positioned itself as a high-performance electrode material for energy storage devices [13–18]. Despite the impressive properties of graphene, the conventional graphite anode in Lithium-Ion Batteries (LIB) faces challenges meeting the growing demands of new storage technologies and the electronic devices market due to its low energy density [19]. Consequently, there is a pressing need to identify advanced electrode materials with enhanced capacities.

In recent years, the study of 2D materials, beyond graphene, has reached new heights, driven by their improved charge carrier ability and higher energy density compared to conventional anode materials [20]. The small volume-to-surface area ratio and exposed surface of a 2D structure allows for controlled manipulation of material properties through impurity doping or defect formation [20–24]. For instance, the synthesis of 2D phosphorene (Black-P) with a honeycomb structure has garnered attention for its reported ultra-high electron mobility of up to $10^4 \text{ cm}^2/\text{V-s}$ [25,23].

However, black phosphorus, while promising, is unstable at room temperature and has a fixed band gap, limiting its use in optoelectronics devices. Another notable 2D material, black Arsenic Phosphorous (b-AsP), has emerged with higher stability at room temperature and modulation properties such as a tunable bandgap compared to black phosphorene [21]. Researchers, including Zhang et al., have proposed the incorporation of AsP in doped atoms, resulting in a transition from semiconductor to metal properties, making it a potential electrode

^{*} Corresponding author.
E-mail addresses: anuragchauhan@dtu.ac.in (A. Chauhan), kapil@ieee.org (K. Sharma), sudhanshu.choudhary@UND.edu (S. Choudhary).

<https://doi.org/10.1016/j.asej.2024.102632>
Received 26 October 2023; Received in revised form 7 December 2023; Accepted 26 December 2023
Available online 16 January 2024
2090-4479/© 2024 THE AUTHORS. Published by Elsevier BV on behalf of Faculty of Engineering, Ain Shams University. This is an open access article under the CC BY license (<http://creativecommons.org/licenses/by/4.0/>).

1. **Anurag Chauhan**, Kapil Sharma, and Sudhanshu Choudhary
“Implementation of Fault Tolerant Arithmetic Logic Unit Using mCell” in the
2nd International Conference on Atomic, Molecular, Material, Nano and
Optical Physics with Applications (ICAMNOP- 2023)



2. **Anurag Chauhan**, Kapil Sharma, and Sudhanshu Choudhary “Transition Metal-induced Magnetization in (6,0) SiCNT” in the 2nd International Conference on Recent Advances in Functional Materials (RAFM-2024).



CURRICULUM VITAE

Anurag Chauhan

Assistant Professor, Department of Electronics and Communication Engineering,
Delhi Technological University

Email: anurag2305chauhan@gmail.com

Professional Summary:

A highly motivated Assistant Professor with over 7 years of experience in the field of VLSI and nanoelectronics. Proven track record in research, teaching, and supervision of students. Adept in utilizing advanced technologies and tools for research and development. Recipient of multiple research excellence awards and active member of IEEE.

Key Achievements:

- Successfully supervised 10+ M.Tech and B.Tech student projects, leading to significant research contributions and publications.
- Published 5 high-impact journal articles in reputed journals with a focus on VLSI and nanoelectronics.
- Received the Commendable Research Award in REA 2022 and REA 2023.

Education:

- **PhD in Nanoelectronics**
Delhi Technological University, 2018-2024
Thesis Title: 'Transition Metal Induced High Spin Polarization in Zigzag SiCNT and Black Arsenic Phosphorus: Materials for Spintronic Applications'
- **M.Tech in VLSI Design and Embedded Systems**
National Institute of Technology, Kurukshetra, 2013-2015
- **B.Tech in Electronics and Communication Engineering**
Guru Gobind Singh Indraprastha University, 2009-2013

Technical Skills:

- **Tools & Software:** Cadence Virtuoso, LTspice, Xilinx, MATLAB, Synopsys QuantumATK
- **Programming Languages:** VHDL, Verilog
- **Technologies:** VLSI, Spintronics, Optoelectronics, Nanoelectronics

Professional Experience:

- Warden for the VVS- Boys Hostel (2019- Present)
- Lab In-charge of PCB Lab (2018-19)
- Lab In-charge of Microwave Engineering. Lab (2020- December 2022)
- Faculty In-charge for the LIC Lab (April 2022 - January 2023)
- Panel member for Online Document Verification shortlisting of Delhi Assembly Research Committee (DARC)
- Various committee memberships for convocation, cultural festivals, and academic audits at DTU
- Faculty Advisor and Coordinator for multiple student societies and events
- Member of the Departmental NBA and IQAC committees

Supervision and Guidance of Students:

- **M.Tech:**
 - Bharti Gahlot, "A Novel DTMOS Based CCCDCC With its Applications" (2017-19, Passed)
 - Ashish Suri, "Cognitive Energy Harvesting System Under Finite Battery Constraints" (2017-19, Passed)
 - Abhishek, "Comparison of Power and Performance of Full-Adder Using Dynamic CMOS LOGIC, NORA LOGIC, AND NORA Logic with MTCMOS Of sub-45 nm Technology Node" (2018-20, Passed)
 - Prateek Tomar, "MoS₂/Cd_{0.90}Zn_{0.10}Te_{0.93}Se_{0.07} vdW Interacted Heterostructure for Photovoltaic Applications with Enhanced Absorption in Visible Region" (2018-20, Passed)
 - Ajit Bandhu, "Comparison of Different Types of Multipliers using Parallel Prefix Adders" (2019-21, Passed)
 - Divyansh Singh, "Implementation of nanowire reconfigurable FET as a biosensor with improved sensitivity" (2021-23, Passed)
 - Richa Dubey, "Implementation of Ternary Logic Using CNTFET" (2022-24, Under Progress)

- **B.Tech Groups Supervised:**

- Reva Gupta, Sumegha Agarwal, "Robotic Hand" (2017-18, Passed)
- Sandeep Kumar Yadav, Sanjeev Kumar, "Autonomous Rubik's Cube Solver Robot" (2017-18, Passed)
- Ritesh Mehta, Sanjeev Kumar Tomar, Shalini, "Advanced Medicine Dispenser and Monitoring System" (2018-19, Passed)
- Kartikeya Malhotra, Lalit Prakash Yadav, Rishabh Choudhary, "Fingerprint and GSM based Door Locking System" (2018-19, Passed)
- Kapil Kumar, Kartik Nerwal, Lalit Kumar Tanwar, Meghna, "ALU Implementation Using Robust Dual Mode Pass Transistor Logic" (2020-21, Passed)
- Kirandeep Kaur Saini, Rushil Domah, Nitin Rajput, "Performance Analysis of Optical Communication System for Various Filtering Operations Using MIMO FSO System Under Fog Condition" (2020-21, Passed)
- Archana Kumari, Priyanka Meena, "FSO based Simulation and Performance Analysis for Underground Trains" (2020-21, Passed)
- Richa Sharma, Rohit Kumar, "Performance Analysis of 4-Bit Multiplier Using 90nm Technology" (2021-22, Passed)
- Priyanshu Yadav, Prithvi Kumar, Prince Kumar, "Power Theft Detection System" (2021-22, Passed)
- Shivank Sharma, Shorya Kumar, Shreyas Jain, "A Novel Low-Power Full Adder Architecture Using Magnetic Cells" (2022-23, Passed)
- Chetan Batra, Harish Tripathi, Himanshu Kumar, "New 14T Hybrid Full Adder: Minimising Power and Maximizing Speed" (2023-24, Passed)
- Siddharth, Umang Aggarwal, "Design and Implementation of a Ternary Logic Memory Cell Using MTJ and CNFET" (2023-24, Passed)

Publications:

Journals

- A. Chauhan, K. Sharma, and S. Choudhary, "Transition metal induced-magnetization and spin-polarisation in black arsenic phosphorous," *Ain Shams Eng. J.*, p. 102632, 2024, doi:10.1016/j.asej.2024.102632. (Impact Factor: 6.0)
- Chauhan, A., Sharma, K. & Choudhary, S. "Transition metal induced-magnetization in zigzag SiCNTs," *J Comput Electron* 22, 964–970 (2023). doi:10.1007/s10825-023-02030-y (Impact Factor: 2.1)
- Chauhan, A., Tomar, P. "First-Principles Study of Enhanced Absorption in Van der Waals Heterostructure of MoS₂/Cd_{0.90}Zn_{0.10}Te_{0.93}Se_{0.07} in the Visible Region," *J. Electron. Mater.* (2022). doi:10.1007/s11664-022-09901-3 (Impact Factor: 2.1)

- Chauhan, A., Maahich, A. & Pal, J. "First-principles calculations of the electronic and optical properties of WSe₂/Cd_{0.9}Zn_{0.1}Te van der Waals heterostructure," *J Comput Electron* (2021). doi:10.1007/s10825-021-01659-x (Impact Factor: 2.1)
- Choudhary, S., Chauhan, A. "First-principles study of spin transport in CrO₂-SiCNT-CrO₂ magnetic tunnel junction," *J Comput Electron* 14, 852–856 (2015). doi:10.1007/s10825-015-0725-x (Impact Factor: 2.1)

International Conference Proceedings

- A. Chauhan and R. Dubey, "CNTFET-based Design of Ternary Adders based on GDI Technique," 2023 3rd International Conference on Innovative Mechanisms for Industry Applications (ICIMIA), Bengaluru, India, 2023, pp. 1369-1373, doi: 10.1109/ICIMIA60377.2023.10426029.
- A. Chauhan, A. K. Meena and A. Kumar, "Performance Analysis of 4-Bit Multiplier using 90nm Technology," 2022 2nd International Conference on Intelligent Technologies (CONIT), 2022, pp. 1-5, doi: 10.1109/CONIT55038.2022.9848209.
- L. Mahor, A. Chauhan and P. Tiwari, "Parity Preserving Reversible Design Using FinFETs," 2019 1st International Conference on Signal Processing, VLSI and Communication Engineering (ICSPVCE), 2019, pp. 1-6, doi: 10.1109/ICSPVCE46182.2019.9092779
- A. Chauhan, L. Mahor and P. Tiwari, "Low Power Quaternary Adder Using CNFET," 2020 IEEE VLSI DEVICE CIRCUIT AND SYSTEM (VLSI DCS), 2020, pp. 109-114, doi: 10.1109/VLSIDCS47293.2020.9179898.
- A. Chauhan, K. K. Saini, N. Rajput and R. Domah, "Implementation of High Performance 4-Bit ALU using Dual Mode Pass Transistor Logic," 2021 International Conference on Intelligent Technologies (CONIT), 2021, pp. 1-4, doi: 10.1109/CONIT51480.2021.9498553
- A. Chauhan, A. Kumari, P. Meena and S. K. Meena, "Performance Analysis of Optical Communication System for Various Filtering Operations Using MIMO FSO System under Fog Condition," 2021 International Conference on Intelligent Technologies (CONIT), 2021, pp. 1-5, doi: 10.1109/CONIT51480.2021.9498509
- A. Chauhan, R. Verma, A. Joshi and R. Sharma, "Design and Performance Analysis for Underground Trains using Optisystem," 2021 International Conference on Intelligent Technologies (CONIT), 2021, pp. 1-4, doi: 10.1109/CONIT51480.2021.9498461.

Awards and Honors:

- Awarded Commendable Research Award in Research Excellence Awards 2023 at Delhi Technological University
- Awarded Commendable Research Award in Research Excellence Awards 2022 at Delhi Technological University

Teaching Experience:

- **Assistant Professor**
Delhi Technological University
2016 - Present
Courses Taught:
 - Electromagnetics (Undergraduate)
 - Linear Integrated Circuits (Undergraduate)
 - Control Systems (Undergraduate)
 - VLSI Design (Undergraduate)
 - Digital Electronics (Undergraduate)
 - Electronics and Communication Engineering for Mechanical Engineers (Undergraduate)
 - CMOS Analog IC Design (Undergraduate)

Professional Memberships:

- IEEE Member since 2020

Technical Skills:

- Cadence Virtuoso
- LTspice
- Xilinx
- MATLAB
- Synopsys QuantumATK

Professional Activities:

- Participated and successfully completed 2 weeks Industrial Training Program on "Cyber Security and Networking" conducted by BSNL from 06/07/2023 to 22/07/2023.
- Participated in the One-week Online Faculty Development Programme on "Recent Tools and Techniques for Quality Research-RTTQR 2023" organized by the Department of Computer Science, Banasthali Vidyapith during 15/03/2023 to 20/03/2023.
- Attended 2 days workshop titled "Hands on Training on Latex" organised by Department of Electronics and Communication Engineering, Delhi Technological University, Delhi from 26/09/2022 to 27/09/2022.
- Volunteered as proctor to guide and oversee competing teams for the IEEE Xtreme 16.0 programming competition that hosted +14,600 participants on 22nd October 2022.
- Participated & successfully completed AICTE Training And Learning (ATAL) Academy Two Week FDP on "Leadership Excellence" in hybrid mode from 02/01/2023 to 07/01/2023 and 16/01/2023 to 20/01/2023 at Deenbandhu Chhotu Ram University of Science and Technology, Haryana.
- Received A-Grade in Refresher Course in Data Science and Machine Learning from 5th March to 19th March 2020 by UGC-HRDC, University of Mumbai.
- 4 Weeks Orientation/ Induction Programme for Faculty in Universities of Higher Education from 4th June to 1st July 2020 organised by Teaching Learning Centre, Ramanujam College, University of Delhi sponsored by Ministry of Human Resource Development, Pandit Madan Mohan Malviya, National Mission on Teachers and Teaching.
- Attended 2 weeks of online industrial training on "Internet of Things- A Project-based Learning using Virtual IoT Lab" organised jointly by National Institute of Technical Teachers Training and Research Chandigarh and Xtrans Solutions Pvt. Ltd., Bangalore from 8th to 17th July 2020.
- Attended 2 weeks online industrial training on "Artificial Intelligence and Machine Learning- A Project- based Learning Approach" organised jointly by National Institute of Technical Teachers Training and Research Chandigarh and Xtrans Solutions Pvt. Ltd., Bangalore from 22nd July to 5th August 2020.
- Attended AICTE, Quality Improvement Scheme (AQIS) Funded One week Online Short Term Training Programme (STTP) on Teaching-Learning Pedagogies organized by A.G. Patil Polytechnic Institute from 07.09.2020 to 12.09.2020.
- Attended one-week FDP on " Advanced Pedagogical Techniques" from 28/10/2020 to 05/11/2020 organised by Teaching Learning Centre, Ramanujam College, University of Delhi sponsored by Ministry of Human Resource Development, Pandit Madan Mohan Malviya, National Mission on Teachers and Teaching.
- Successfully completed eight modules of AICTE approved NITTT Swayam MOOCs in February 2021.
- Participated in One day E-Workshop on the theme of "Entrepreneurial Ecosystem and start-up" held on 30th September 2021, organized by

Department of Electronics and Communication Engineering, Delhi Technological University, Delhi, India.

- Attended Two Days IEEE Workshop on "INTERNET OF THINGS (IoT): THE FUTURE OF CONNECTIVITY" jointly organized by IEEE Standards Association, ECE Department DTU, IEEE Delhi Section, IEEE Delhi CS Chapter and IEEE Delhi ComSos Chapter during 28-29 October 2021.
- Participated in One-Week online Short Term Training Program on “Recent Advances and Challenges in Computer Vision” held from 03rd Dec to 07th Dec, 2021 organized by Department of Electronics & Communication Engineering, Delhi Technological University, Delhi-110042, India.
- Participated in One-Week Online Faculty Development Program on the theme of “Machine Learning Applications in Signal Processing and Wireless Networks” held on December 20th-24th, 2021, organized by Department of Electronics and Communication Engineering, Delhi Technological University, Delhi, India.
- Participated in One-Week online international Faculty Development Program on "Computational Techniques for Electromagnetics" organized by the Department of ECE, DTU, India in collaboration with Xiangshan Laboratory (XSL), Zhongshan Institute of CUST, China and ARK Infosolutions Pvt. Ltd. India during December 27-31, 2021.
- Participated & completed successfully AICTE Training And Learning (ATAL) Academy Online Elementary FDP on "Wireless Sensor Networks and IoT" from 10/01/2022 to 14/01/2022 at Delhi Technological University, Delhi.
- Participated in the 3 days FDP on "NBA Accreditation Procedures" conducted by NITTR, Chennai, from 09/05/2022 to 11/05/2022 at Delhi Technological University, Delhi.

References:

Prof. Kapil Sharma

Department of Information Technology, Delhi Technological University

Email: kapil@ieee.org

Phone: +91-9717470444

Dr. Sudhanshu Choudhary

Sudhanshu Choudhary, PhD

Instructor of Electrical Engineering,

School of Electrical Engineering and Computer Science (SEECs)

University of North Dakota

Email: sudhanshu.choudhary@und.edu

Phone: +1 701-314-3388

Declaration:

I hereby declare that the information provided above is true to the best of my knowledge and belief.

Anurag Chauhan

Date: 03/09/2024